1963

A statistical investigation of the diurnal temperature variation during the polar night at McMurdo Sound, Antarctica

Barrigar, Donald B.

Monterey, California: U.S. Naval Postgraduate School

A STATISTICAL INVESTIGATION OF THE DIURNAL TEMPERATURE VARIATION DURING THE POLAR NIGHT AT McMURDO SOUND, ANTARCTICA.

DONALD B. BARRIGAR

Mont 254

A STATISTICAL INVESTIGATION OF THE DIURNAL TEMPERATURE VARIATION DURING THE POLAR NIGHT AT McMURDO SOUND, ANTARCTICA

* * * * * * * * * * *

Donald B. Barrigar

A STATISTICAL INVESTIGATION OF THE DIURNAL TEMPERATURE VARIATION DURING THE POLAR NIGHT AT McMURDO SOUND, ANTARCTICA

by

Donald B. Barrigar

Lieutenant, United States Navy

Submitted in partial fulfillment of the requirements of the degree of

MASTER OF SCIENCE

IN

METEOROLOGY

United States Naval Postgraduate School

Monterey, California

1963

A STATISTICAL INVESTIGATION OF THE DIURNAL TEMPERATURE VARIATION DURING THE POLAR NIGHT AT McMURDO SOUND, ANTARCTICA

by

Donald B. Barrigar

This work is accepted as fulfilling
the thesis requirements for the degree of
MASTER OF SCIENCE
IN
METEOROLOGY
from the
United States Naval Postgraduate School

ABSTRACT

It is observed that normally, during the polar night, 24-hour periods with a clear sky and light to moderate winds have their lowest temperatures in the middle of the period, and the highest temperatures occur at the beginning and end. For cloudy and windy periods, the shape of the temperature curve is reversed, with the maximum temperature occurring near the middle of the period. Despite many efforts by various investigators no physical explanation could be found for this variation.

Hisdal discovered that for clear skies and low wind speed, the same shape of temperature variation curve occurs, whether the starting time is 0000 hr, 1200 hr, or 1400 hr. Thus, the abnormal behavior of the temperature variation appears to be influenced primarily by the statistical bias involved in the selection criteria.

This investigation, using six years of surface data, divides the diurnal temperature variation for various special types of days into two parts, the meteorological or diurnal variation and the superimposed statistical bias. Finally, the meteorological diurnal temperature variation, based upon all observations during the six year period, is determined.

The writer wishes to express his appreciation for the advice and guidance given him by Professor W. van der Bijl of the U. S. Naval Postgraduate School in this investigation.

TABLE OF CONTENTS

LIST OF ILLUSTRATIONS

LIST OF TABLES

LIST OF ABBREVIATIONS AND SYMBOLS

C_m	constant, dependent upon the meteorological influence
C_s	constant, dependent upon the statistical bias
e	temperature due to random fluctuations
GCT	Greenwich Civil Time
g_i	Lamont correction
hh	hour of observation (GCT)
m	subscript denoting the meteorological contribution to total temperature
Met	meteorological; free from statistical or random influences
M_i	temperature due to the meteorological influence at observation time i
R	reduction factor, representing the factor by which the variance in the statistical bias will be reduced if a diagonal average is used, rather than a column average
s	subscript denoting the statistical bias contribution to total temperature
S_j	temperature due to the statistical bias at time j
t	total temperature, equal to the sum of the meteorological, statistical, and random temperature contributions
T_i	three-hourly temperature observation ($i = 0,1,2,----,n$)
T_{iL}	temperature, corrected by the Lamont correction
Var	variance
Δt	time increment between temperature observations
σ^2	variance of a single-observation random error
ϕ	subscript denoting a contribution to the total temperature

1. Introduction

In his meteorological investigations with the Norwegian-British - Swedish Antarctic expedition of 1949 - 1952, V. Hisdal [1] discusses a much pondered peculiarity of the diurnal temperature variation during the polar night. For the various polar stations investigated, days with clear skies and/or light to moderate winds had their minimum temperatures near 1200 GCT, whereas for the cases of overcast skies and/or windy days the opposite type of diurnal variation occurred; that is, a maximum temperature near 1200 GCT.

Concerning this strange temperature behavior, Simpson [2, p.72] wrote in 1919:

> I have spent more time over this problem than over any other discussed in this work ..... the investigation has led only to negative results.

In 1951 Court [3] could still not explain this temperature behavior. He wrote:

> Why should the maximum temperature on clear days during the antarctic night occur, almost without exception, in the hour after midnight? Simpson pondered this problem longer than any other of the many he investigated in compiling the meteorological reports of the last Scott expedition, without developing a satisfactory hypothesis.

Rouch [4] also found a daily temperature variation during the dark season, based on an analysis of the data both from the Charcot expeditions and from the Bird expeditions. He wrote that the average daily variation

> is a simple curve with a maximum around 1 or 2 A.M. and minimum after noon .... I cannot give a satisfactory explanation.

Hisdal's explanation for this phenomenon was simply that a physical explanation was not necessary at all. It could be explained in terms of an "automatic" daily variation which results from the nature of the type of day selected. For example, Hisdal [5, p.104] has shown that if a type of day is characterized by the presence of a temperature inversion, it will usually have a lower average temperature than the non-inversion days. This means that if the average diurnal temperature curve is computed using only the inversion-type days (having lower temperatures), the non-inversion days (having higher temperatures) will automatically tend to give a contribution near both edges of the 24-hour time span. The result of this automatic daily variation, shown schematically in figure 1, is that it superimposes a statistical bias upon any given diurnal variation that might be present. Moreover, the magnitude of the bias could be large enough to mask the diurnal variation completely.

An interesting fact is that Hisdal's explanation for the peculiar behavior of the diurnal temperature variation is apparently an independent discovery of the theory that Bartels [6] described in his Gottingen dissertation of 1922.

Hisdal demonstrated this statistical bias explicitly by considering two diurnal temperature variation curves for polar stations, based on data for dark season days with wind speeds less than 15 miles per hour and cloudiness less than five-tenths. The first curve begins at 0000 GCT and has a minimum temperature at 1200 GCT. The second begins at

(a)

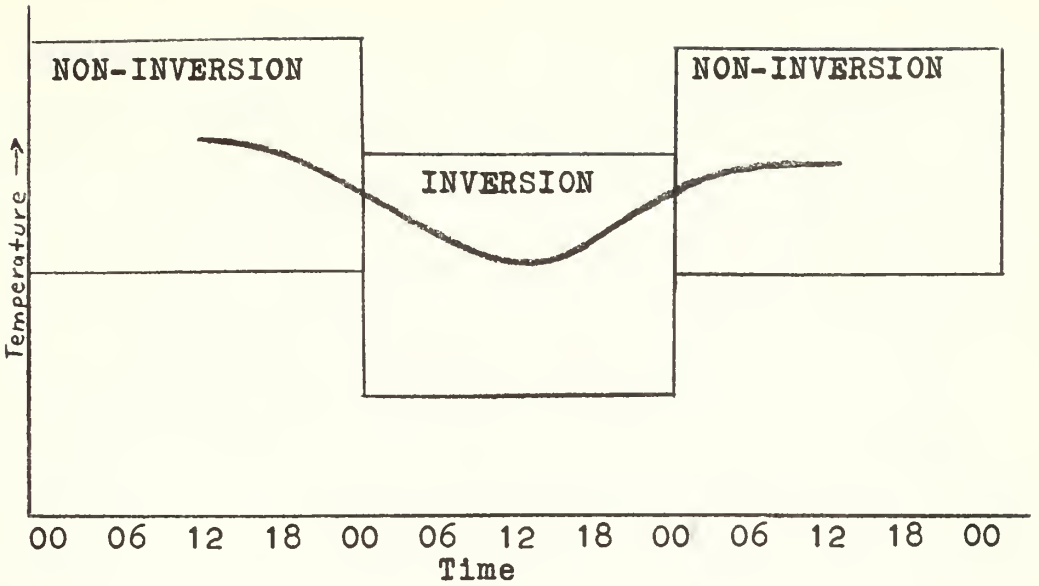

(b)

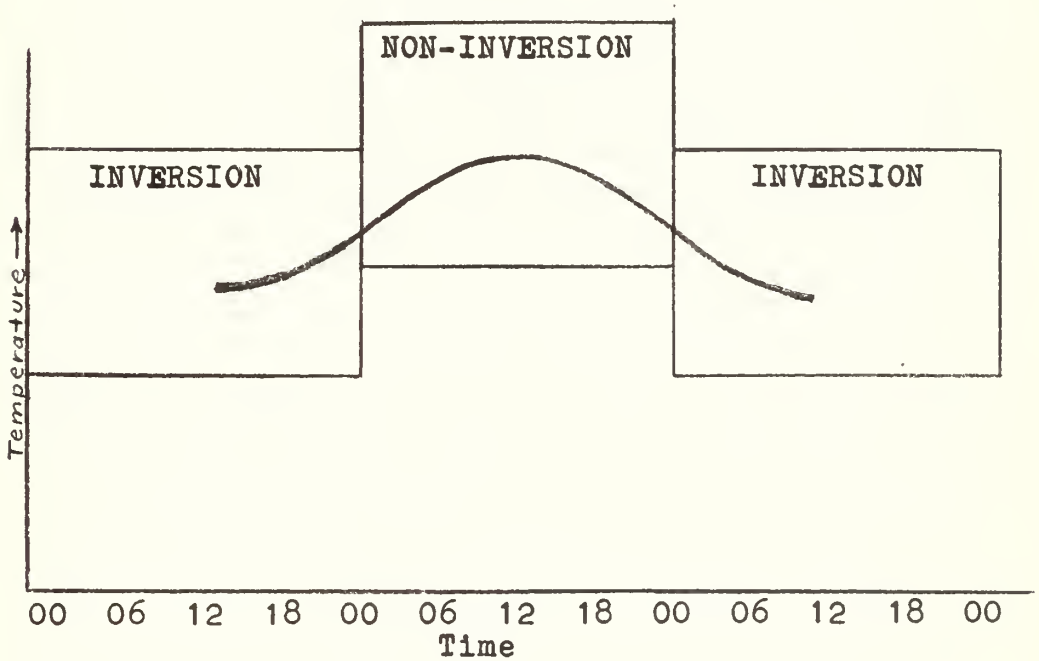

Figure 1

Schematic diagram showing the statistical bias effect

1200 GCT and has a minimum at approximately 0000 GCT. If there were a uniform diurnal temperature variation, the minimum temperatures should always occur at the same local time. Moreover, varying the initial time of the graph should not change the time of occurrence of the minimum. A logical explanation of the difference in these diurnal temperature variations is that the minima were primarily due to the statistical bias, not by diurnally different physical processes.

W. van der Bijl [7, p.149] also supports the theory of a "statistical bias" in his investigation of the diurnal pressure variation in northwest Europe. His study discloses a similar automatic diurnal variation due to data-selection bias. The basis of selection was that each day had to be in the month of December and have at least 5.7 hours of insolation. These criteria resulted in a diurnal trend with low pressure at the beginning and end of the period, with high pressure in the middle.

Thus, it has been shown that the existence of a "statistical bias" or "automatic diurnal variation" gives a reasonable explanation of the behavior of the temperature trend at polar stations during the dark season. However, Hisdal in his investigation did not deduce the mean meteorological diurnal variation of temperature, even though a knowledge of the effect of the statistical bias made this deduction possible.

The purpose of this study is to compute the mean meteorological or diurnal temperature variation during the polar night. As a secondary purpose, the temperature variations

induced by the statistical case-selection procedure will also be computed.

2. Data and Processing

The data used in this investigation were obtained from the National Weather Records Center, Asheville, North Carolina. The meteorological information consisted of punched IBM cards of surface data at three-hourly intervals from McMurdo Sound, Antarctica (78S, 166E), for the years 1956 through 1961. Figure 2 shows the geographical location of the area concerned.

The duration of the polar night at McMurdo sound was determined by the use of the solar altitude curves prepared by LeVasteau [8] . These indicated that the duration of the dark season was from 20 March through 20 September. However, this period does not eliminate twilight effects and incoming solar radiation due to unusual atmospheric refraction conditions. Therefore, the shorter period, 15 May through 15 August, was used in order to insure complete darkness.

In processing the punched data cards, the IBM 82 card sorter was used to select observations for the 15 May through 15 August period. Then the card data was transferred to a magnetic tape by use of the IBM 1401 printer. The magnetic tape was subsequently used in conjunction with a program for the Control Data Corporation 1604 digital computer, in order to determine:

(1) the mean diurnal variations of temperature, cloudiness, atmospheric pressure, and wind direction for various years;

(2) the same as (1), except for various starting times of the period;

(3) the same as (2), except for periods other than 24 hours;

(4) the total six-yearly mean variations as stated in (1), (2), and (3) above;

(5) and the Lamont correction for the above mentioned curves.

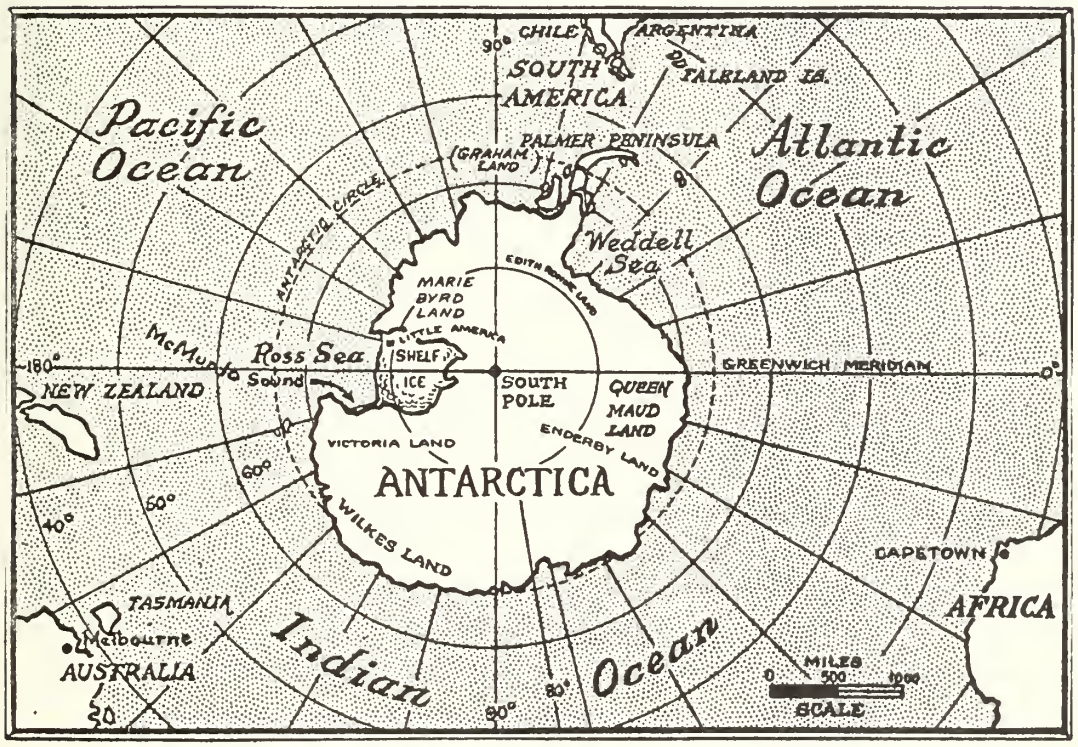

Figure 2

Geographical location of McMurdo Sound, Antarctica

3. The Lamont correction

The Lamont correction was mentioned in section 2 as one of the computer subroutines. The purpose of this correction is to make the starting value of a continuous parameter and the final value of the parameter equal to each other. This technique simplifies the study of any cyclical variations and is especially valuable in determining a diurnal variation.

A more complete discussion of the Lamont correction is presented by Conrad and Pollak [9] . For this study the corrected temperature was computed, using equation (2):

$$T_{iL} = g_i + T_i \qquad (2)$$

$$g_i = \frac{i(T_o - T_n)}{n} \qquad (3)$$

where T_{iL} = corrected temperature

T_i = sequence of three-hourly temperature observations ($i = 0, 1, 2, \ldots\ldots\ldots\ldots, n$)

g_i = Lamont correction.

A typical application of the Lamont correction follows. For this purpose, use is made of equations (2) and (3), and the hypothetical temperature observations given in table 1. The computed values of T_{iL} are summarized in the lower half of table 1.

given $T_o = 10$

$T_4 = 2$

$n = 4$

thus $g_i = \left(\frac{2-10}{4}\right)i = (-2)i$,

and $T_{iL} = (-2)i + T_i$.

Table 1

Some hypothetical temperature observations(T_i) and the resulting Lamont-corrected temperatures(T_{iL})

Hour of observation (GCT)	00	06	12	18	24
i	0	1	2	3	4
T_i	2	3	6	9	10
g_i	0	-2	-4	-6	-8
T_{iL}	2	1	2	3	2

It must be noted that the temperatures as corrected by the Lamont procedure are quite different than the original, uncorrected temperatures. However, since the present investigation deals only with the meteorological temperature cycle (i.e. the T_{iL} values), actual values of temperature are not important.

If the actual temperature values were desired, it would be necessary to maintain a table of corrections, as well as the corrected values.

4. Theoretical discussion of the method used to separate the meteorological diurnal variation and the statistical variation

As previously explained, the apparent diurnal temperature variation observed during the polar night for special types of days may be considered to be the sum of the meteorological variation and an effect resulting from statistical bias. Moreover, the major purpose of this study is to determine an estimate of these two components.

In order to illustrate how this dichotomy may be performed, it will be helpful to consider first how a particular observed daily temperature variation is "built up" by combining a meteorological influence with a statistical one. After the total diurnal variation has been constructed, it will once again be separated into its original components. This example will serve to illustrate how the actual data for this study may be treated to derive the meteorological and statistical variations.

First, consider that the set of T_{iL} values listed in table 1 are representative of the meteorological variation. These temperatures will remain fixed for the particular hours for which they were reported (e.g., the meteorological influence for 0600 GCT will always be 1F, regardless of the starting time of the period).

Next, consider a purely hypothetical statistical variation as listed in table 2. As previously pointed out by Hisdal, the statistical bias is not fixed at a particular value for a particular observation time, but depends upon the starting time of the period selected. To illustrate this,

assume first that the starting time of the 24-hour period in table 2 is 0000 GCT. Then the statistical bias for 0600 GCT would be 1F, since it would be the second observation reported. On the other hand, if 0600 GCT were the starting hour of the 24-hour period, the 0600 GCT bias would be 3F. Thus, the statistical influence may be thought of as a wave which is free to move through the diurnal or meteorological wave with contributions dependent upon the starting time of the 24-hour period.

Table 2

Hypothetical statistical bias for each 6-hourly observation time in a 24-hour period

Observation time i	Temperature(F)
1st	3
2nd	1
3rd	0
4th	1
5th	3

Now, using the meteorological influence from table 1 and the statistical influence from table 2, the "total" temperatures will be computed for various starting times, as shown in table 3.

The values of total temperature for the various 24-hour periods are summarized in table 4. The smaller numbers adjacent to the total temperature are the meteorological and statistical contributions to the total, as follows.

Table 3

Total temperature variation resulting from the statistical and meteorological variations from tables 1 and 2 respectively, for various starting times

Starting time: 0000 GCT

Hour:	00	06	12	18	00
Statistical:	3	1	0	1	3
Meteorological:	2	1	2	3	2
Total:	5	2	2	4	5

Starting time: 0600 GCT

Hour:	06	12	18	00	06
Statistical:	3	1	0	1	3
Meteorological:	1	2	3	2	1
Total:	4	3	3	3	4

Starting time: 1200 GCT

Hour:	12	18	00	06	12
Statistical:	3	1	0	1	3
Meteorological:	2	3	2	1	2
Total:	5	4	2	2	5

Starting time: 1800 GCT

Hour:	18	00	06	12	18
Statistical:	3	1	0	1	3
Meteorological:	3	2	1	2	3
Total:	6	3	1	3	6

t_m^s; where t = total

s = statistical influence

m = meteorological influence.

The total temperature variations in table 4 are typical of those obtained from the CDC 1604 computer program. They are plotted in figure 3 in order to show the effect the statistical influence has in shifting the time of the daily minimum for various starting times of the hypothetical 24-hour period.

Now, the next step in this discussion is to perform a dichotomy upon the total temperature values found in table 4 in order to determine the original values of meteorological and statistical variation contributions. A more general proof of the separation method is given in section 5. Specifically, the method to be used is the same as that utilized by van der Bijl in his investigation of diurnal pressure variations. It consists of averaging the values of table 4 in either of two ways: by columns, to determine the meteorological influence, or diagonally, to determine the statistical influence. Once either of these averages has been computed, the other may be determined by subtraction from the total values. These methods are shown below. The notation used is as follows: $t_{\phi,hh}$

t = temperature (F)

ϕ = m; refers to meteorological influence

ϕ = s; refers to statistical influence

hh = hour of observation (GCT).

Table 4

Hypothetical total temperatures
for various 24 hour periods

Hour (GCT)	00	06	12	18	24/00	06	12	18
Temperature (F)	5^{3}_{2}	2^{1}_{1}	2^{0}_{2}	4^{1}_{3}	5^{3}_{2}			
	3^{1}_{2}	4^{3}_{1}	3^{1}_{2}	3^{0}_{3}	3^{1}_{2}	4^{3}_{1}		
	2^{0}_{2}	2^{1}_{1}	5^{3}_{2}	4^{1}_{3}	2^{0}_{2}	2^{1}_{1}	5^{3}_{2}	
	3^{1}_{2}	1^{0}_{1}	3^{1}_{2}	6^{3}_{3}	3^{1}_{2}	1^{0}_{1}	3^{1}_{2}	6^{3}_{3}

Figure 3: Hypothetical total temperature variation curves for various starting times of the period, based upon the values found in table 4.

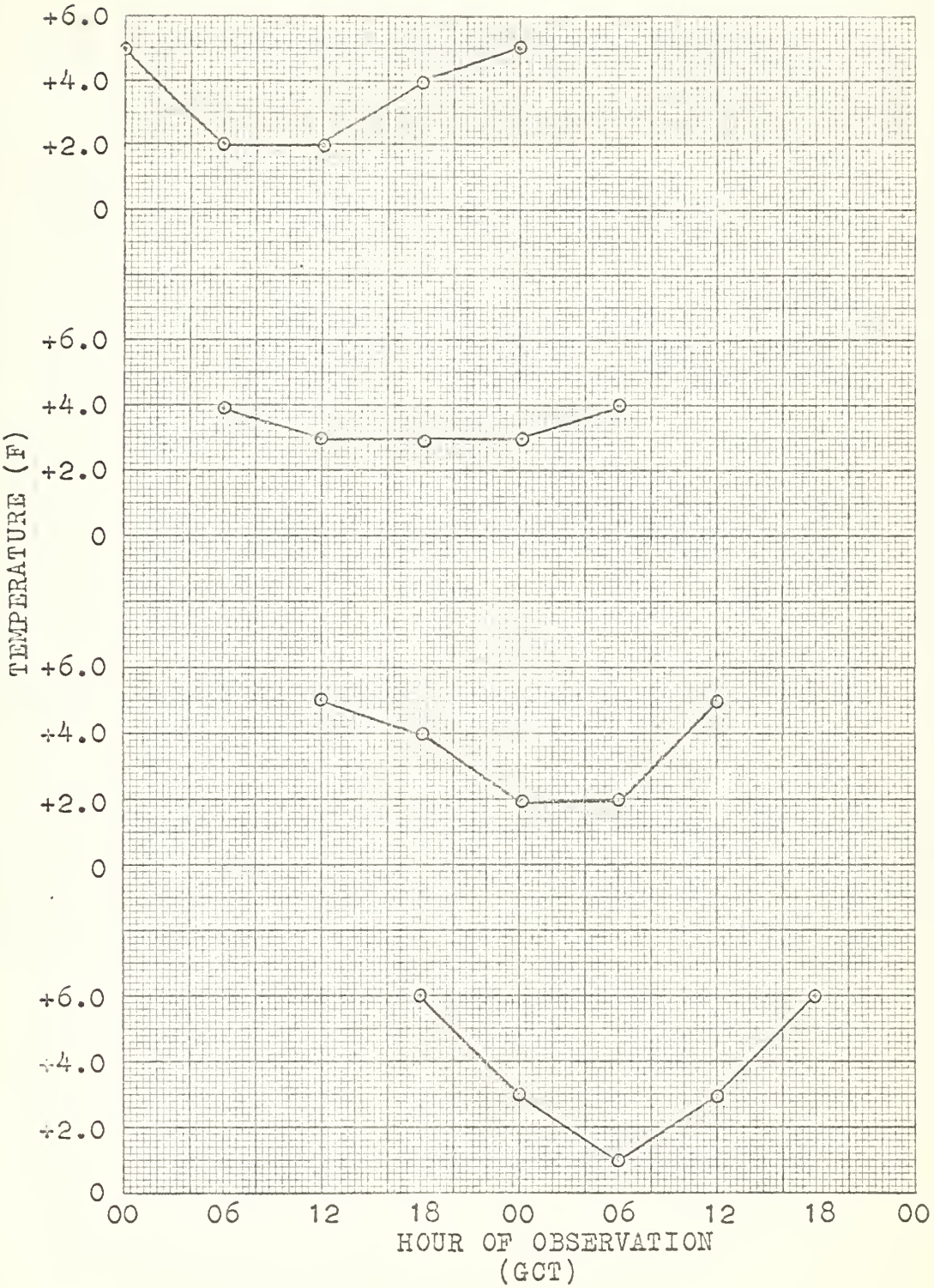

Averaging by columns, and subtracting the constant value of the statistical bias, results in the meteorological variation.

$$t_{m,00} = \left(\frac{5+3+2+3}{4}\right) - \left(\frac{3+1+0+1}{4}\right) = \frac{13}{4} - \frac{5}{4}$$
$$= 2$$

$$t_{m,06} = \left(\frac{2+4+2+1}{4}\right) - \left(\frac{1+3+1+0}{4}\right) = \frac{9}{4} - \frac{5}{4}$$
$$= 1$$

$$t_{m,12} = \left(\frac{2+3+5+3}{4}\right) - \left(\frac{0+1+3+1}{4}\right) = \frac{13}{4} - \frac{5}{4}$$
$$= 2$$

$$t_{m,18} = \left(\frac{4+3+4+6}{4}\right) - \left(\frac{1+0+1+3}{4}\right) = \frac{17}{4} - \frac{5}{4}$$
$$= 3$$

$$t_{m,24} = \left(\frac{5+3+2+3}{4}\right) - \left(\frac{3+1+0+1}{4}\right) = \frac{13}{4} - \frac{5}{4}$$
$$= 2$$

Averaging diagonally (assuming the 24-hour period begins at 0000 GCT), and subtracting the constant value of the meteorological influence, results in the statistical influence.

$$t_{s,00} = \left(\frac{5+4+5+6}{4}\right) - \left(\frac{2+1+2+3}{4}\right) = \frac{20}{4} - \frac{8}{4}$$
$$= 3$$

$$t_{s,06} = \left(\frac{2+3+4+3}{4}\right) - \left(\frac{1+2+3+2}{4}\right) = \frac{12}{4} - \frac{8}{4}$$
$$= 1$$

$$t_{s,12} = \left(\frac{2+3+2+1}{4}\right) - \left(\frac{2+3+2+1}{4}\right) = \frac{8}{4} - \frac{8}{4}$$
$$= 0$$

$$t_{s,18} = \left(\frac{4+3+2+3}{4}\right) - \left(\frac{3+2+1+2}{4}\right) = \frac{12}{4} - \frac{8}{4}$$
$$= 1$$

$$t_{s,24} = \left(\frac{5+4+5+6}{4}\right) - \left(\frac{2+1+2+3}{4}\right) = \frac{20}{4} - \frac{8}{4}$$
$$= 3$$

In this example we have recovered the values of the meteorological and statistical influences, assumed originally in constructing the values of total temperature.

One difficulty in applying these methods to actual data lies in the fact that the constant terms which are subtracted from the averages of total temperature are not immediately apparent. This difficulty, however, is of no great concern, when the temperature trend and not the actual temperature <u>per se</u> is under investigation.

For the sake of completeness, the next section will illustrate how the use of these constants may be eliminated.

5. Elimination of the constant term, when computing the statistical bias

The purpose of this section is to illustrate how the constant term may be eliminated, when computing the statistical bias. The only known temperature values are those of total temperature, found in table 4. The hourly meteorological contributions are unknown.

The notation used is as specified in section 4, except for the following:

C_m = a constant which is dependent upon the meteorological influence,

C_s = a constant which is dependent upon the statistical bias.

The column averages, computed in section 4, become:

$$t_{m,00} = \frac{13}{4} - C_s,$$

$$t_{m,06} = \frac{9}{4} - C_s,$$

$$t_{m,12} = \frac{13}{4} - C_s, \qquad C_s = \frac{t_{s,00} + t_{s,06} + t_{s,12} + t_{s,18}}{4}$$

$$t_{m,18} = \frac{17}{4} - C_s,$$

$$t_{m,24} = \frac{13}{4} - C_s.$$

Next, if the averaging is done diagonally, using 0000 GCT as the starting time, the following temperatures result:

$$t_{s,00} = \frac{20}{4} - C_m,$$

$$t_{s,06} = \frac{12}{4} - C_m, \qquad C_m = \frac{t_{m,00} + t_{m,06} + t_{m,12} + t_{m,18}}{4},$$

$$t_{s,12} = \frac{8}{4} - C_m,$$

$$t_{s,18} = \frac{12}{4} - C_m ,$$

$$t_{s,24} = \frac{20}{4} - C_m .$$

Making the appropriate substitution for C_m in the last set of equations,

$$t_{s,00} = \frac{20}{4} - \frac{t_{m,00} + t_{m,06} + t_{m,12} + t_{m,18}}{4}$$

$$= \frac{20}{4} - \frac{1}{4}\left[\left(\frac{13}{4} + \frac{9}{4} + \frac{13}{4} + \frac{17}{4}\right) - 4C_s\right]$$

$$= \frac{20}{4} - \frac{1}{4}\left(\frac{13}{4} + \frac{9}{4} + \frac{13}{4} + \frac{17}{4}\right) - \left(\frac{t_{s,00} + t_{s,06} + t_{s,12} + t_{s,18}}{4}\right)$$

$$t_{s,00} = 5 - \frac{52}{16} + \frac{t_{s,00} + t_{s,06} + t_{s,12} + t_{s,18}}{4} .$$

$$\therefore 3t_{s,00} - t_{s,06} - t_{s,12} - t_{s,18} = 7 . \qquad (4)$$

Similarily, for the starting times 06, 12 and 18 h, we obtain, respectively:

$$t_{s,00} - 3t_{s,06} + t_{s,12} + t_{s,18} = 1 , \qquad (5)$$

$$t_{s,00} + t_{s,06} - 3t_{s,12} + t_{s,18} = 5 , \qquad (6)$$

$$t_{s,00} + t_{s,06} + t_{s,12} - 3t_{s,18} = 1 . \qquad (7)$$

Equations (4) through (7) comprise a set of four linear, homogeneous equations in four unknowns, which can be readily solved using the usual mathematical techniques. Such a solution produces the following:

$$t_{s,00} = 3$$

$$t_{s,06} = 1$$

$$t_{s,12} = 0$$

$$t_{s,18} = 1$$

$$t_{s,24} = t_{s,00} = 3 .$$

Thus, it is seen that if specific values of statistical bias or meteorological effect are desired, a set of homogeneous equations must be solved. However, as was stated in section 4, this present study does not require specific temperature values, but rather their relative values. Therefore, the constants C_s and C_m will not be removed from the computed diurnal averages.

6. General discussion of the actual results

In general, the results of this study can be separated into four parts. The first is the set of 24-hour temperature variation curves, figures 4 through 25. These curves were drawn in order to determine to what degree statistical bias is apparent, when dealing with actual data. Also, in these curves the criteria used in selection of the type of day to be investigated were varied. The extreme cases considered were (1) wind speed greater than 15 kt, cloudiness greater than five-tenths; and (2) wind speed calm, cloudiness equal to zero.

The second set of curves, figures 26 through 30 are the 48-hour variations for various pairs of days selected. The selection criteria are comparable to those specified for the 24-hour variation curves. The major purpose of the 48-hour curves is to show that the statistical bias effect is not restricted to a 24-hour period.

The third set, figures 31 through 34, comprise the 18-hour and the 72-hour variations. These curves are also included in the study to show how periods of various length effect the statistical bias.

The fourth set of curves, figures 35 through 42, show the relationship between temperature variation and variations of atmospheric pressure, cloudiness, and wind direction. The purpose of this set is to aid in giving some explanation for the peculiarities found in the daily temperature trend.

In all of these curves the abscissa is the hour of observation in Greenwich Civil Time, which is the same time scale

that Hisdal used in his investigation. It is convenient to use Greenwich Civil Time rather than local time, since the reporting times of surface observations are in GCT.

If it is desired to obtain the diurnal variation, based on local time, add 11 hours to the observation times in Greenwich Civil Time. However, it must be remembered that local time loses its significance during the polar winter season, since the noon hour has no more sunshine than the "witching hour".

7. The diurnal temperature variation for special selections of days

Table 5 summarizes the comparison between the expected curvatures of the diurnal variations for selected types of day and various starting times of the period considered. The expected curvature is based on the discussion in section 1. There it was pointed out that days with high wind speed and/or cloudy skies will have above-normal average values of temperature, resulting in a convex diurnal temperature curve. Days with low wind speed and/or clear skies have below-normal mean temperatures, resulting in a concave diurnal temperature curve. In table 5 the shape of the daily meteorological course of temperature agrees favorably with the expected shape. However, as the criteria are made more restrictive, the agreement becomes worse, due to the increasing contributions arising from random effects as the sample size is reduced. (The effects of randomness are considered in section 11.)

Table 6 contains a summary of the expected shape and actual shape of the statistical bias curves for the various types of day selected. The table also contains information concerning the time of maxima or minima in the mean meteorological curves and the range of temperature fluctuations involved. It is seen that the actual shape of the statistical bias curves agrees with the expected shape quite well. However, as in table 5, making the selection criteria more restrictive produces more pronounced random errors, due to the reduction of the sample size. For instance, figure 21 is based upon only seven days. The result is that no

Table 5

Summarized results of the total temperature variation curves for various starting times

Figure	Criteria wind speed (kt)	Criteria cloudiness (tenths)	Expected Shape concave	Expected Shape convex	Actual Shape concave	Actual Shape convex	Actual Shape neither
4	≥15	≥5		X	4	2,3	1
6	≤15	≤5	X		1,3,4		2
8	≤8	≤5	X		1,2,3,4		
10	≤5	≤5	X		3,4		1,2
12	≤4	≤5	X		3,4		1,2
14	≤3	≤5	X		1,3,4		2
16	≤2	≤5	X		1,3,4		2
18	= 0	≤5	X		1,3,4		2
20	= 0	= 0	X		3	2	1,4
22	≥2 ≤15	≤5	X		3	4	1,2
24	≤15	≤10	X		1,3,4		2

1: Starting time = 0000 GCT
2: Starting time = 0600 GCT
3: Starting time = 1200 GCT
4: Starting time = 1800 GCT

Table 6

Summarized results of the 0000 GCT to 0000 GCT
meteorological and statistical temperature variations

Figure	Criteria		Statistical Variation			Meteorological Variation		
	wind (kt)	clouds (tenths)	concave shape	convex shape	neither	max. temp at___ GCT	min. temp at___ GCT	range of variation
5	≥15	≥5		E,A		00	00	1.75
7	≤15	≤5	E,A			18	06	1.25
9	≤8	≤5	E,A			12	06	1.50
11	≤5	≤5	E,A			03,18	06,21	2.10
13	≤4	≤5	E,A			03,18	06,21	1.60
15	≤3	≤5	E		A	03,15	06,21	3.20
17	≤2	≤5	E,A			09,15,21	06,12,18	5.00
19	=0	≤5	E		A	15,21	06,18	4.20
21	=0	=0	E		A	15,21	06,18	5.20
23	2< ≤15	≤5	E,A			12,18	03,15	7.00
25	≤15	≤10	E,A			03,12	06,21	1.50

E: Expected Shape
A: Actual Shape

organized statistical influence is apparent in this case. In contrast, figure 7 is based on 174 days and the statistical bias has a definitely concave-shaped curve.

One peculiarity that occurs in the set of temperature variation curves is the 2100 GCT maximum, appearing in the statistical bias curves. This maximum, which would occur at 0800 local time, gives an unnatural appearance to the bias curves. Therefore, considerable time was spent in determining the cause of the peculiarity. One resulting conclusion is that the 2100 GCT maximum is associated with the criterion of calm winds, since it appears in all curves in which calm winds are included, except those of figure 21. Here the maximum occurs at 1800 GCT. However, this latter figure is based on only seven days and one should be careful not to attribute undue significance to such a small sample.

An attempt was made to exclude the calm days in computing the mean diurnal temperature variation in order to determine whether the 2100 GCT maximum would disappear from the statistical bias. The results are contained in figures 5 and 23, in which the maximum does not appear. However, the criterion for figure 23 (wind speed between two and 15 kt) was too restrictive and only four days could be used.

Further investigation revealed how the calm-day observations affected the statistical bias curves. This matter is explained in more detail in section 11. It will suffice the present discussion to say that the maximum in the statistical bias curve resulted from calculating the bias through the use

of a total temperature curve which had an above-normal random contribution at 2100 GCT.

It is interesting to note that the 18-hour statistical bias curve, figure 32, does not contain a maximum comparable the the 2100 GCT maximum. Therefore, it is doubtful that such a maximum would occur with an independent selection of data.

Figure 4: Total temperature variation curves with variation in starting time of the period. (wind speed ≥ 15 kt; cloudiness ≥ 5/10)

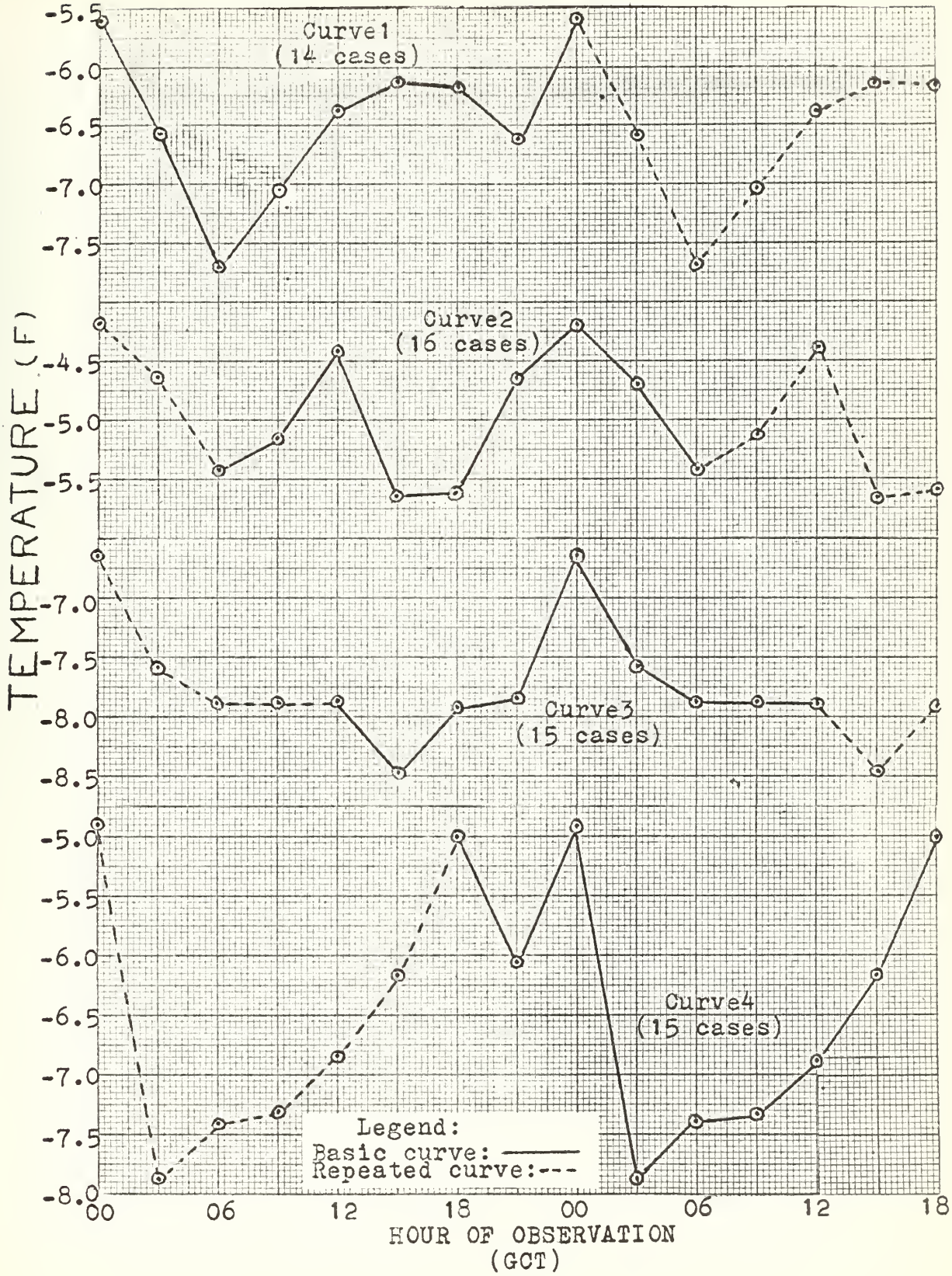

Figure 5: Comparison of the total temperature variation with the meteorological (Met.) and the statistical bias variations.
(wind speed ≥15 kt; cloudiness ≥5/10)

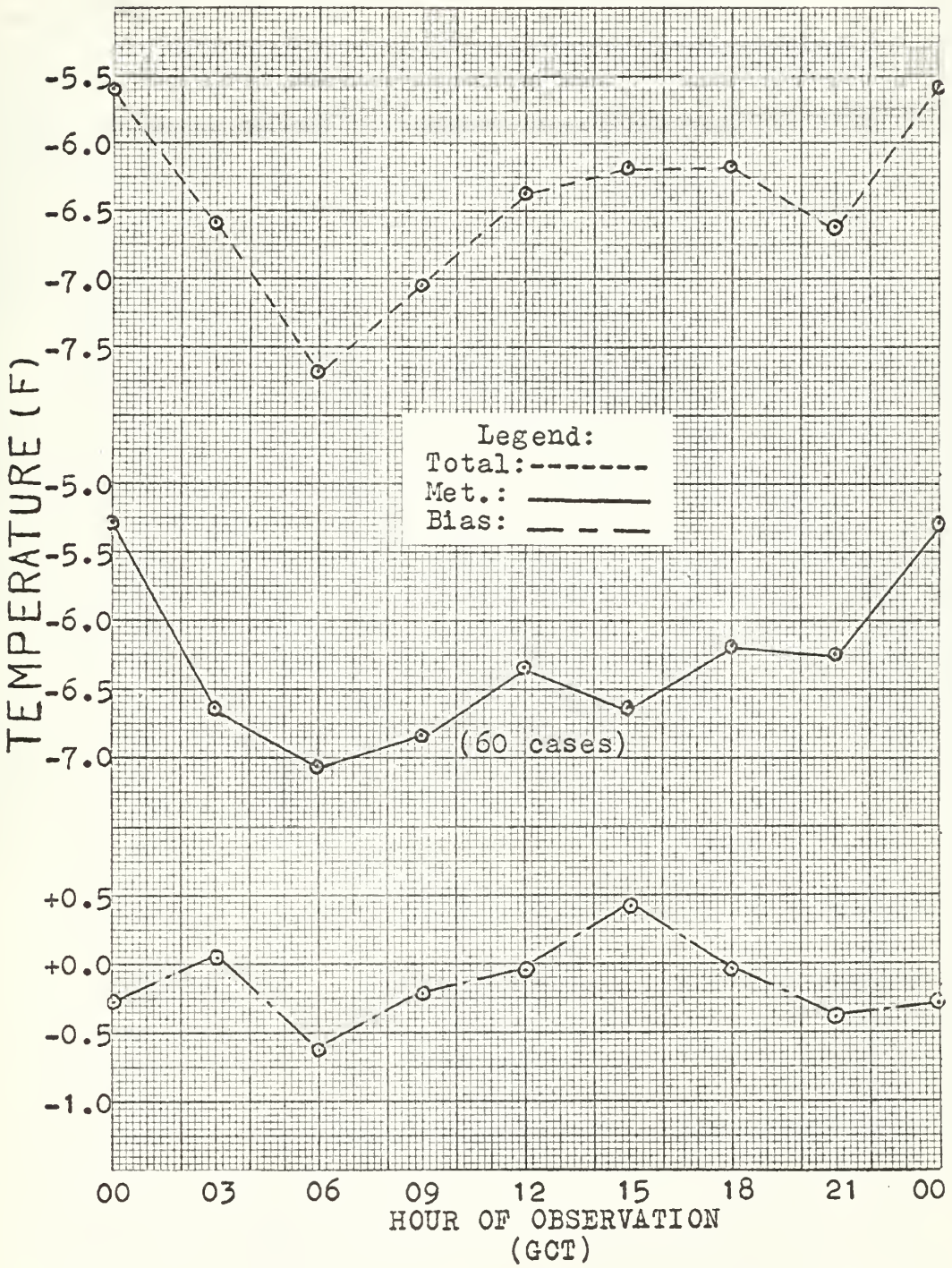

Figure 6: Total temperature variation curves with variation in starting time of the period. (wind speed ≤ 15 kt; cloudiness ≤ 5/10)

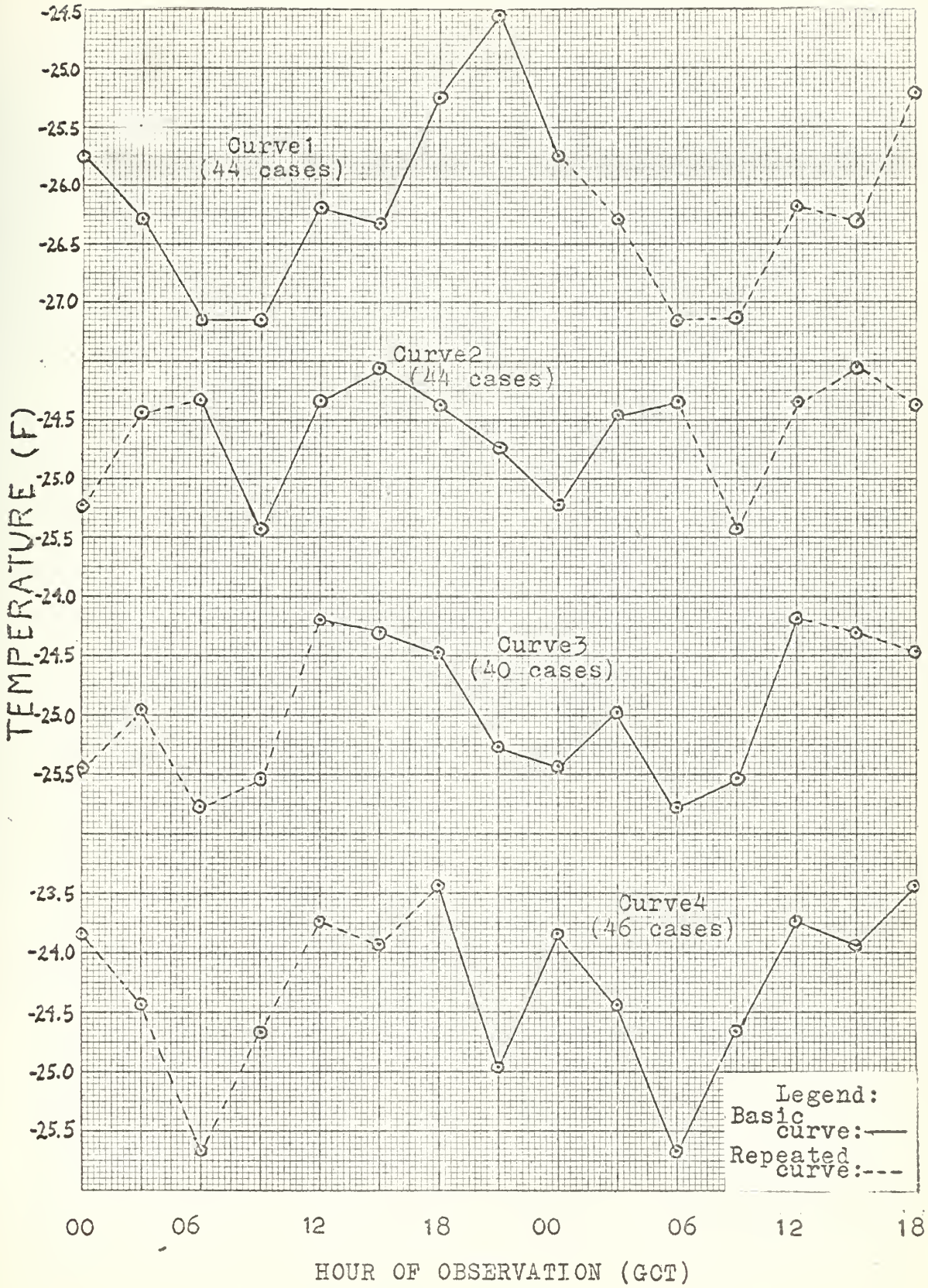

Figure 7: Comparison of the total temperature variation with the meteorological (Met.) and the statistical bias variations.
(wind speed ≤ 15 kt; cloudiness ≤ 5/10)

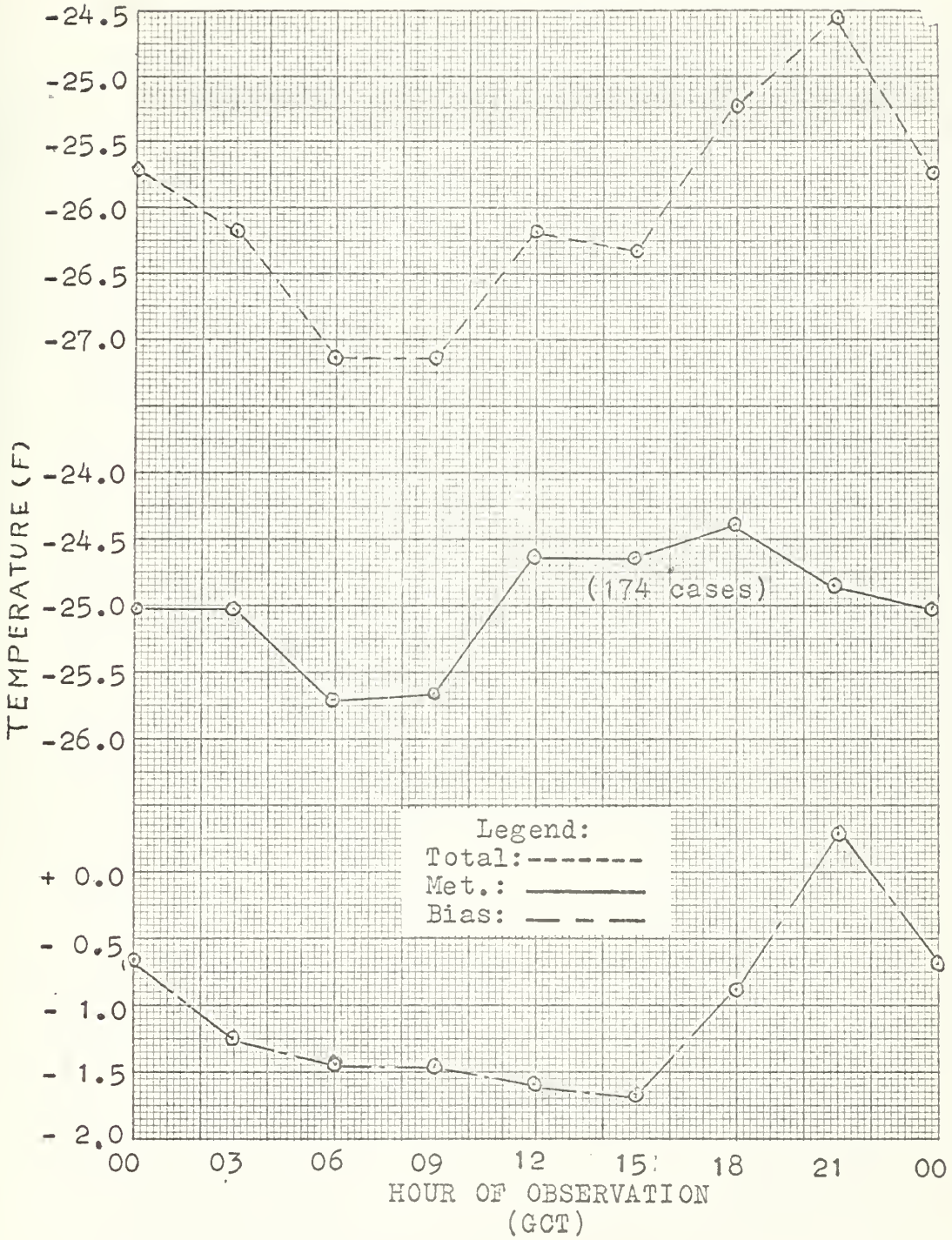

Figure 8: Total temperature variation curves with variation in starting time of the period. (wind speed ≤ 8 kt; cloudiness ≤ 5/10)

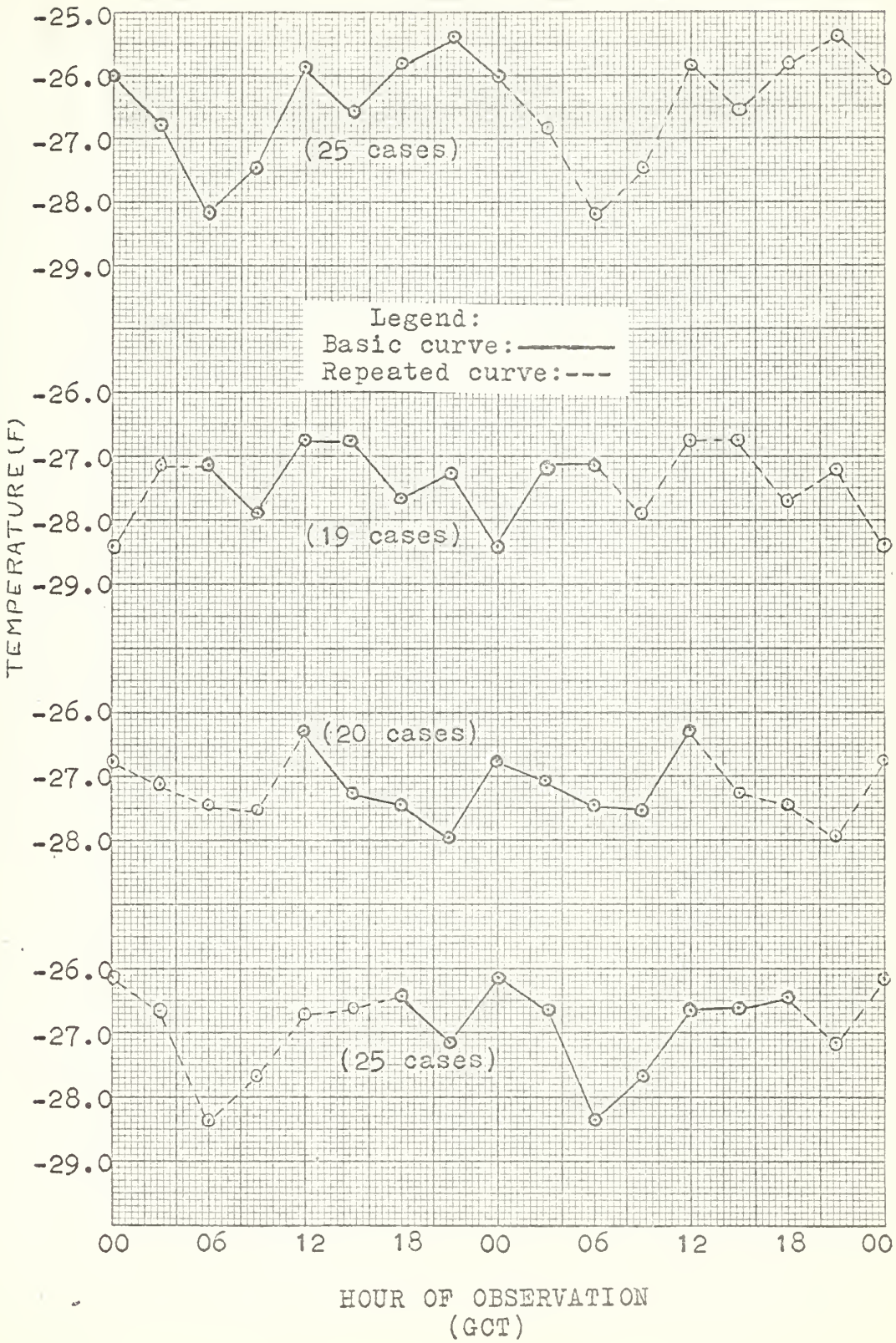

Figure 9: Comparison of the total temperature variation with the meteorological and the statistical bias variations.
(wind speed ≤ 8 kt; cloudiness ≤ 5/10)

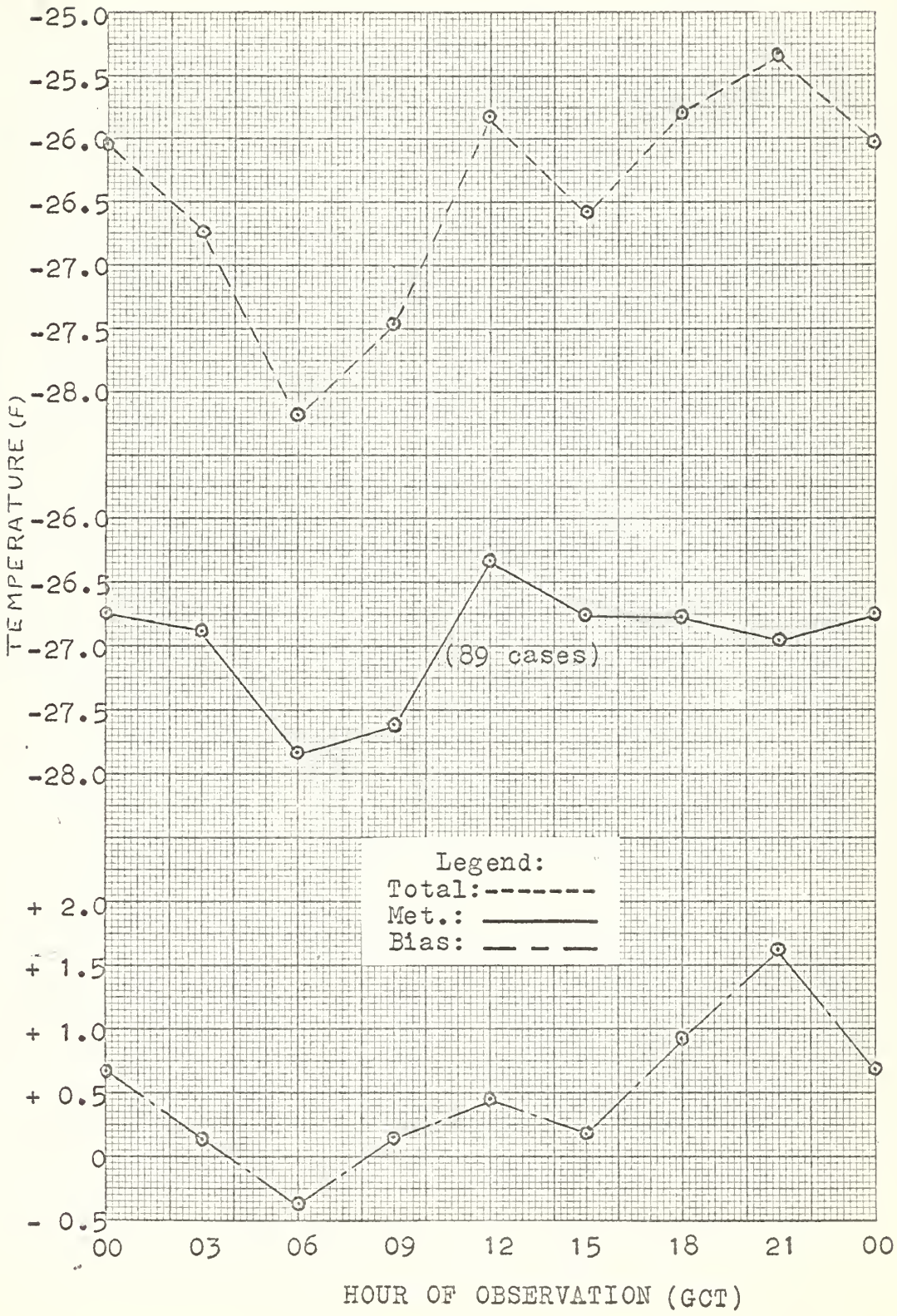

Figure 10: Total temperature variation curves with variation in starting time of the period. (wind speed ≤5 kt; cloudiness≤5/10)

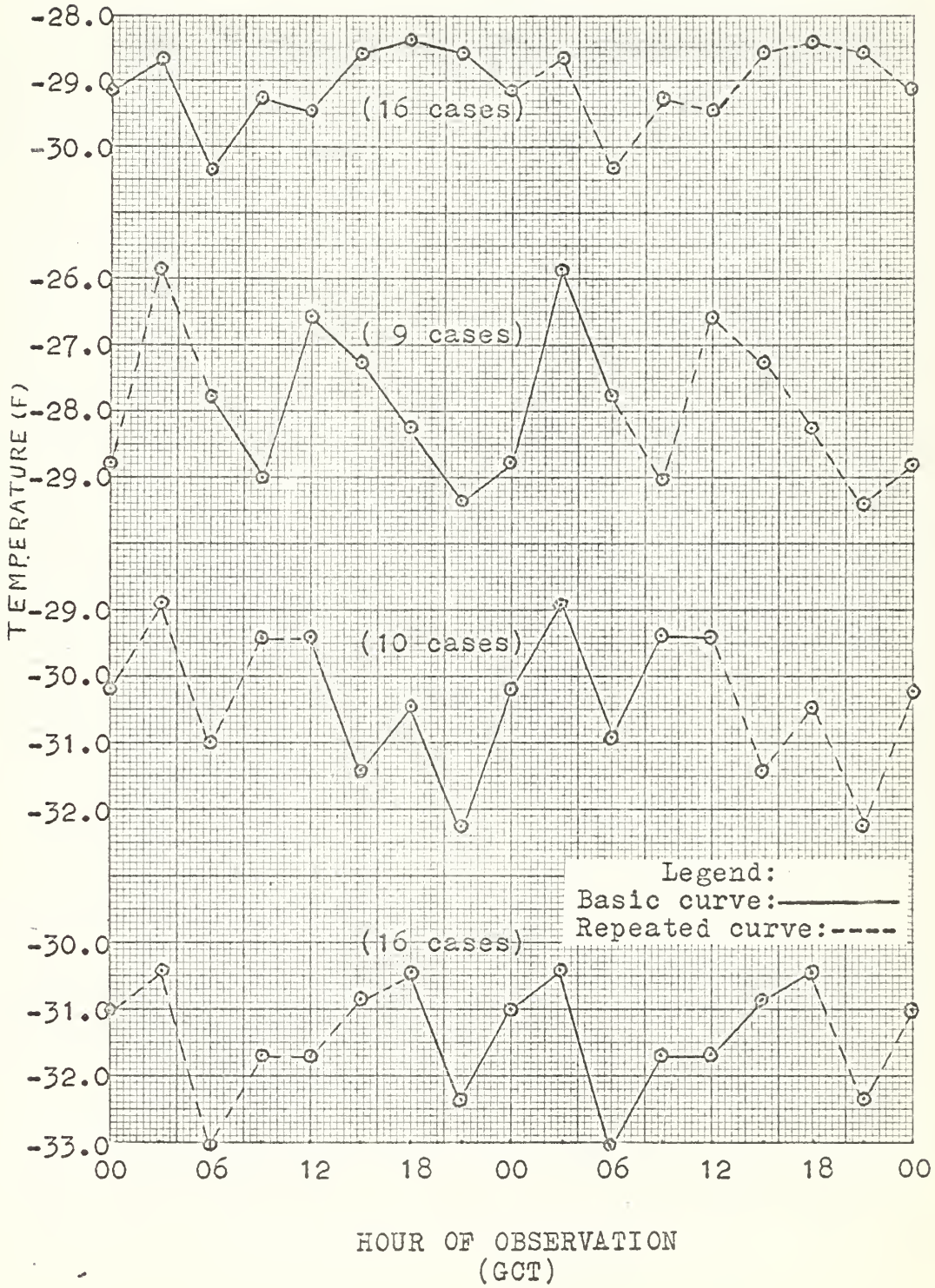

Figure 11: Comparison of the total temperature variation with the meteorological and the statistical bias variations.
(wind speed ≤ 5 kt; cloudiness ≤ 5/10)

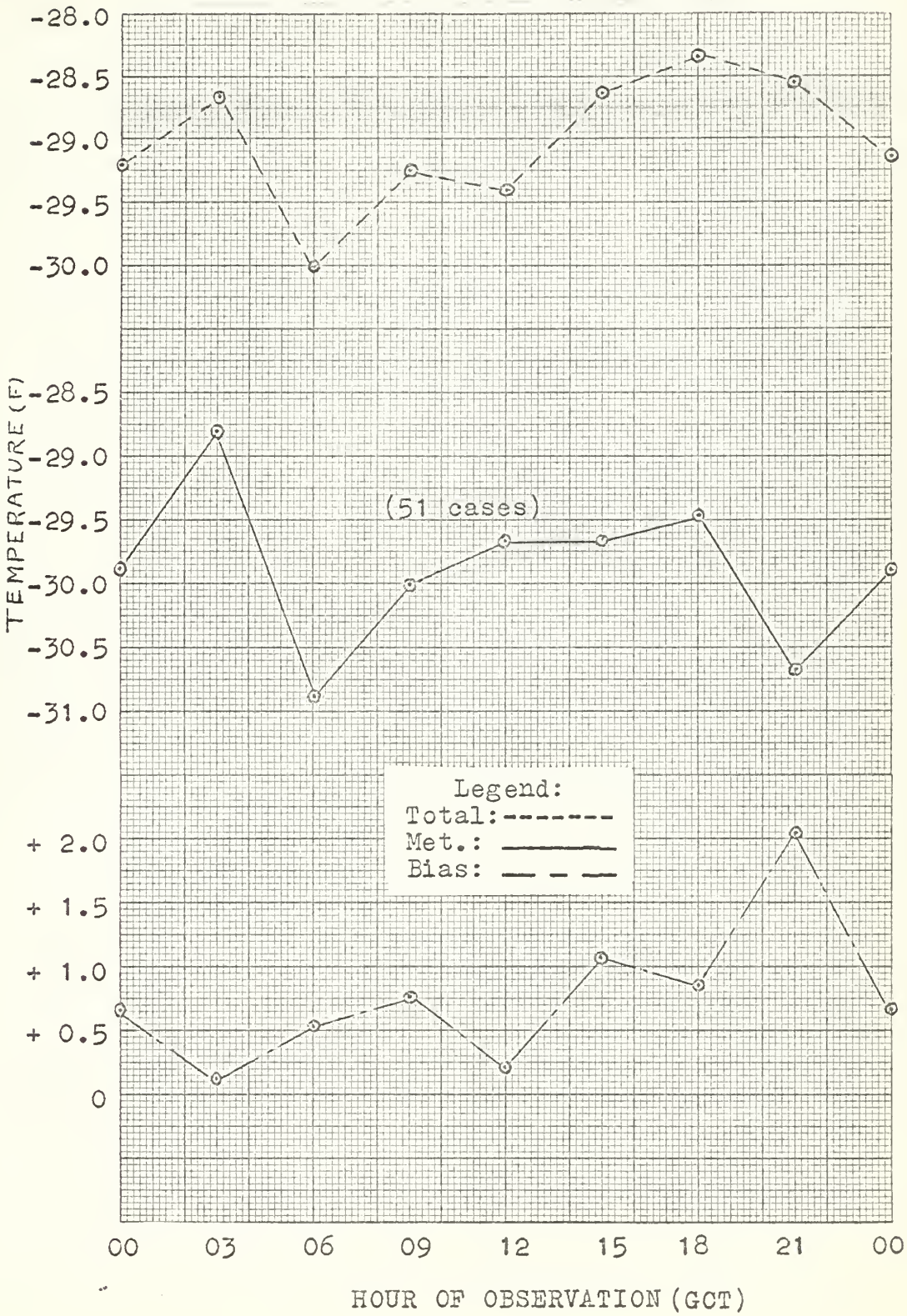

Figure 12: Total temperature variation curves with variation in starting time of the period. (wind speed ≤ 4 kt; cloudiness ≤ 5/10)

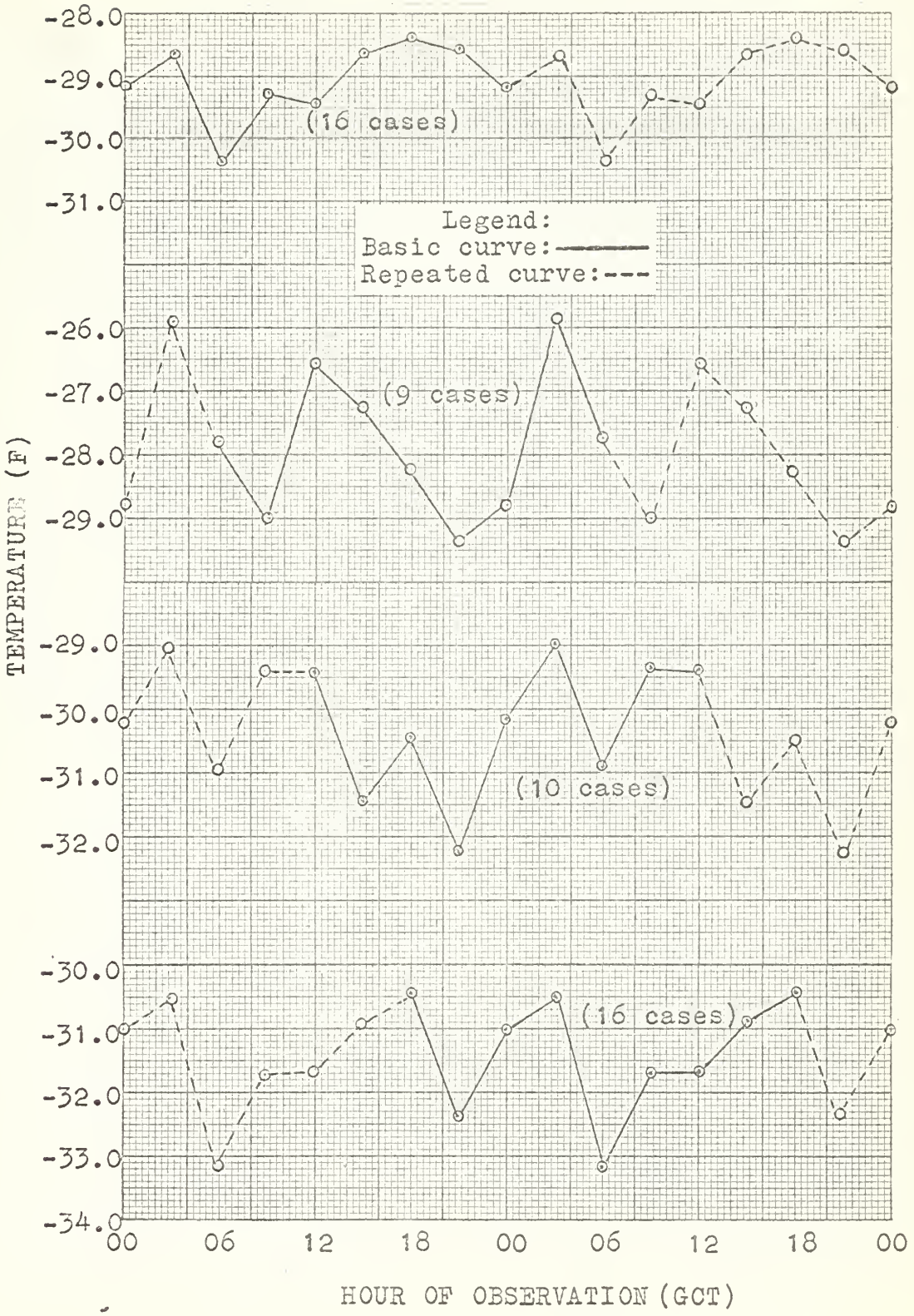

Figure 13: Comparison of the total temperature variation with the meteorological and statistical variations.

(wind speed ≤ 4 kt; cloudiness ≤ 5/10)

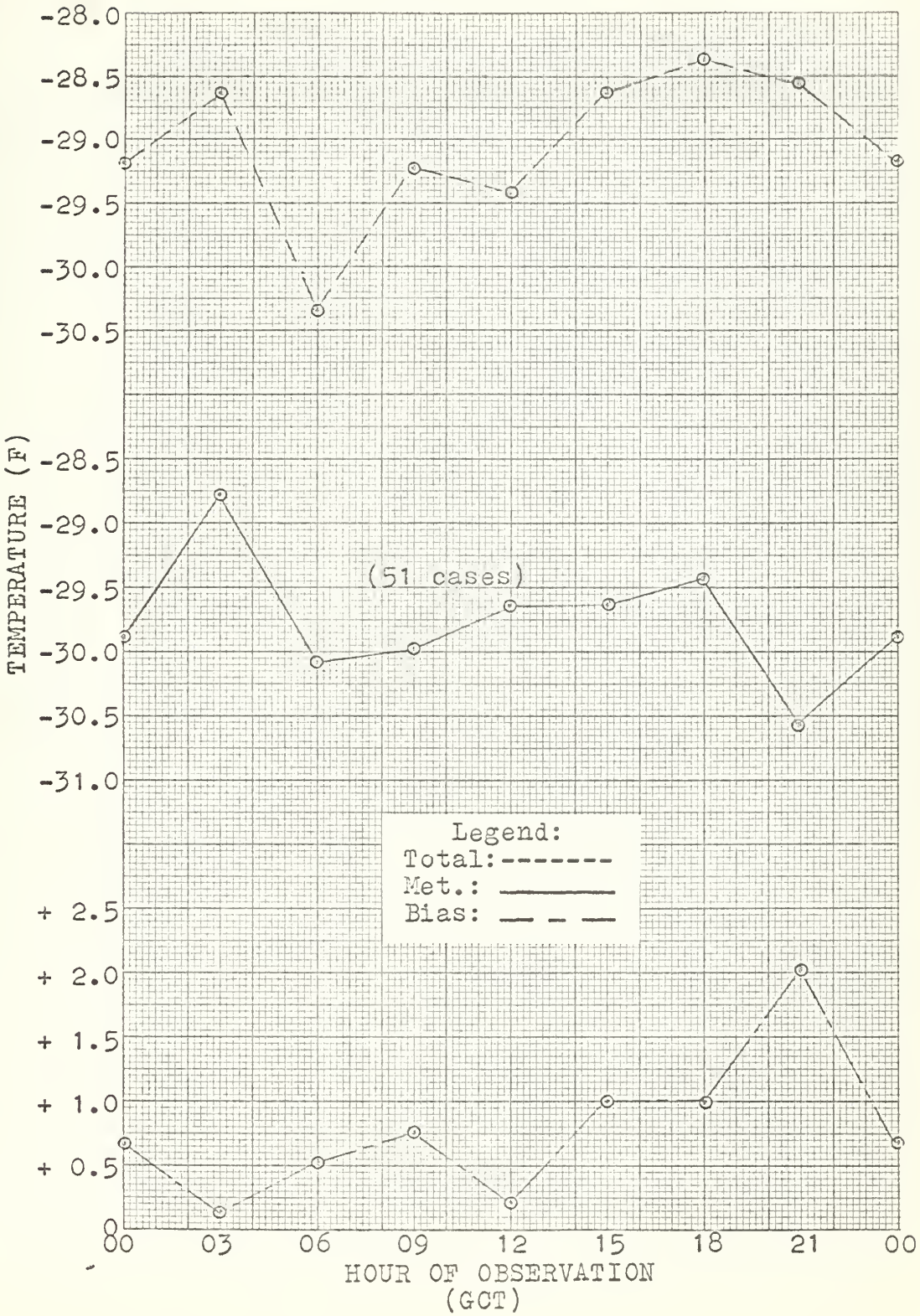

Figure 14: Total temperature variation curves with variation in starting time of the period. (wind speed ≤ 3 kt; cloudiness ≤ 5/10)

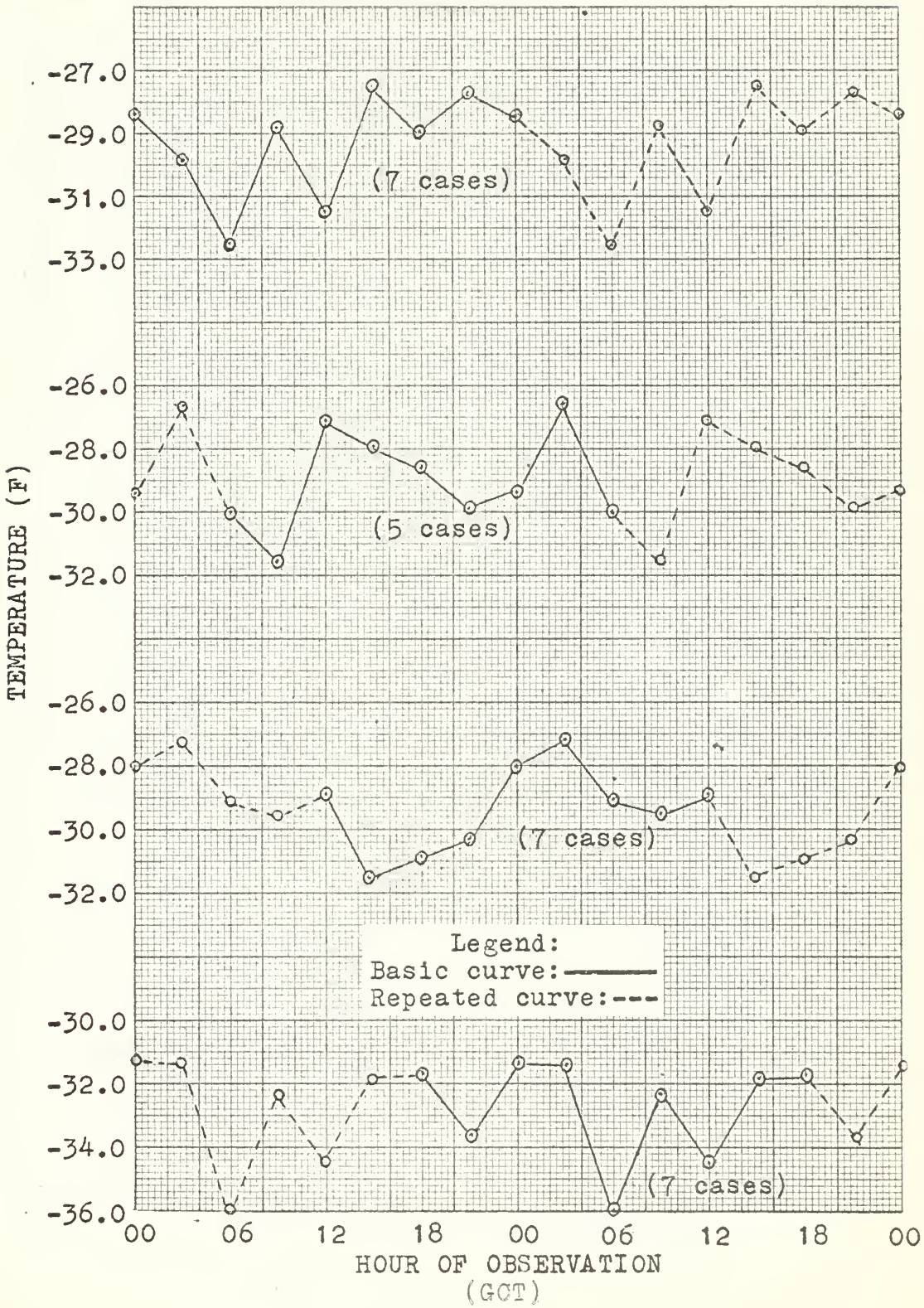

Figure 15: Comparison of the total temperature variation with the meteorological and statistical bias variations.

(wind speed ≤ 3 kt; cloudiness ≤ 5/10)

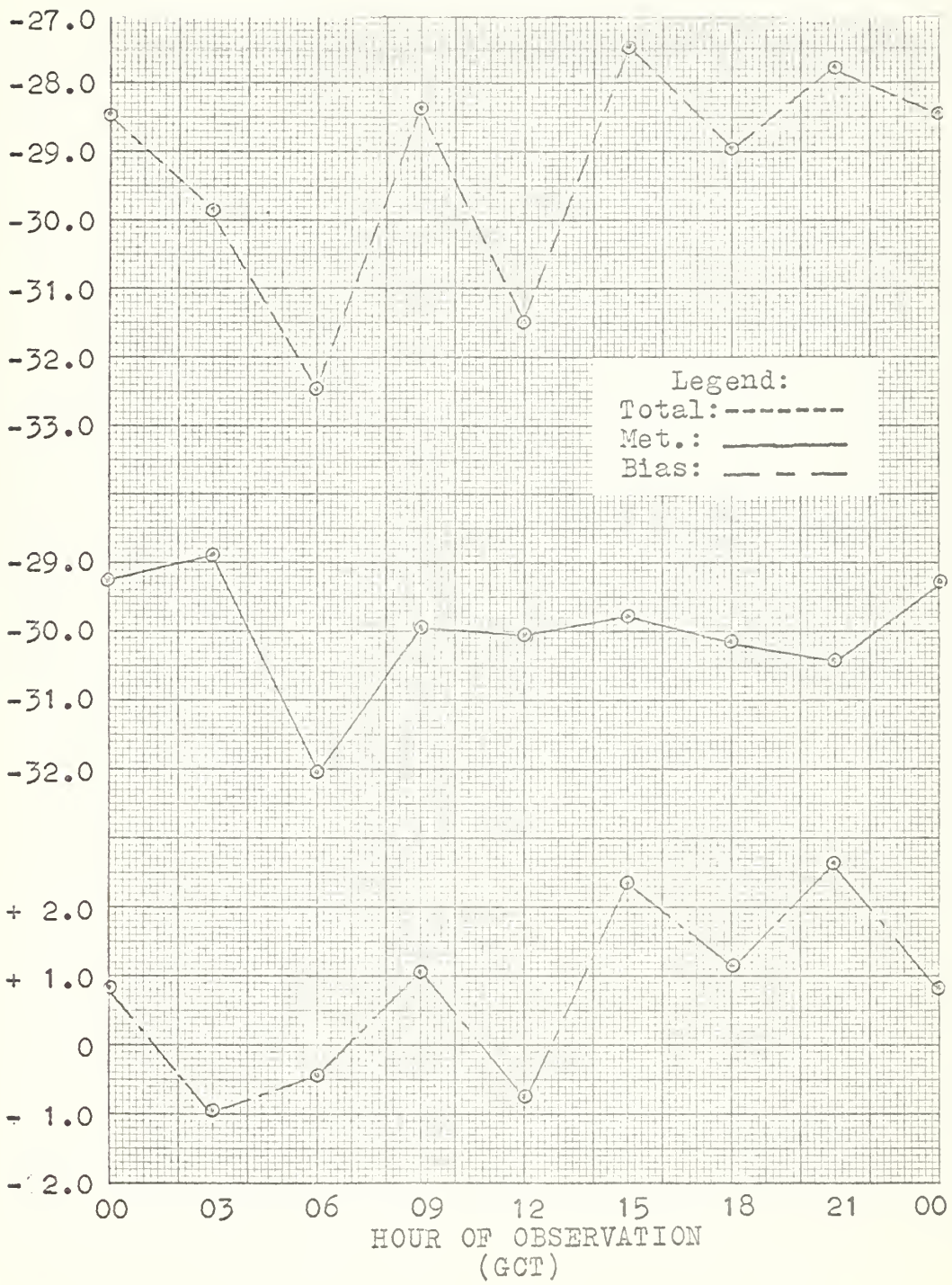

Figure 16: Total temperature variation curves with variation in starting time of the period. (wind speed ≤ 2 kt; cloudiness ≤ 5/10)

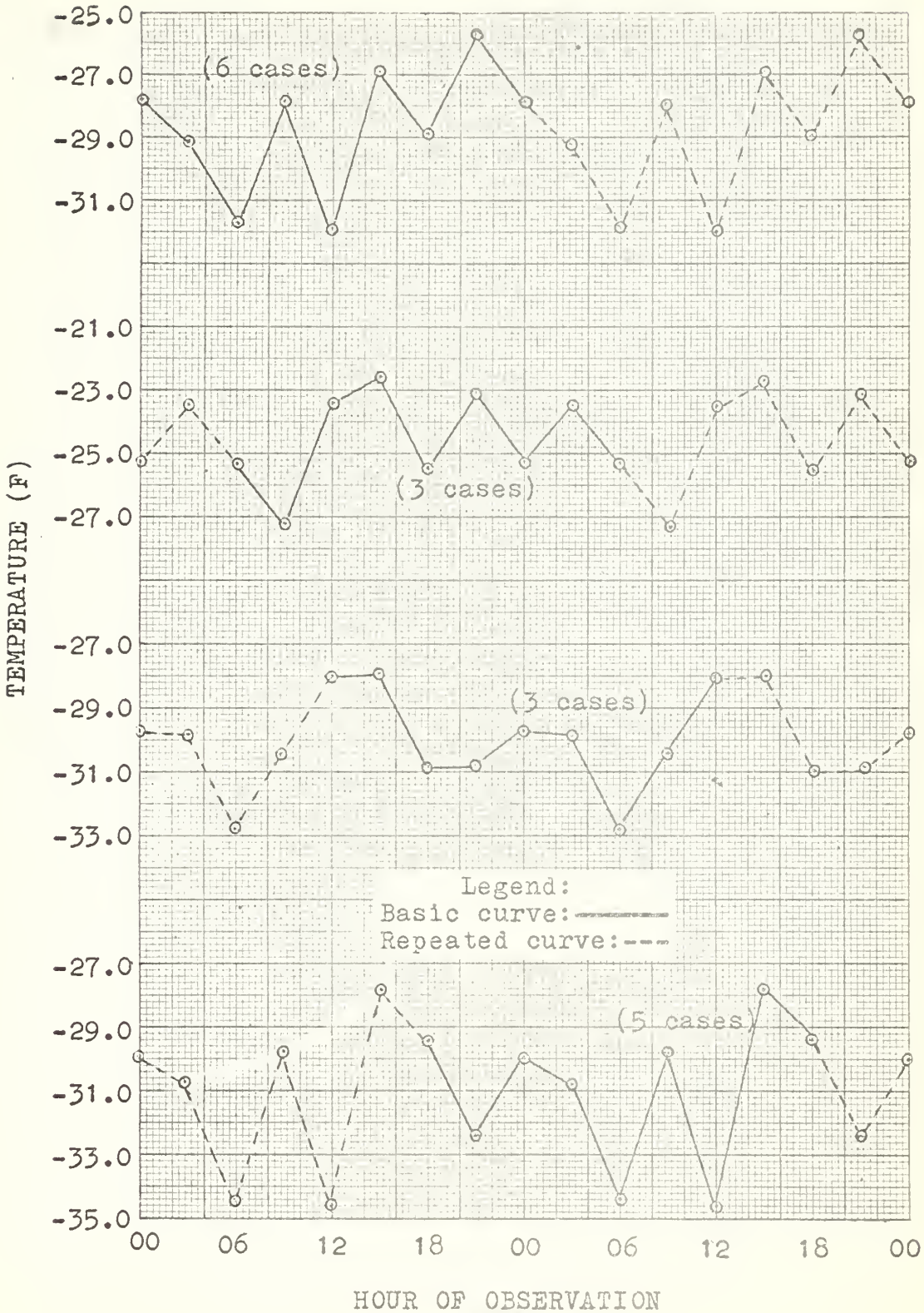

Figure 17: Comparison of the total temperature variation with the meteorological and the statistical bias variations.
(wind speed ≤ 2 kt; cloudiness ≤ 5/10)

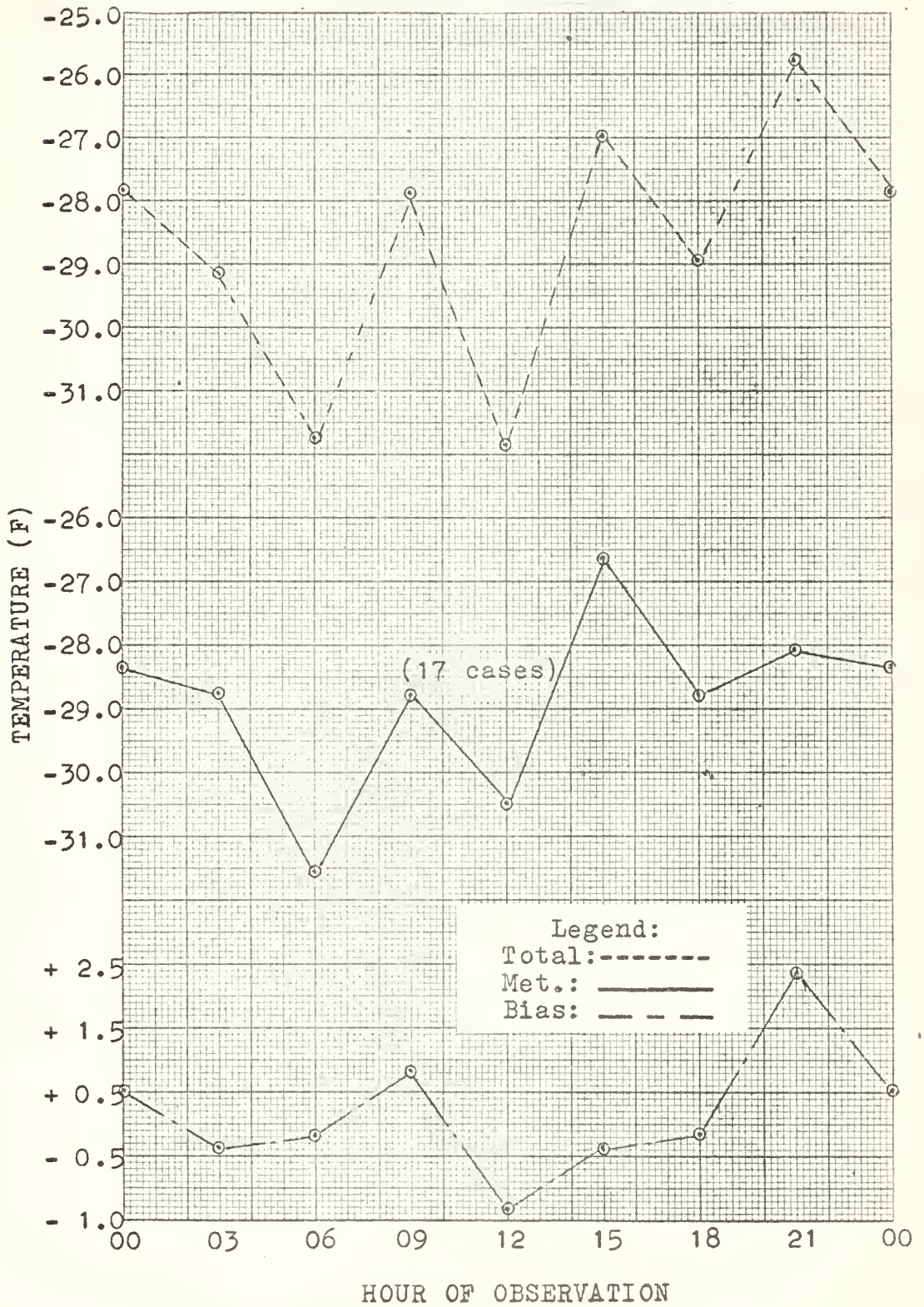

Figure 18: Total temperature variation curves with variation in starting time of the period. (wind speed = 0 kt; cloudiness = 5/10)

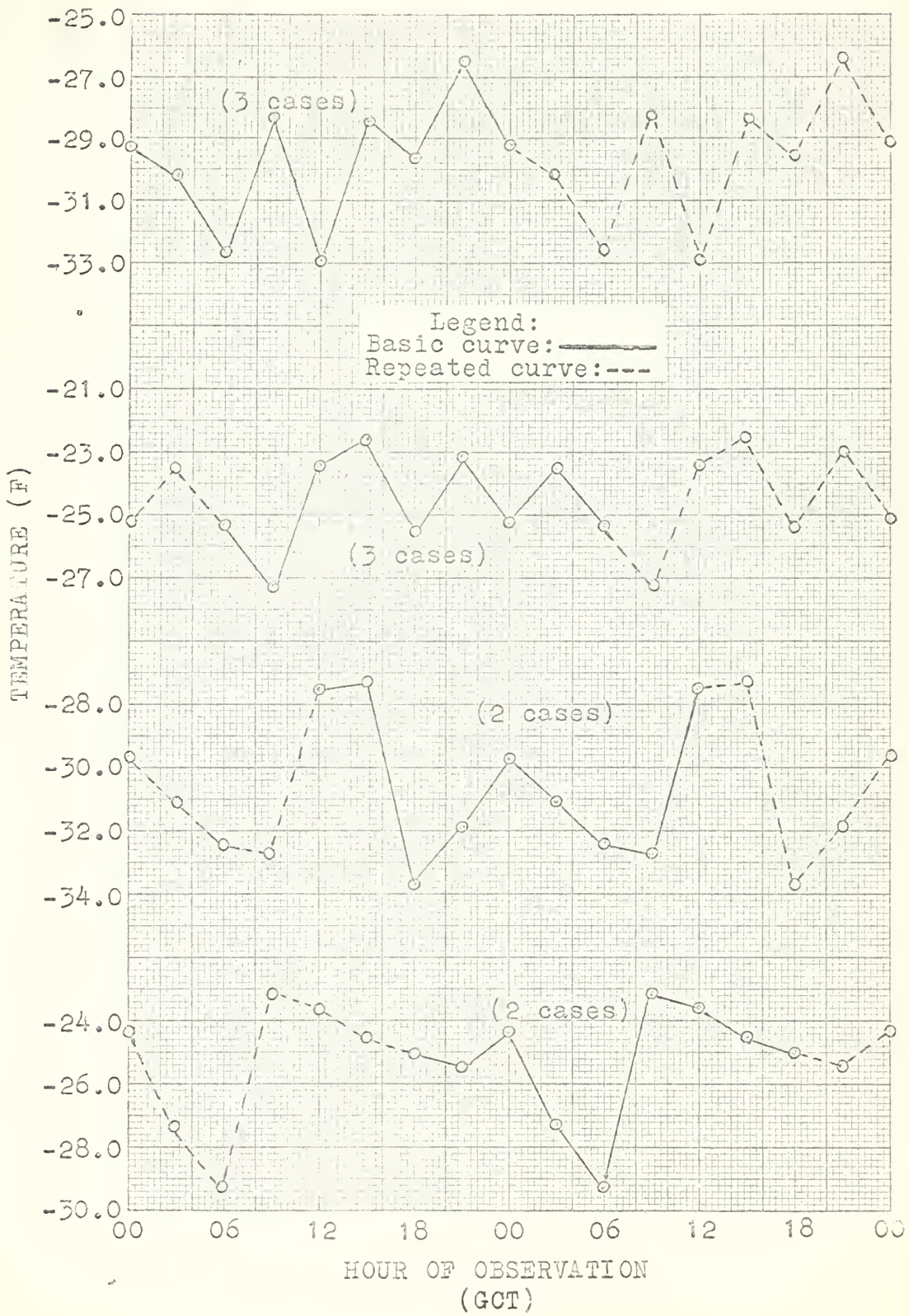

Figure 19: Comparison of the total temperature variation with the meteorological and the statistical bias variations.
(wind speed = 0 kt; cloudiness=5/10)

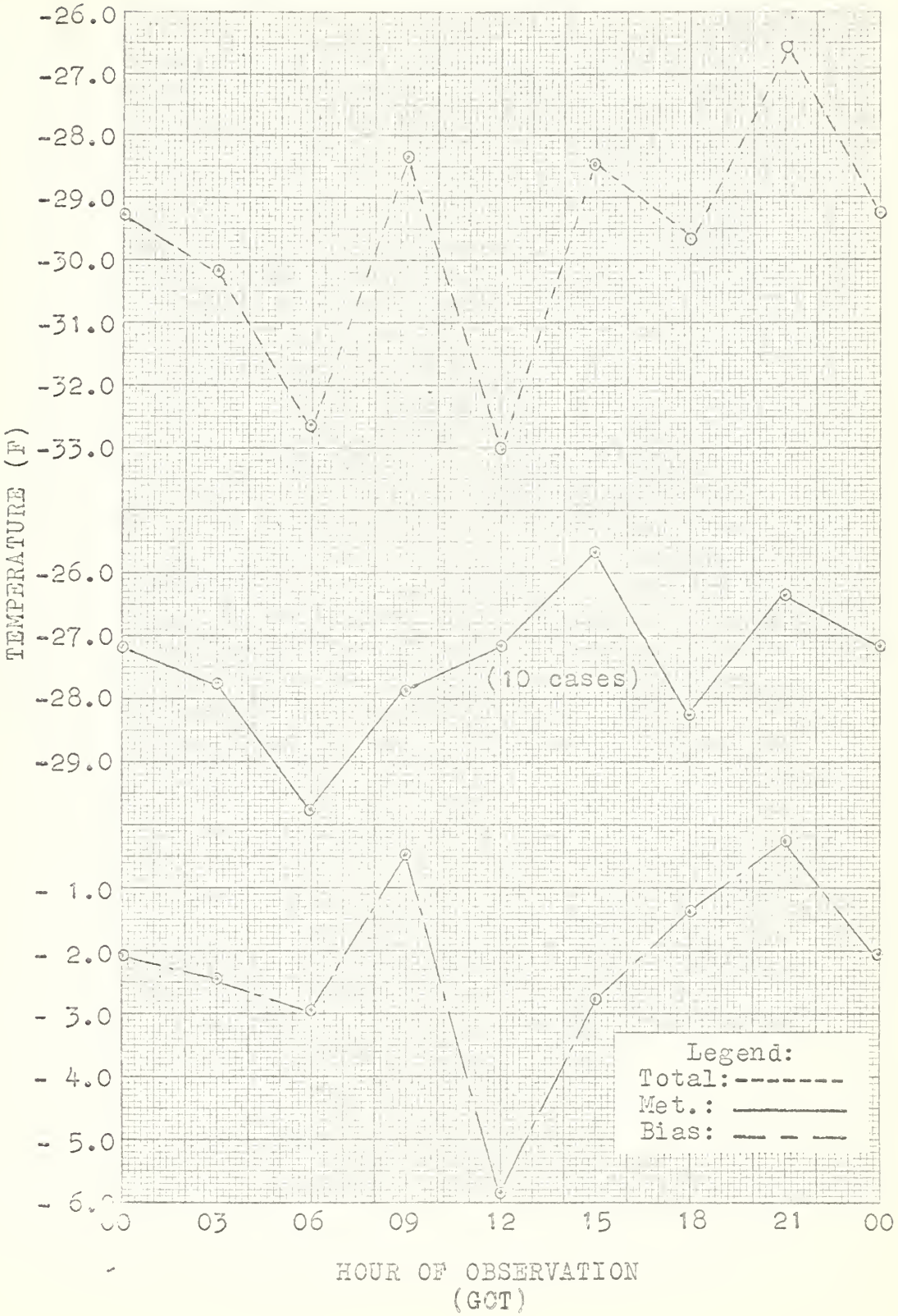

Figure 20: Total temperature variation curves with variation in starting time of the period. (wind speed = 0 kt; cloudiness = 0)

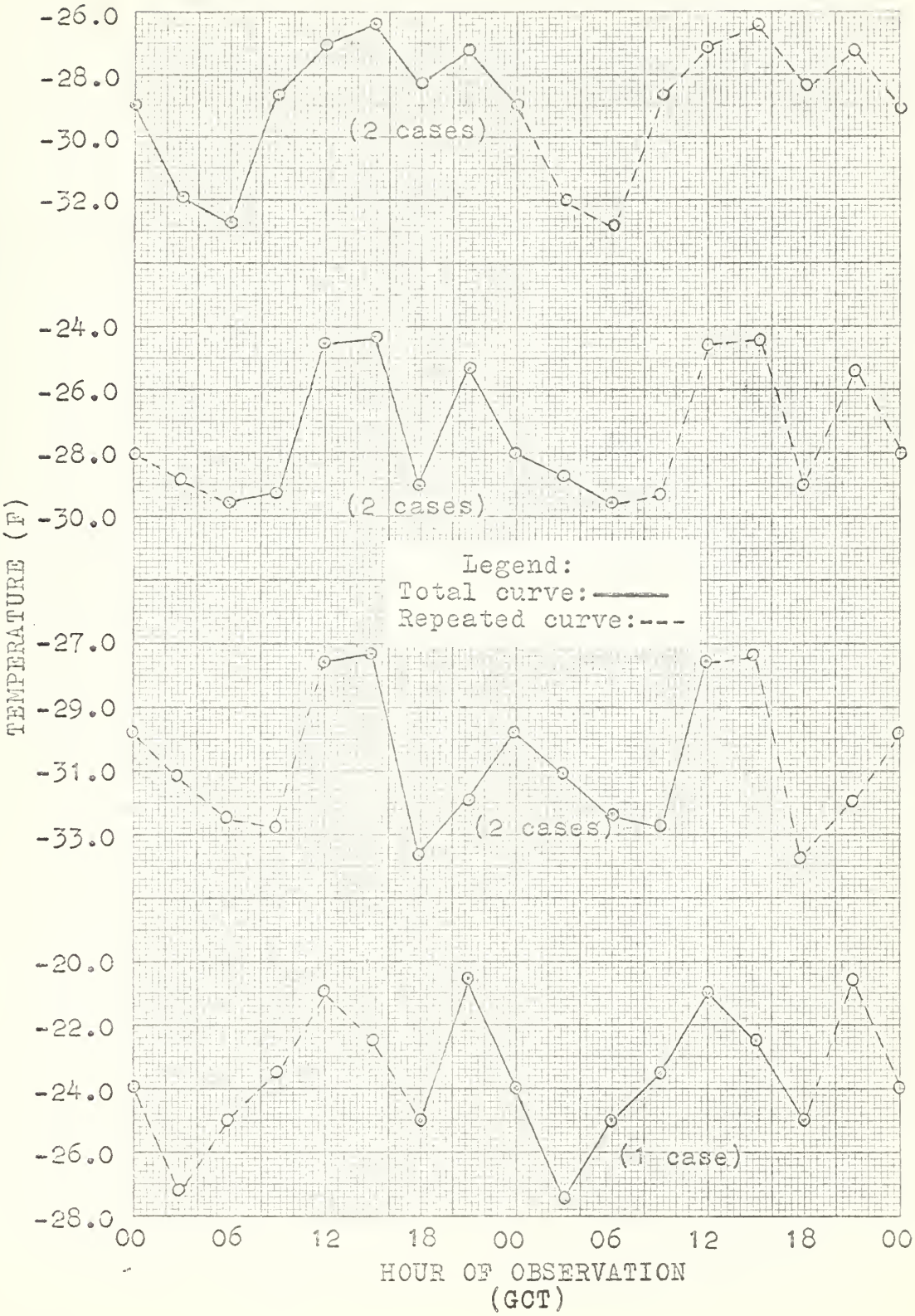

Figure 21: Comparison of the total temperature variation with the meteorological and the statistical bias variations.
(wind speed = 0 kt; cloudiness = 0)

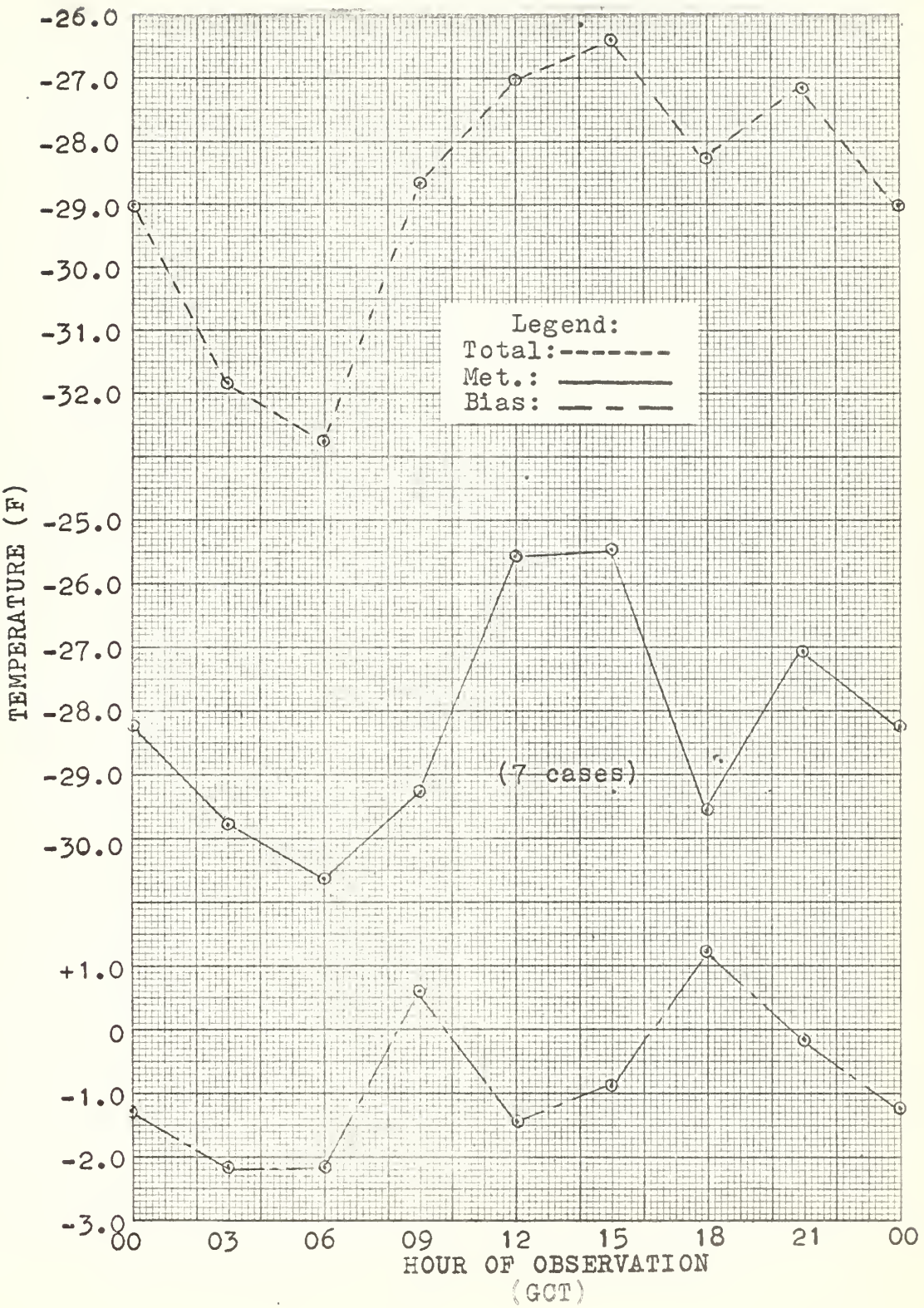

Figure 22: Total temperature variation curves with variation in starting time of the period. (2 kt $\leq$ wind speed $\leq$ 15 kt; cloudiness $\leq$ 5/10)

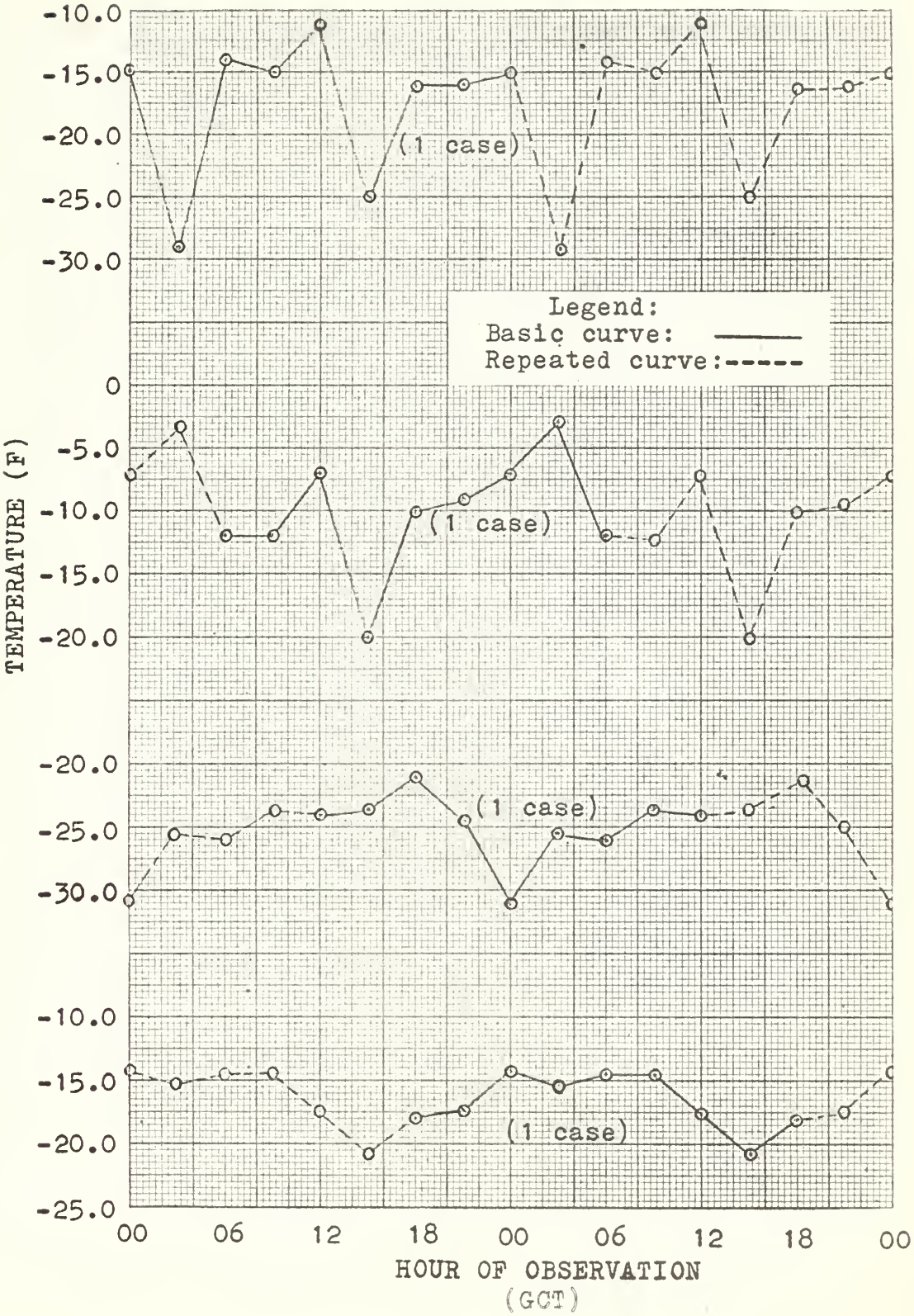

Figure 23: Comparison of the total temperature variation with the meteorological and the statistical bias variations.
(2 kt ≤ wind speed ≤ 15 kt; cloudiness ≤ 5/10)

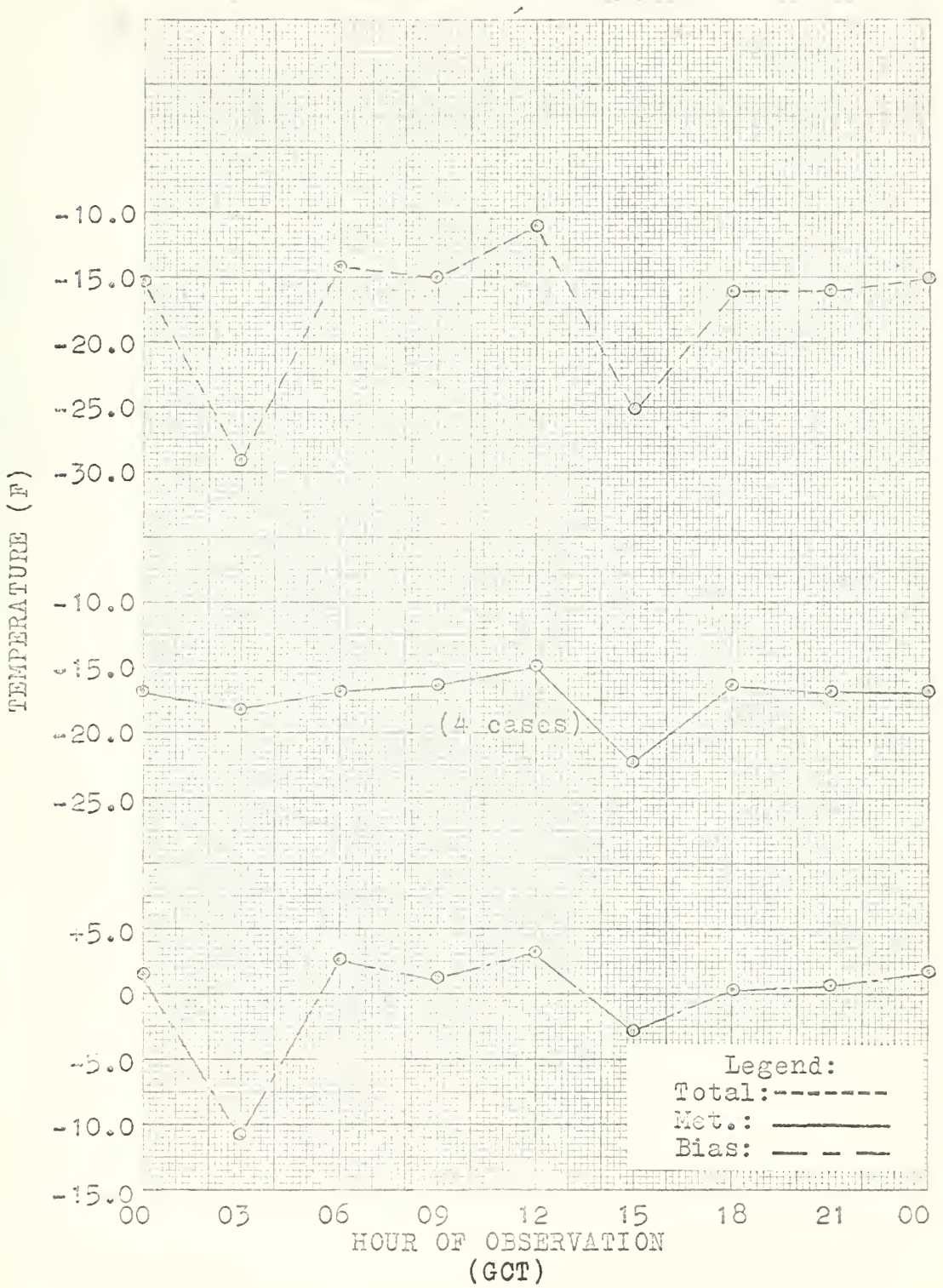

Figure 24: Total temperature variation curves with variation in starting time of the period. (wind speed ≤15 kt; cloudiness ≤10/10)

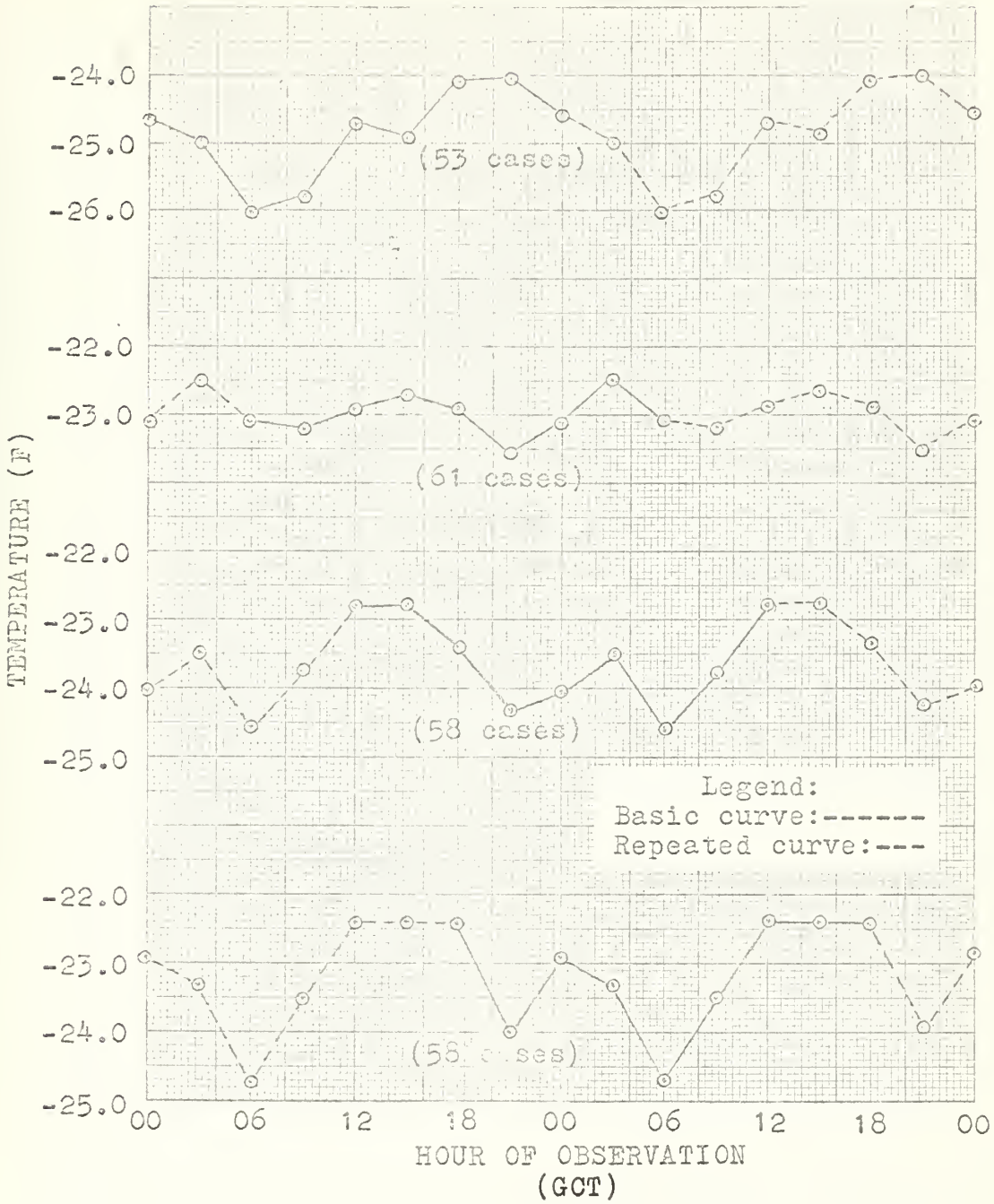

Figure 25: Comparison of the total temperature variation with the meteorological and statistical variations.

(wind speed ≤ 15 kt; cloudiness ≤ 10/10)

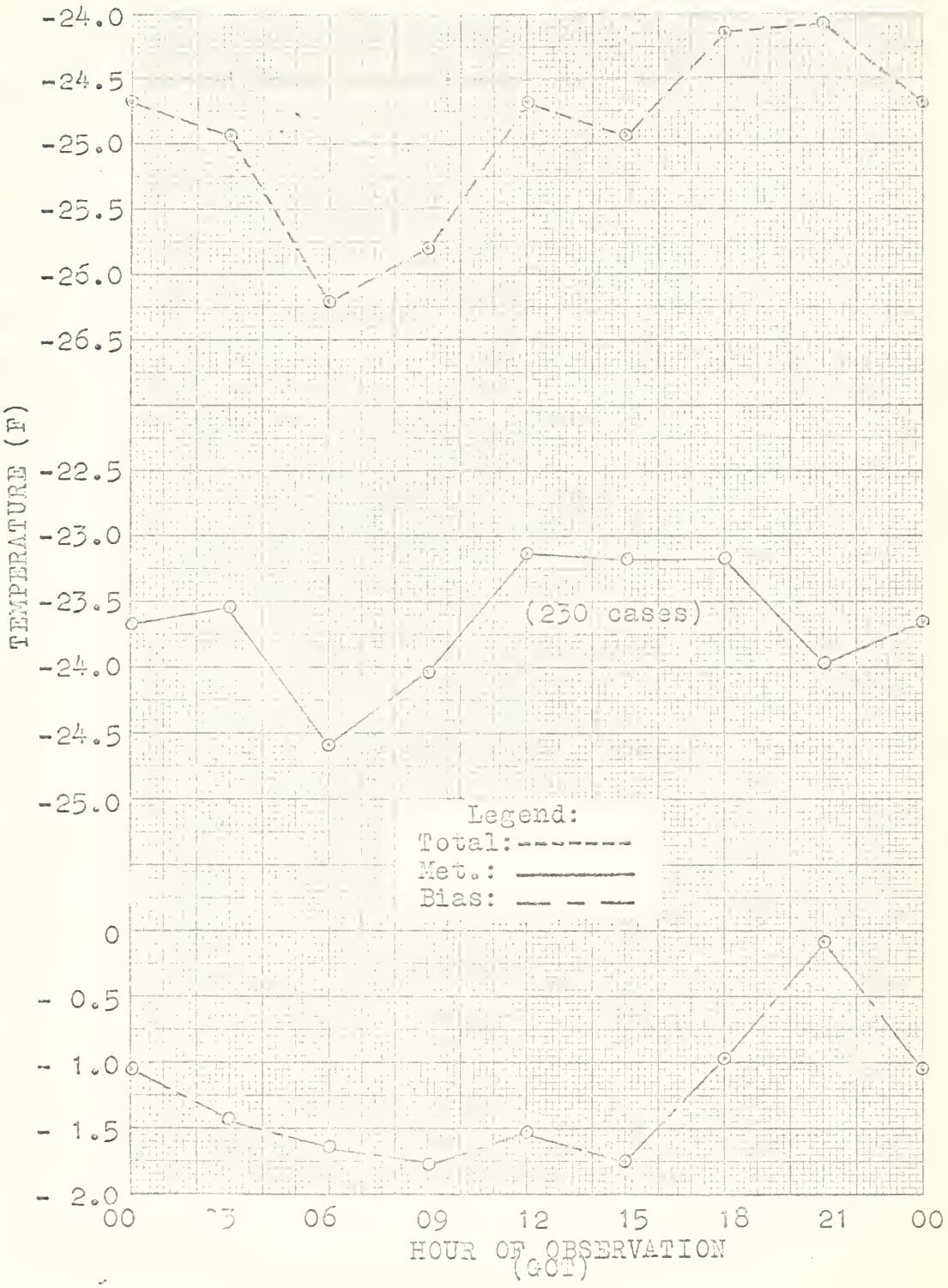

8. 48-hour temperature variation

As previously mentioned, the purpose of the 48-hour temperature variation analysis is to examine whether the statistical bias occurs for periods other than 24 hours. The results of this analysis are presented graphically in figures 26 through 30.

Figure 27 clearly shows an effect of statistical bias. For this figure the selection criteria were windy and/or cloudy periods, which, according to Hisdal, should have their highest temperatures near the middle of the period. This is what actually occurred, but only five 48-hour periods met the specified selection criteria.

In figure 29, a total of 39 periods met the criteria, but the actual results are inconsistent with those expected. According to the discussion of section 1, for days with wind speed less than or equal to 15 knots and cloudiness less than or equal to five-tenths the temperature trend should be concave in shape. In figure 29, the statistical bias is convex. This departure from *a priori* expectation may be due to the random variations included in the total temperature curve, from which the bias was deduced. This idea is treated more thoroughly in section 11.

The last figure in the 48-hour set, figure 30, illustrates the mean 48-hour temperature variation which results when no particular selection criteria are specified. In theory these curves should have negligible statistical bias, considering the discussion in section 1. This theory is essentially borne out

in figure 30, where the mean meteorological variation, obtained by the column averaging method, is very nearly the same as the total variation. Thus, upon subtraction of the meteorological from the total variation, the resulting statistical bias does not appear significantly different from zero.

It should be noted that the conclusion of a zero bias through such a procedure is complicated by end effects due to different starting times. For example, the first two three-hourly temperatures used in computing the 0000 GCT to 0000 GCT mean curve are not included in the 0600 GCT to 0600 GCT curve. Likewise, the last two temperatures in the 0600 GCT to 0600 GCT curve are not included in the 0000 GCT to 0000 GCT curve.

Figure 26: 48-hour temperature variation curves with variation in starting time of the period.
(wind speed ≥15 kt; cloudiness ≥5/10)

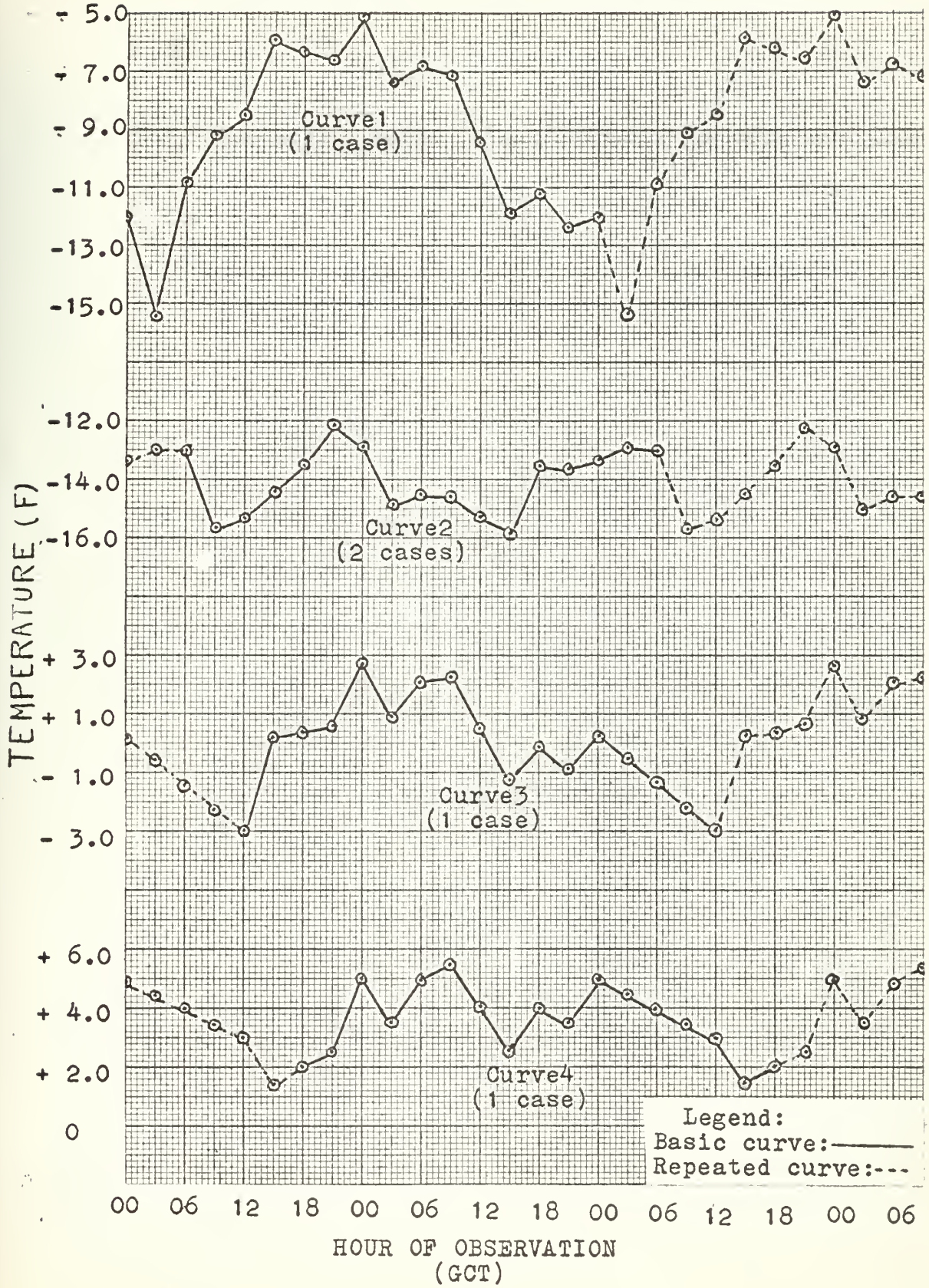

Figure 27: Comparison of the total 48-hour temperature variation with the meteorological and statistical bias variations.

(wind speed ≥ 15 kt; cloudiness ≥ 5/10)

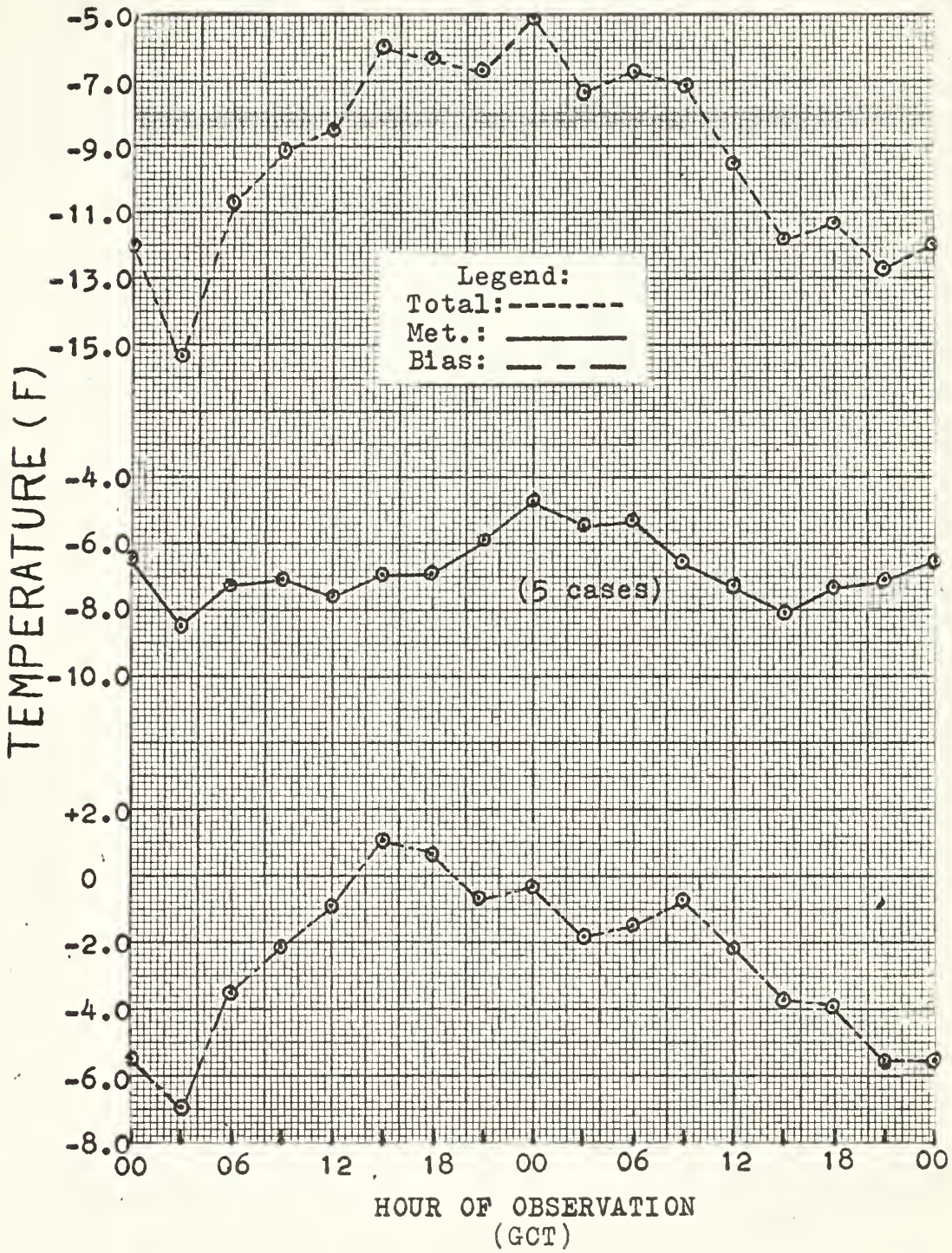

Figure 28: 48-hour temperature variation curves with variation in starting time of the period. (wind speed ≤ 15 kt; cloudiness ≤ 5/10)

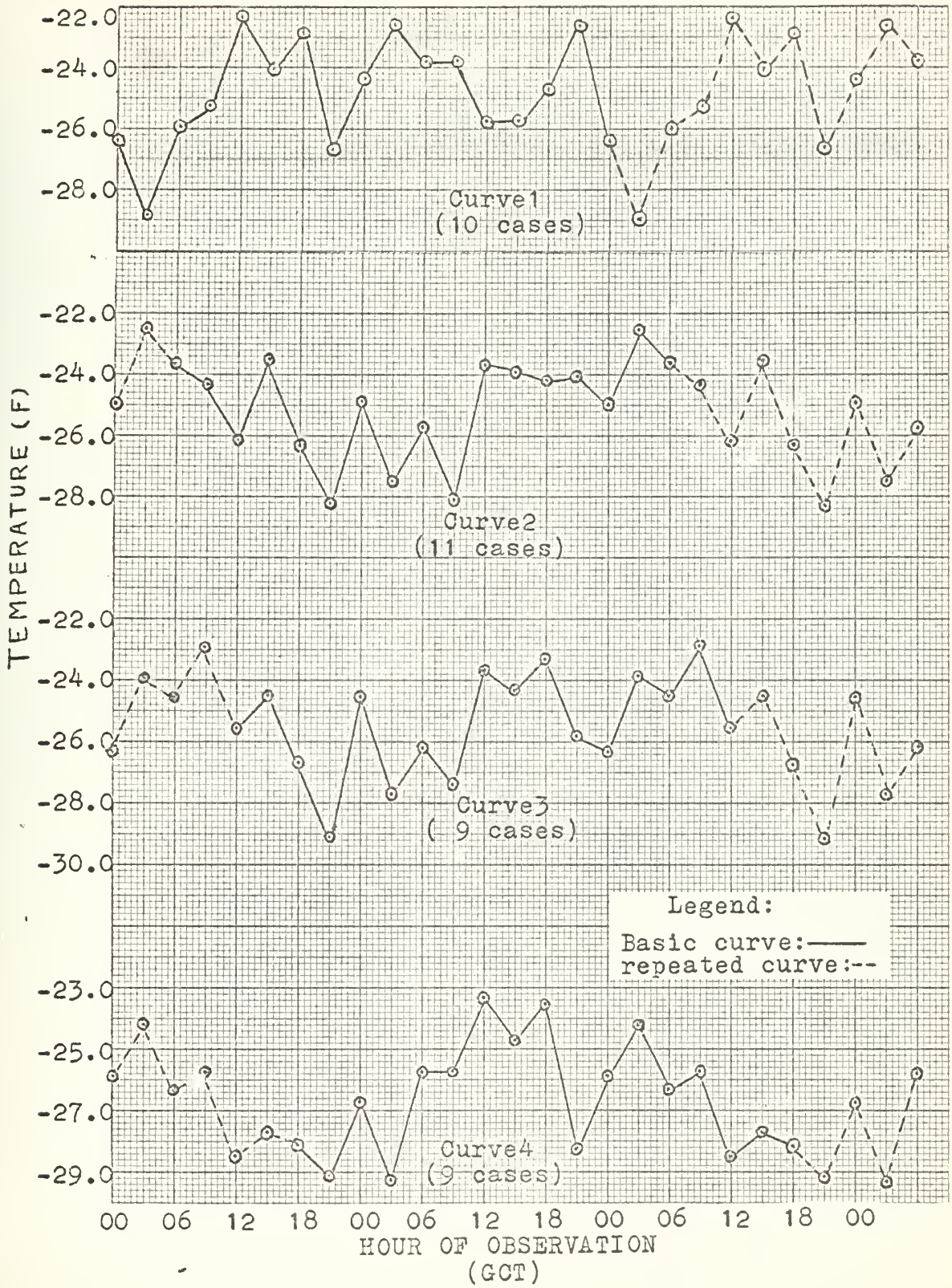

Figure 29: Comparison of the total 48-hour temperature variation with the meteorological and statistical bias variation.

(wind speed ≤ 15 kt; cloudiness ≤ 5/10)

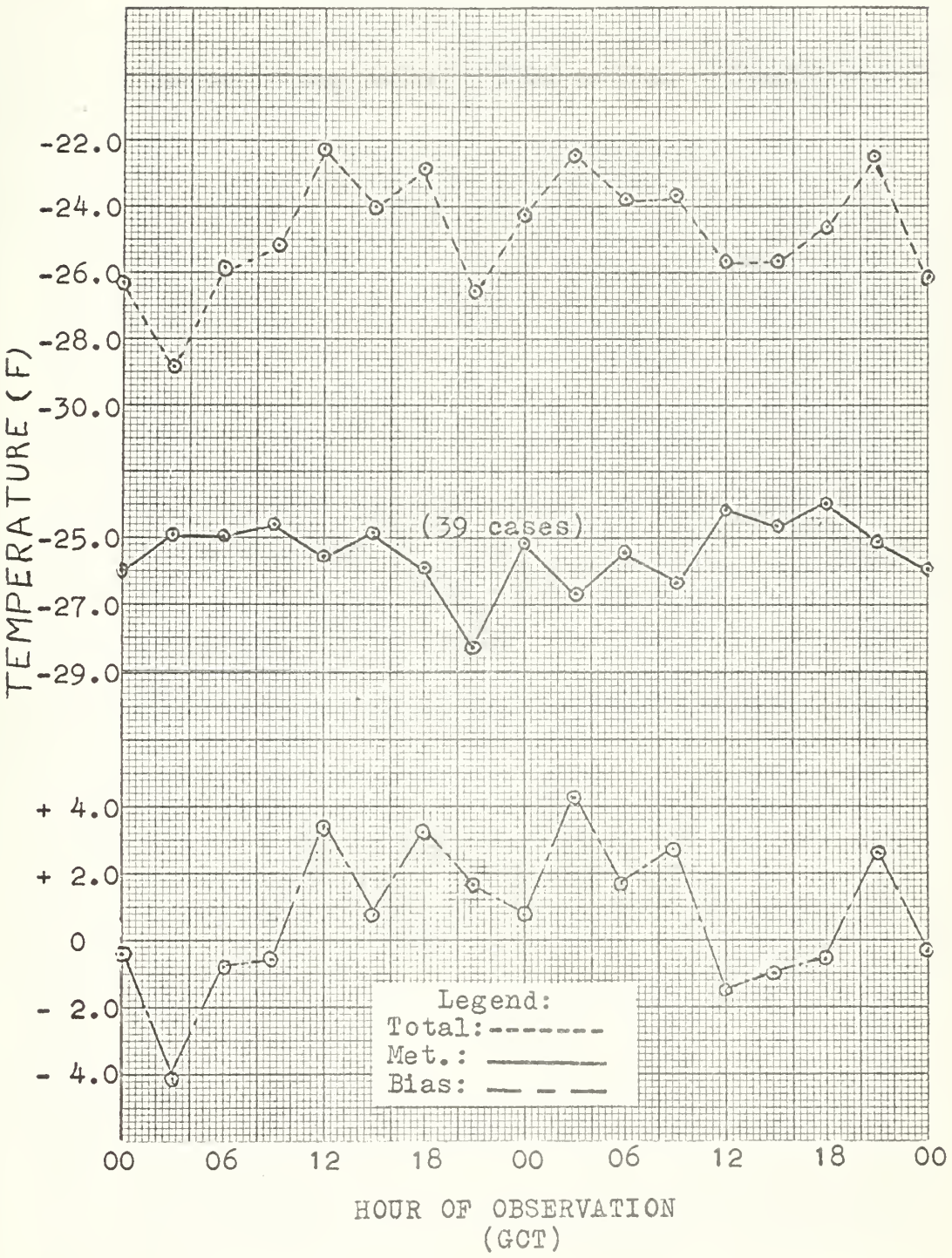

Figure 30: 48-Hour temperature variation curves with variation in starting time of period (for all observations, regardless of windspeed and cloud amount).

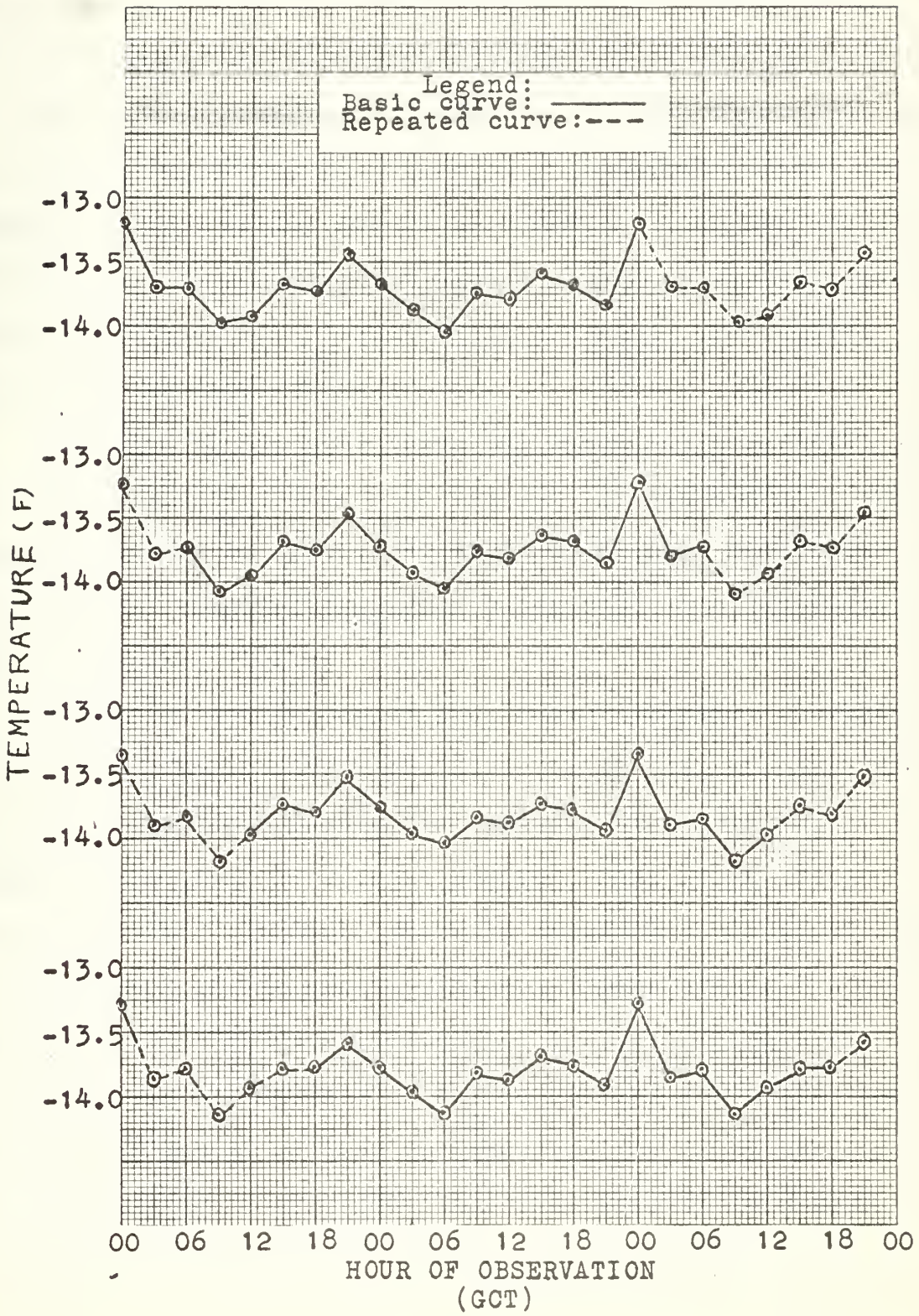

9. 18-hour and 72-hour temperature variations

As with the 48-hour temperature variation, the purpose for studying the 18-hour and 72-hour variations is to demonstrate that a statistical bias effect is not limited to a 24-hour period.

The 18-hour temperature variation curves, figures 31 and 32, clearly depict the existence of a statistical bias. In principle, these curves should be concave, since the criteria specified are wind speed less than or equal to 15 knots and cloudiness less than or equal to five-tenths. The actual curves are, in fact, concave.

In figure 32 the meteorological temperature variation and the statistical bias have been computed by means of the two schemes proposed in section 4; that is, by both the column-averaging and diagonal-averaging processes. The resulting curves are quite similar.

Figures 33 and 34 depict the 72-hour temperature variation curves. These curves are designed to test the hypothesis that the statistical bias effect exists for considerably longer periods than 24 hours. However, they do not support this hypothesis. In fact, there is evidence of an upper limit for the length of the period yielding a bias effect. A possible explanation for this limitation is that the physical mechanism causing the type of day to persist for a long period remains long enough so that the observations on either side of the selected period also meet the criteria. If this were the case, no statistical bias would be evidenced.

A further investigation is necessary in order to determine which synoptic situations at Antarctica are associated with long sequences of similar days.

One difficulty which arises in studying a period as long as 72 hours is that the number of periods meeting the criteria are relatively few. Thus, the statistical significance is greatly reduced compared to that of shorter periods.

Figure31: 18-hour temperature variation curves with variation in starting time of the period.

(wind speed≤15 kt; cloudiness≤5/10)

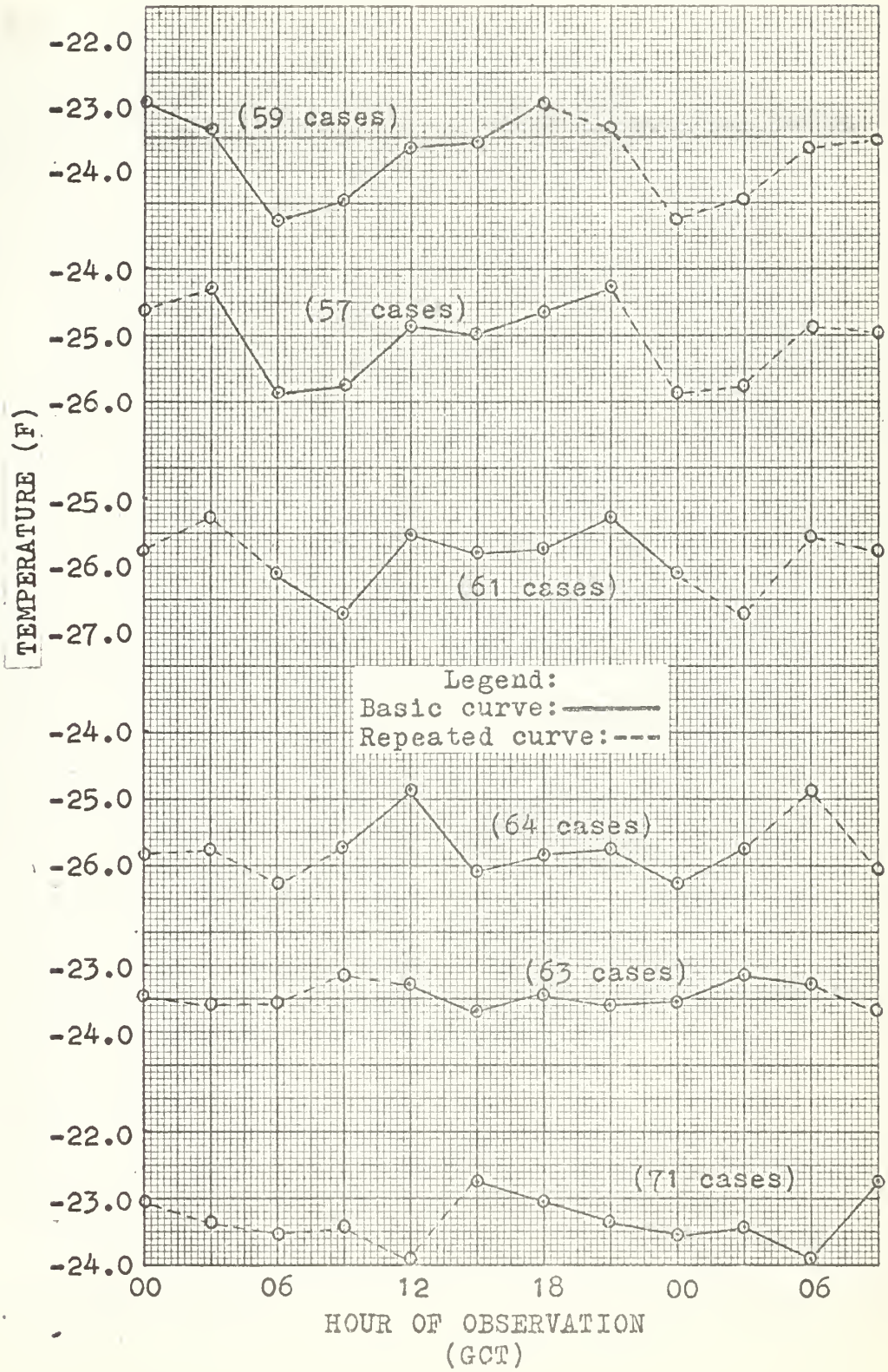

Figure 32: Comparison of the total 18-hour temperature variation with the meteorological and statistical bias variations.

(wind speed ≤15 kt: cloudiness ≤5/10)

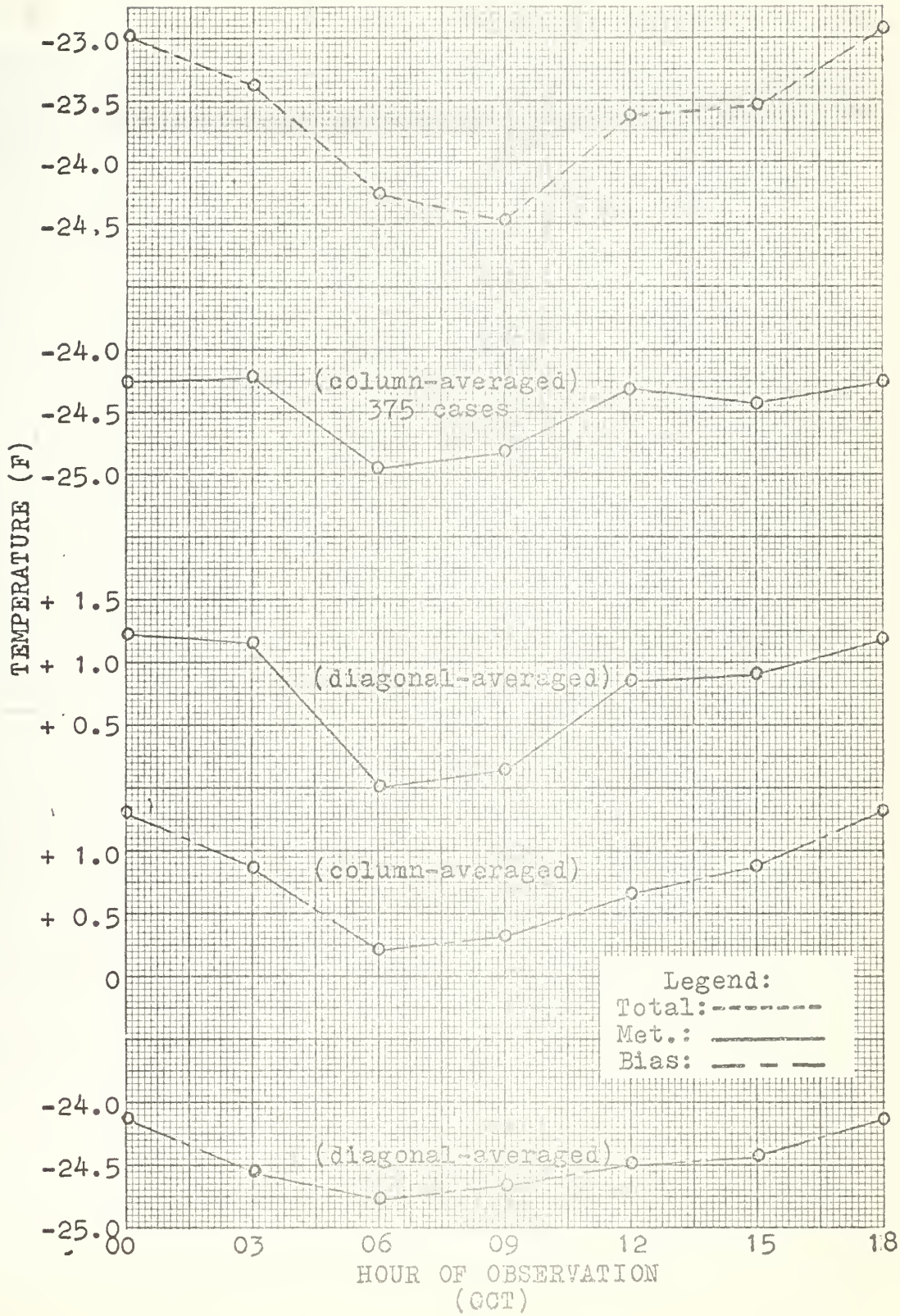

Figure 33: The 72-hour temperature variation with variation in starting time of the period. (wind speed≤15 kt; cloudiness≤5/10)

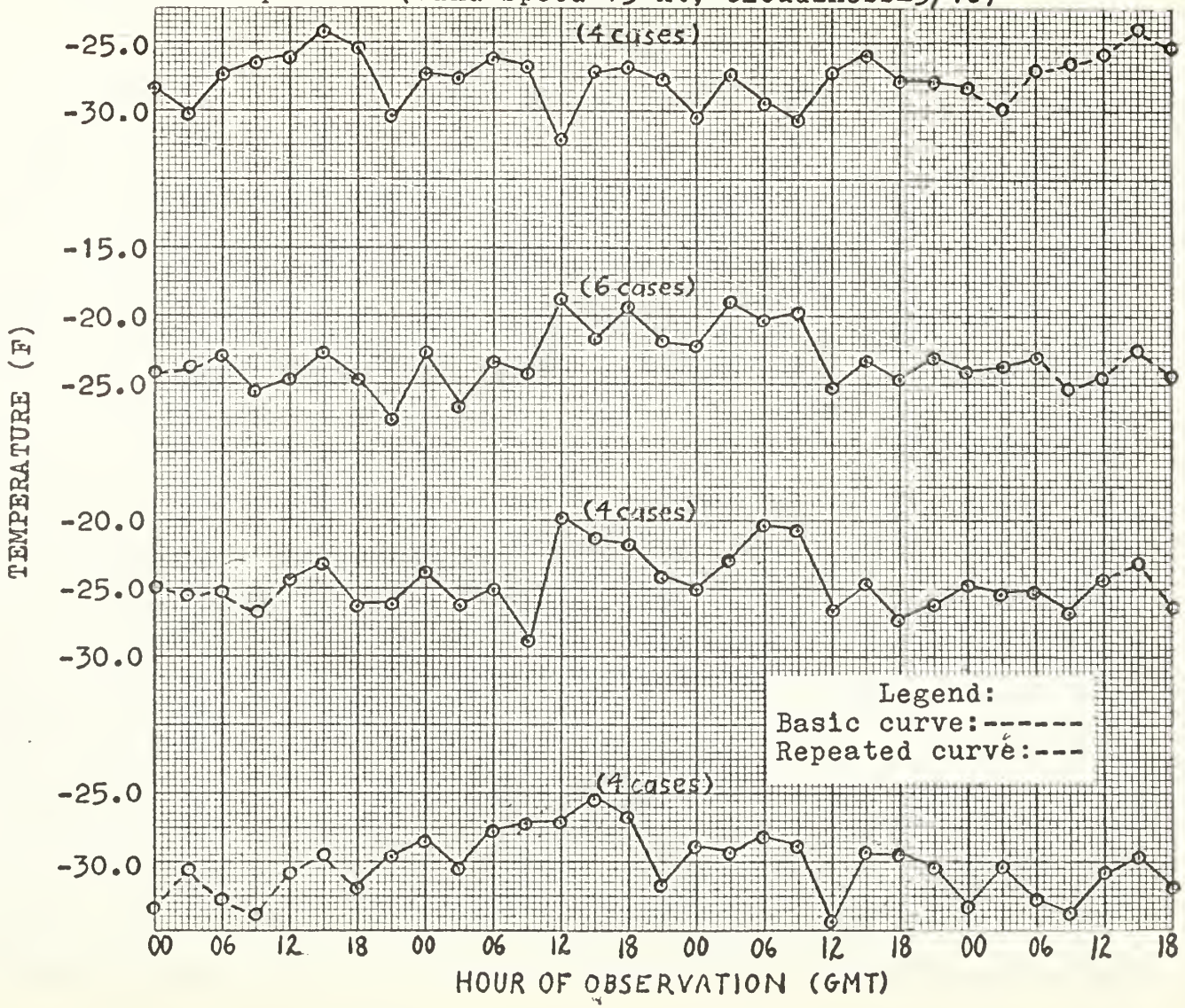

Figure 34: Comparison of the total 72-hour temperature variation with the meteorological and statistical bias variations.

(wind speed ≤ 15 kt; cloudiness ≤ 5/10)

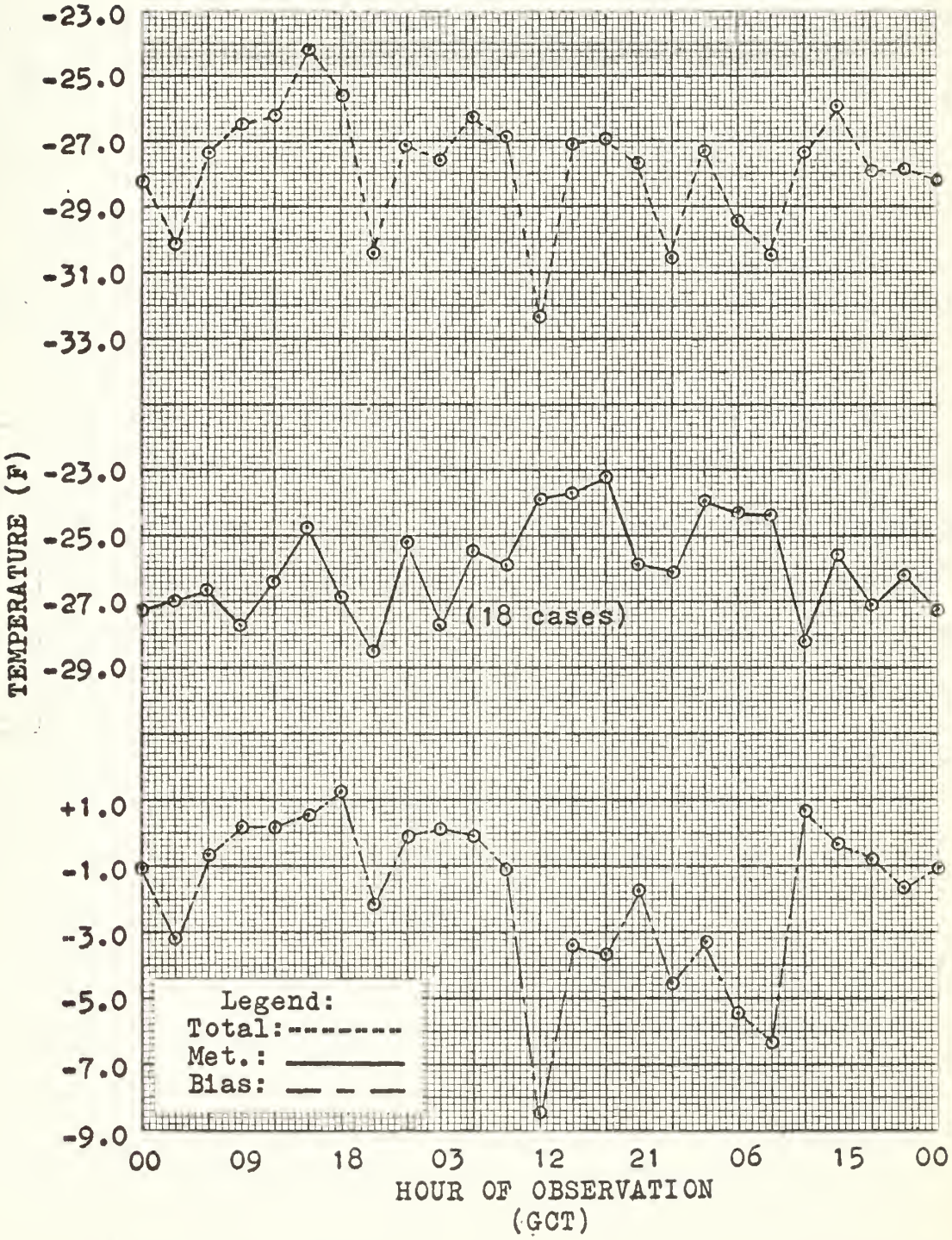

10. The diurnal temperature variation, based upon all observations 1956 - 1961

Figure 35 is a chart of mean diurnal or meteorological temperature variation curves, based on all three-hourly surface observations at McMurdo Sound, during the dark season, for the years 1956 through 1961. The first six of these curves are annual means, based on observations of 93 days. The last curve is the six-year mean diurnal variation, based upon 558 days.

Since no selection criteria were specified for these mean curves, each represents a diurnal temperature variation, that is, one free from statistical bias.

There are two pronounced features of the six-year mean curve. The first is the temperature maximum occurring at 1500 GCT. This maximum, however, may have no particular significance, since it is caused, in part, by the abnormally high 1500 GCT mean temperature which occurred in 1956. Moreover, during the years 1958 through 1961, there is a minimum value at 1500 GCT.

The second feature of the six-year mean diurnal temperature variation curve is the maximum occurring at 0000 GCT. This appears to be a regularly occurring phenomenon, at least for the years included in this study.

In order to discover a possible explanation for the 0000 GCT maximum, the diurnal variations of some other meteorological parameters were plotted in figures 36 through 42. The first of these, figure 36, gives an estimate of the "mean diurnal variation of wind direction." In order to simplify the computation, a scalar-average wind direction was computed

instead of a vector average. However, the diurnal course of wind direction did not reveal a modal value at 0000 GCT. On the other hand, Hisdal [1, p.172] in his investigation did, in fact, obtain a relationship between wind direction and surface temperature, using a histogram of wind direction in conjunction with the diurnal temperature trend. It would be interesting to consider histograms of the wind-direction fluctuation associated with the temperature curves of this study.

The next parameter examined was the diurnal variation of cloudiness. The annual means and six-yearly mean are found in figure 37. This set of curves bears a very close resemblance to the mean curves of diurnal temperature variation, even to the point of having a 0000 GCT maximum. Once again, the conclusion may be drawn that cloudiness plays a very important role in the mean diurnal temperature fluctuation during the polar night. However, it cannot be concluded that the diurnal fluctuation of cloudiness is the cause of the diurnal temperature variation, for then it becomes quite difficult to explain why there should be a systematic periodicity in cloudiness. It seems more reasonable to believe that the two phenomena are due to some common cause.

A relationship between cloudiness and temperature would also be indicated, if a comparison were made between figures 39 and 19. In these curves, the selection criteria were calm wind and cloudiness less than or equal to five-tenths. These criteria were chosen in order to minimize temperature changes due to turbulent mixing associated with higher wind speeds.

Comparing the mean variations in figures 19 and 39, it appears that for periods with calm winds a maximum or minimum of temperature tends to lag the corresponding cloudiness by three hours. Table 7 summarizes some observations of this lag relationship.

Table 7

Time (GCT) of occurrence of maxima/minima for days with wind speed = 0 and cloudiness less than or equal to five-tenths

Cloudiness		Temperature	
Max.	Min.	Max.	Min.
2400		2100	
	2100		1800
1800		1500	
	1500		1200
1200		0900	
	0900		0600
0300		0300	

Since neither mean wind direction nor mean cloudiness yielded a causative explanation of the diurnal variation of temperature, another parameter was investigated. The parameter selected next was the sea-level pressure. Its annual mean diurnal variation and six-year mean are found in figure 40. Also, figure 42 shows a comparison of the six-year mean diurnal pressure variation with that of the corresponding temperature variation, as well as the variation of other parameters.

The important features of the six-year mean diurnal pressure variation is that it has a maximum value at 1200 GCT and a secondary maximum at 0000 GCT. This result agrees with

the results of a recent investigation of Antarctic data by Carpenter [10] . He used two years of three-hourly surface pressure data in making a harmonic analysis to determine the phase and amplitude of the diurnal and semidiurnal pressure waves. Carpenter's results for McMurdo Sound are listed in table 8 which compares favorably with the pressure variation in figure 42.

Table 8

Mean harmonic components of the diurnal pressure wave at McMurdo Sound, after Carpenter [10]

	Ampl.(mb)	Mean time of max.
Diurnal Oscillation	.001	2118 GCT
Semidiurnal Oscillation	.076	1040 GCT

In view of the fact that there is a definite diurnal and semidiurnal pressure fluctuation at McMurdo Sound, the next problem is to determine what influence they have, if any, on the diurnal temperature variation.

Since the semidiurnal variation has its maximum value near 1200 GCT, it is readily apparent that this compressional pressure wave can not account for a temperature minimum which occurs at the same time. The Poisson equation shows that for an adiabatic pressure increase, a temperature increase will result. Moreover, the diurnal pressure wave (maximum at 2118 GCT) has an amplitude of only .001 mb. This pressure increase would result in a temperature increase by adiabatic compression of the order .0002F.

Thus, it is seen that neither the diurnal nor semidiurnal

Figure35: Mean diurnal temperature variation during the polar night for the years 1956 through 1961.

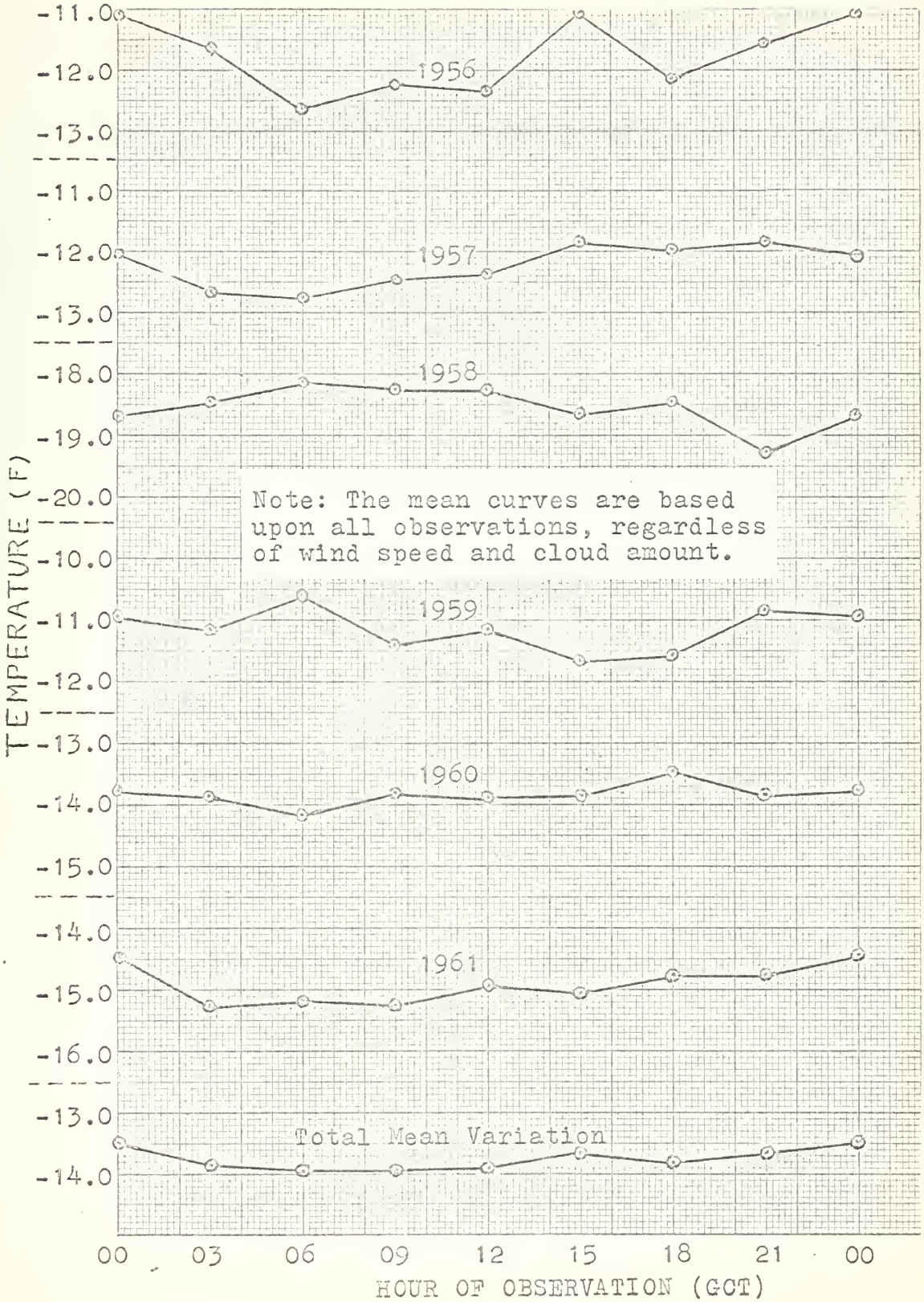

Figure36: Mean diurnal variation of wind direction during the polar night for the years 1956 through 1961, based upon all observations, regardless of wind speed and cloud amount.

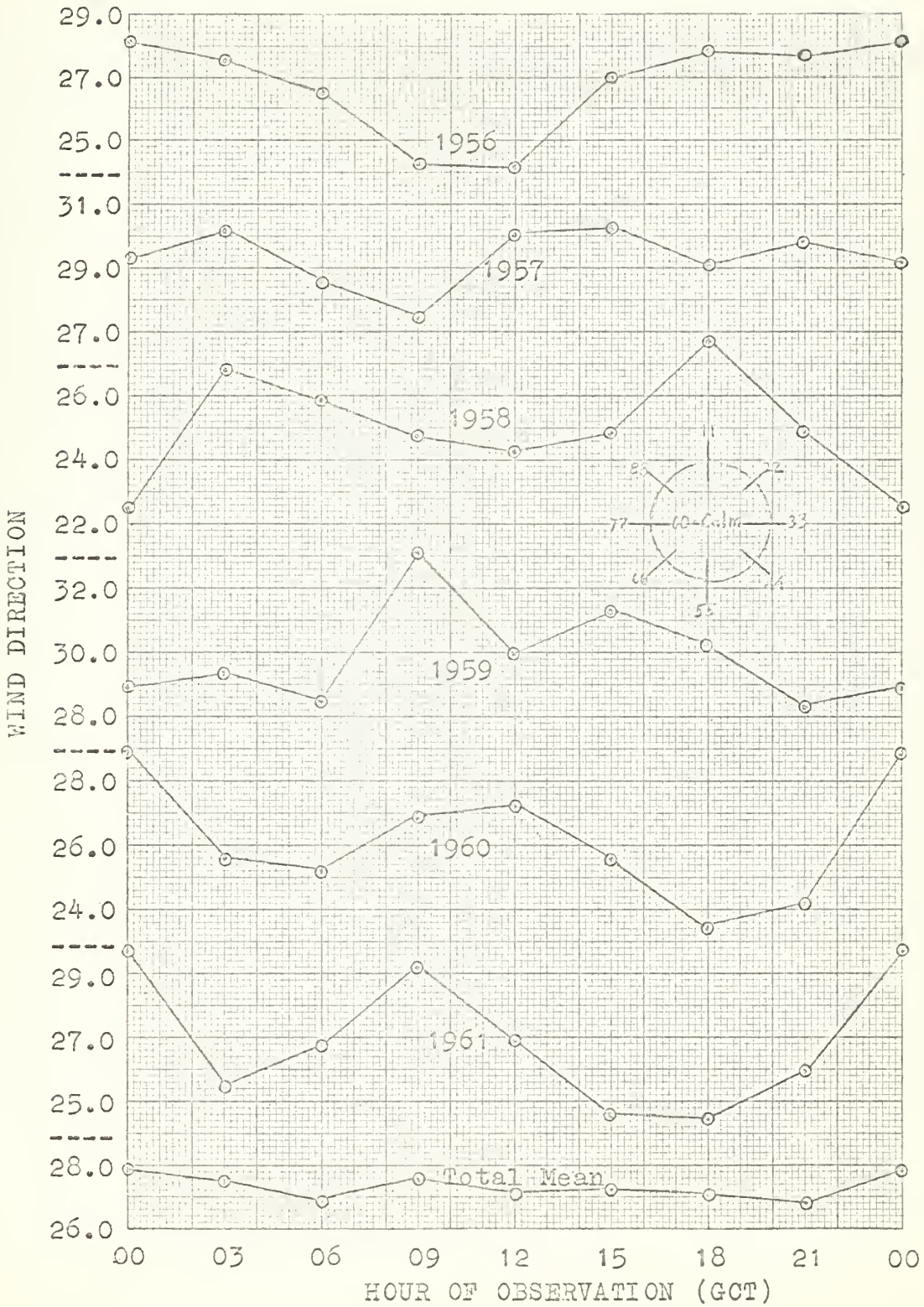

Figure37: Mean diurnal variation of cloudiness during the polar night for the years 1956 through 1961, based upon all observations, regardless of wind speed and cloud amount.

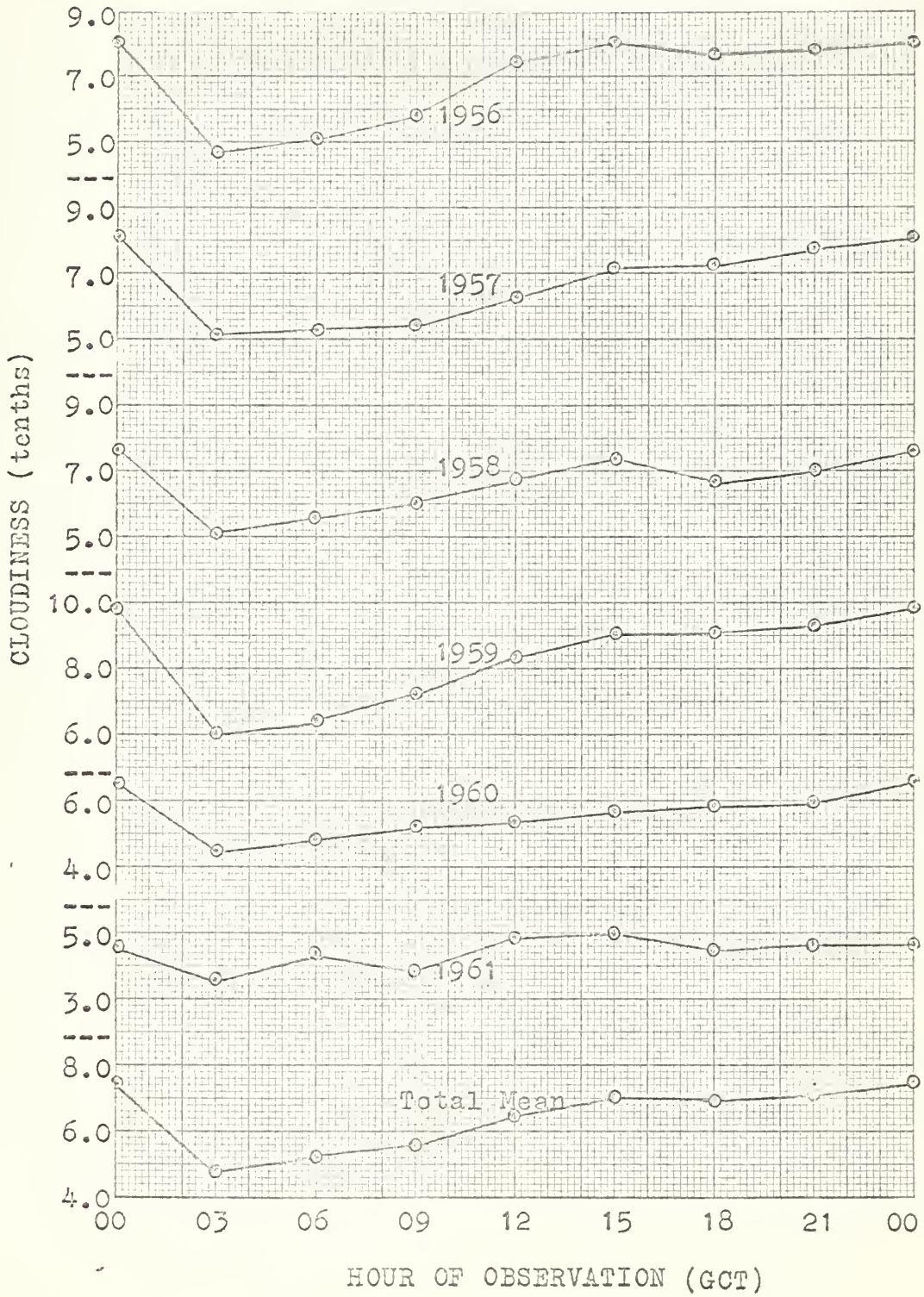

Figure 38: Total cloudiness variation curves with variation in starting time of the period.

(wind speed = 0 kt; cloudiness ≤ 5/10)

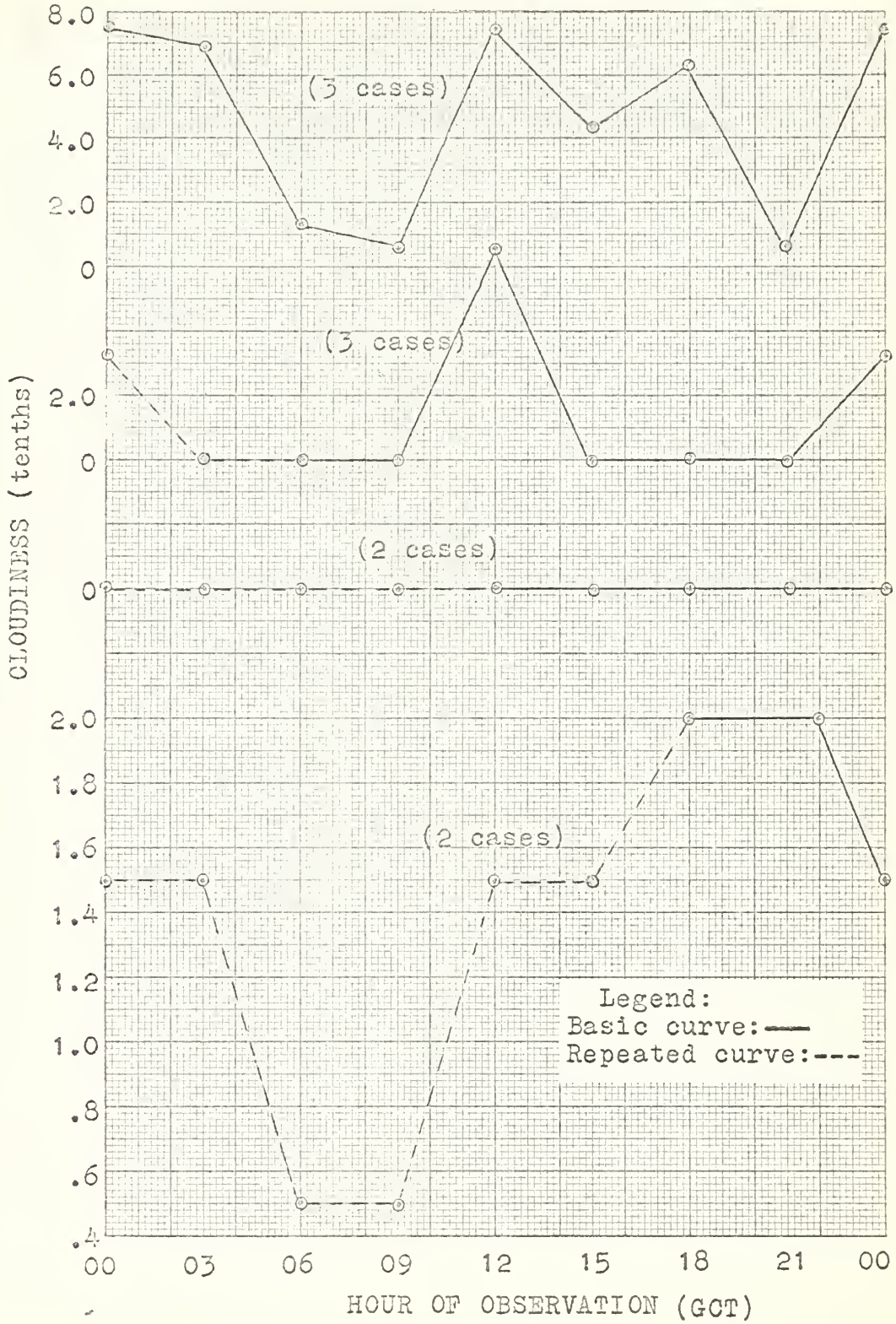

Figure 39: Comparison of the total cloudiness variation with the meteorological and statistical bias variations.

(wind speed = 0 kt; cloudiness ≤ 5/10)

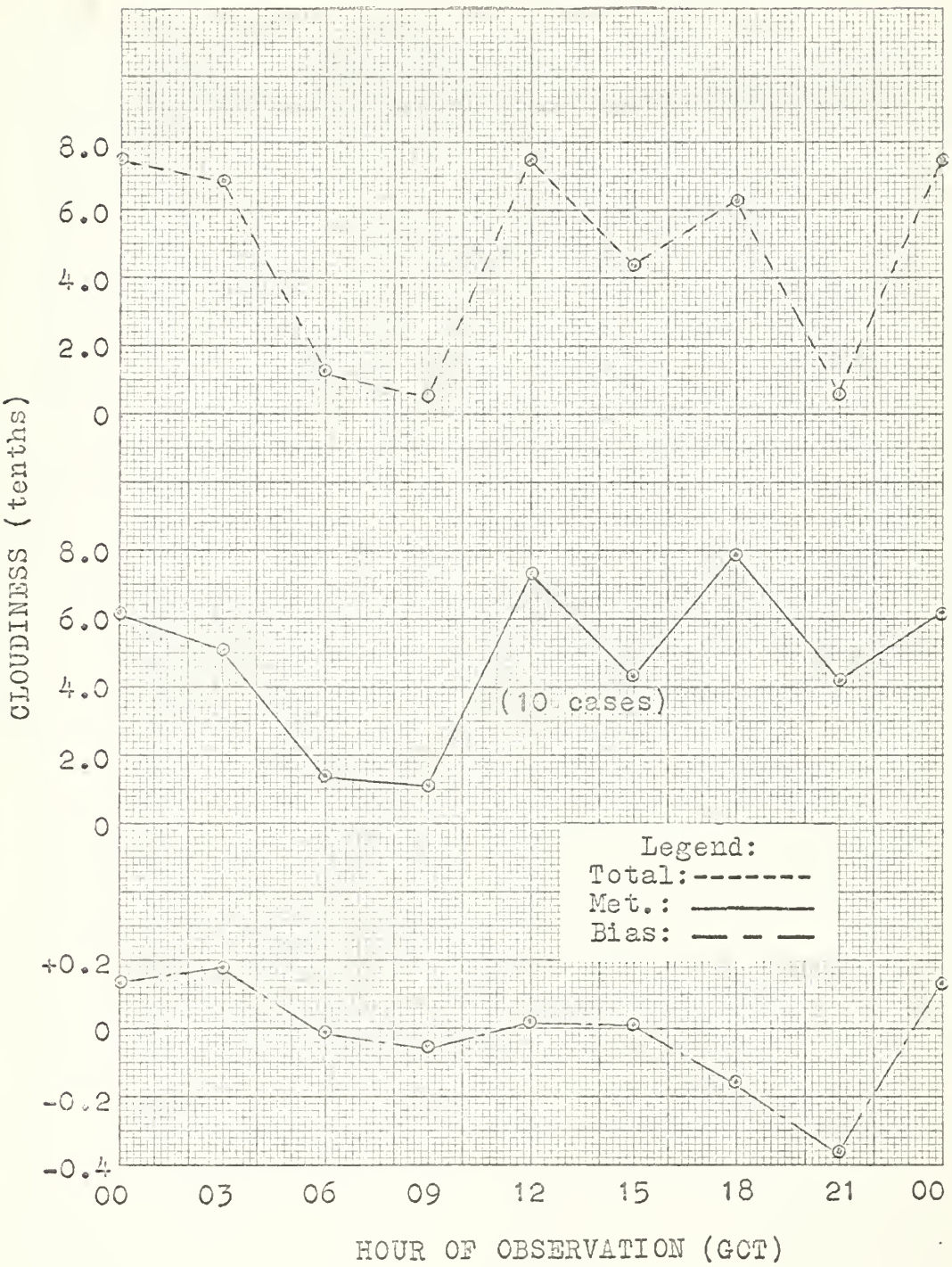

Figure40: Mean diurnal variation of atmospheric pressure during the polar night for the years 1956 through 1961, based upon all observations, regardless of wind speed and cloud amount.

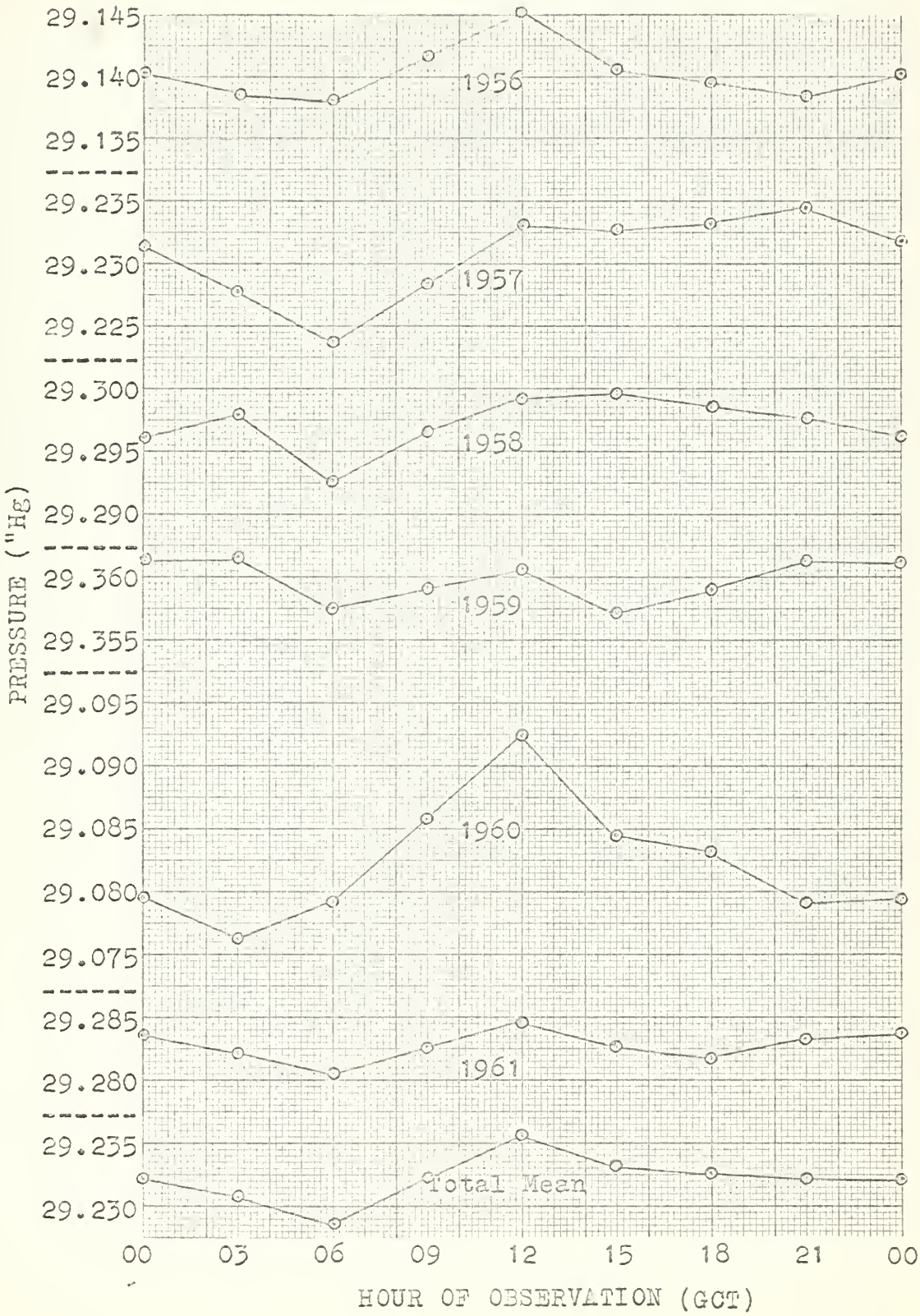

Figure 41: Comparison of the total atmospheric pressure variation with the meteorological and statistical bias variations.

(wind speed = 0 kt; cloudiness = 0)

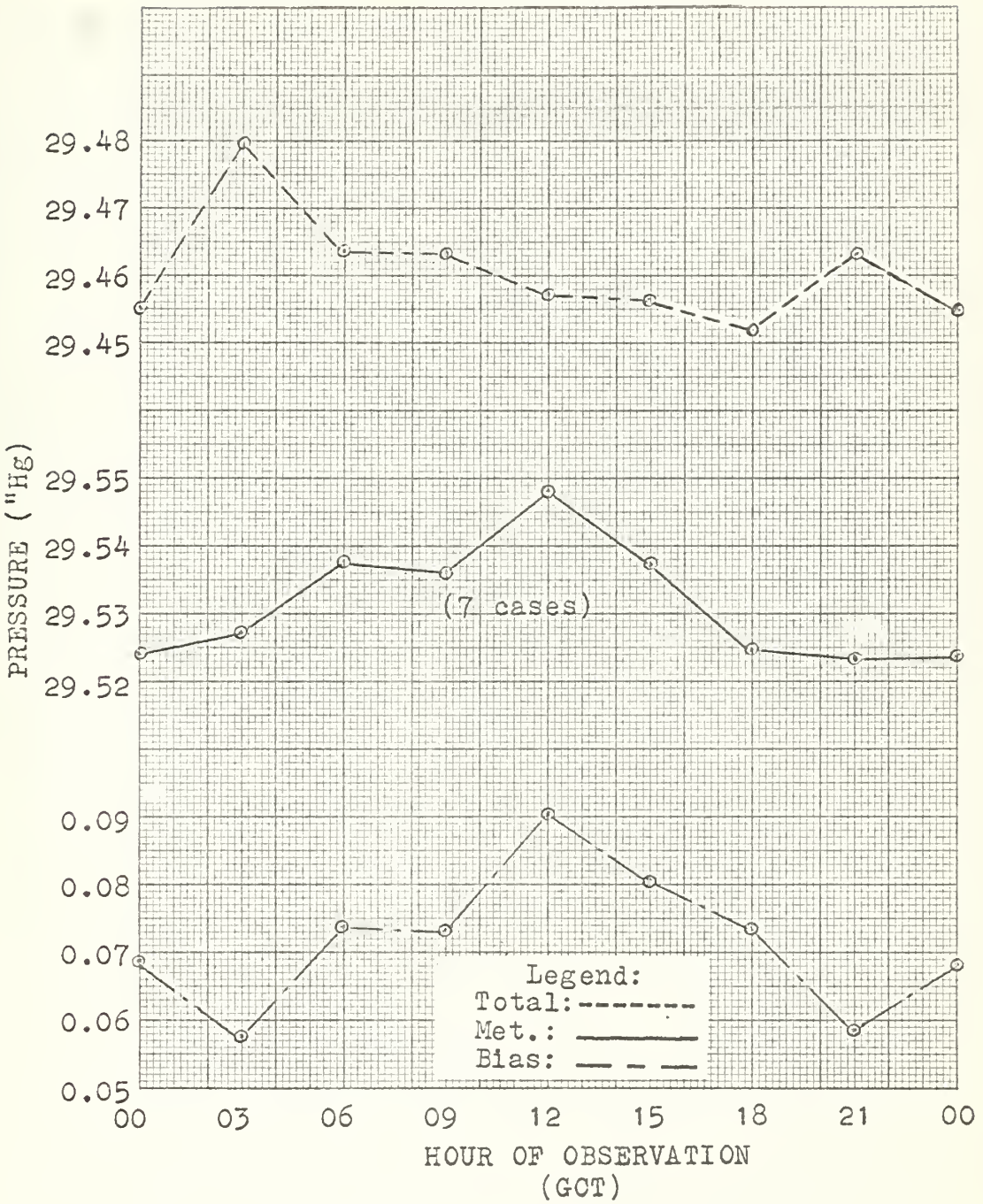

Figure 42: Diurnal variation of temperature, atmospheric pressure, wind direction, and cloudiness during the polar night. These curves are based upon six winters of observations, 1956 through 1961.

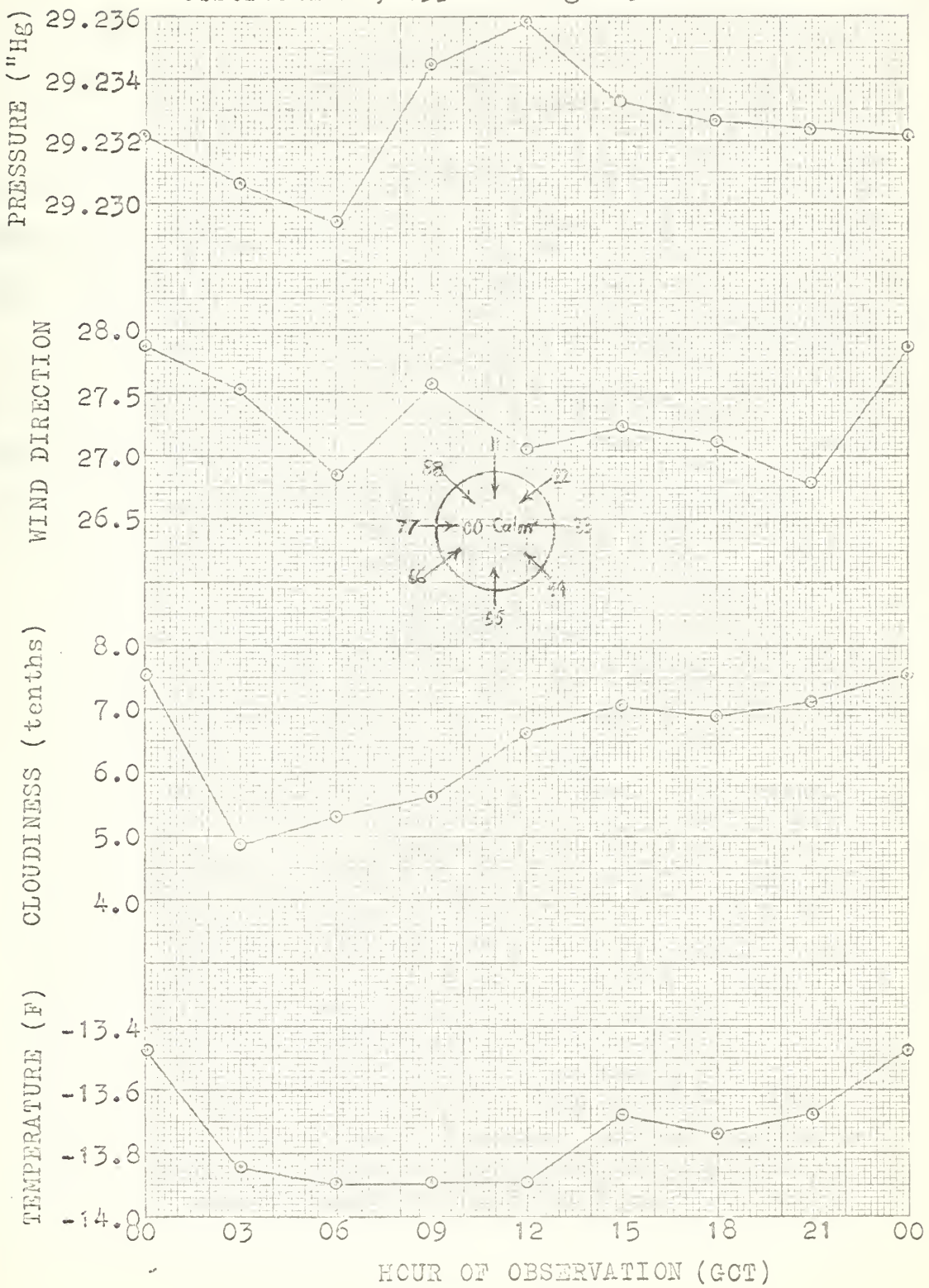

pressure variations can account for the 0000 GCT maximum in the diurnal temperature variation. The diurnal pressure wave is not of sufficient magnitude to affect the diurnal temperature variation, and the semidiurnal pressure wave is 12 hours out of phase with the temperature.

With the foregoing physical factors eliminated as reasonable explanations for the 0000 GCT maximum in the daily temperature curves considered previously, it is necessary to again consider a statistical explanation.

A climatological statistical effect has been proposed as an explanation by van der Bijl, who suggested that the seasonal temperature trend could produce such a maximum. A schematic version of the seasonal effect is shown in figure 43.

Figure 43

Schematic illustration of the seasonal trend effect

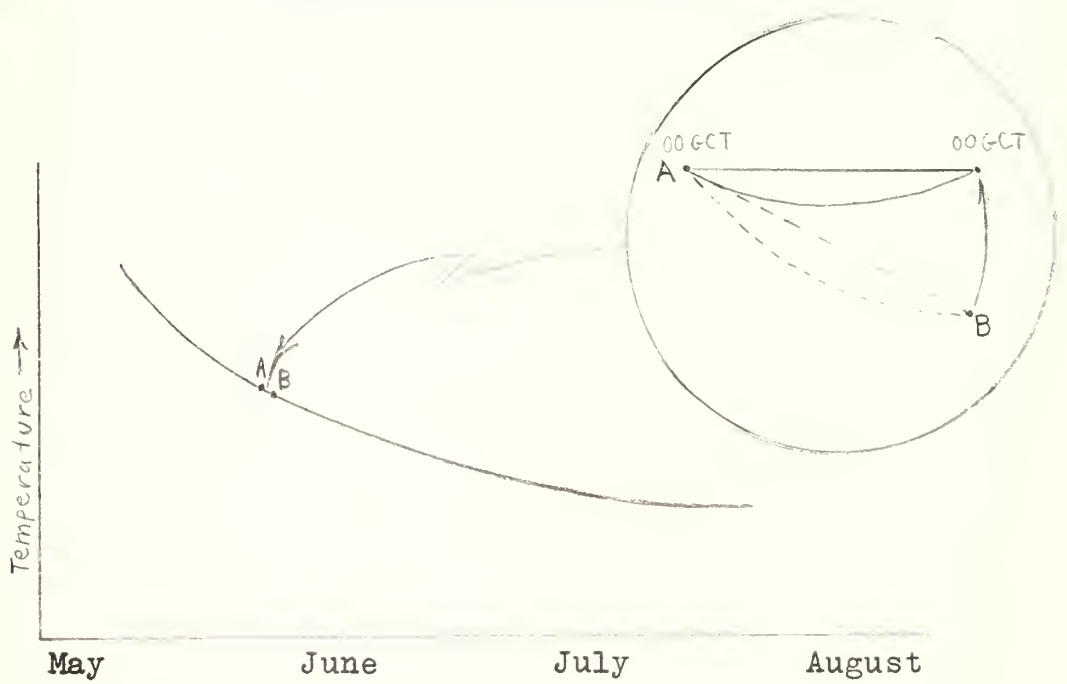

A 24-hour segment of the seasonal temperature trend, denoted AB, is enlarged and shown as a dashed line in the upper right-hand corner of figure 43. The solid lines in the enlarged portion show the segment as corrected by the Lamont procedure.

If the entire temperature trend for the cooling season were divided into 24-hour segments, each would have a concave curvature, because the over-all trend is concave. Now, if these 24-hour segments were averaged for the entire cooling season, the mean would also be concave. This concavity would give the appearance of a diurnal temperature fluctuation, such as that observed in the present investigation.

Figure 35 shows that the concavity of the mean diurnal or meteorological temperature variation produces a temperature range of 0.5F. It is of interest then to determine whether the seasonal temperature trend actually has enough curvature to produce 0.5F in a 24-hour period. In pursuing this investigation, the seasonal temperature trends were plotted for each of the years 1956 through 1961. Also, the six-year mean trend was computed. These curves are shown as figures 44 through 50.

Examination of the seasonal temperature trends reveals that they are not as smooth as was expected. Also, the curvature from the beginning to the end of the dark season is not of sufficient magnitude to cause a five-tenths degree temperature range in a 24-hour segment. Therefore, a temperature-variation model which would increase the curvature of

the average 24-hour segments would substantiate van der Bijl's proposal and yet produce, upon averaging, the long-term mean seasonal temperature curve.

This curvature increase may be accomplished by considering that actual observations of the seasonal temperature trend in a given year are as shown in figure 51. In this figure the dashed line represents the long-term seasonal trend, which is the same as in figure 43. The solid line represents the unsmoothed temperature trend, which shows that relatively long cooling periods during the dark season are interrupted by short periods of above seasonal temperature.

The effect is to produce a series of "spiked" temperature maxima which greatly increase the mean curvature of the average 24-hour segments during the prolonged cooling segments. With this refinement the mean diurnal temperature variation may have enough curvature to produce a range of 0.5F.

A more complete study of the seasonal temperature trend is necessary, however, before its effect on the curvature can be validated. In particular, if the shape of the summer temperature trend is as shown in figure 51, and the total mean diurnal temperature variation for the mid-summer months has a minimum at 0000 GCT, then the seasonal trend effect would have some merit for the summer months also.

Figure 44: Seasonal trend of the temperature during the polar night at McMurdo Sound, Antarctica. (15 May - 15 August, 1956)

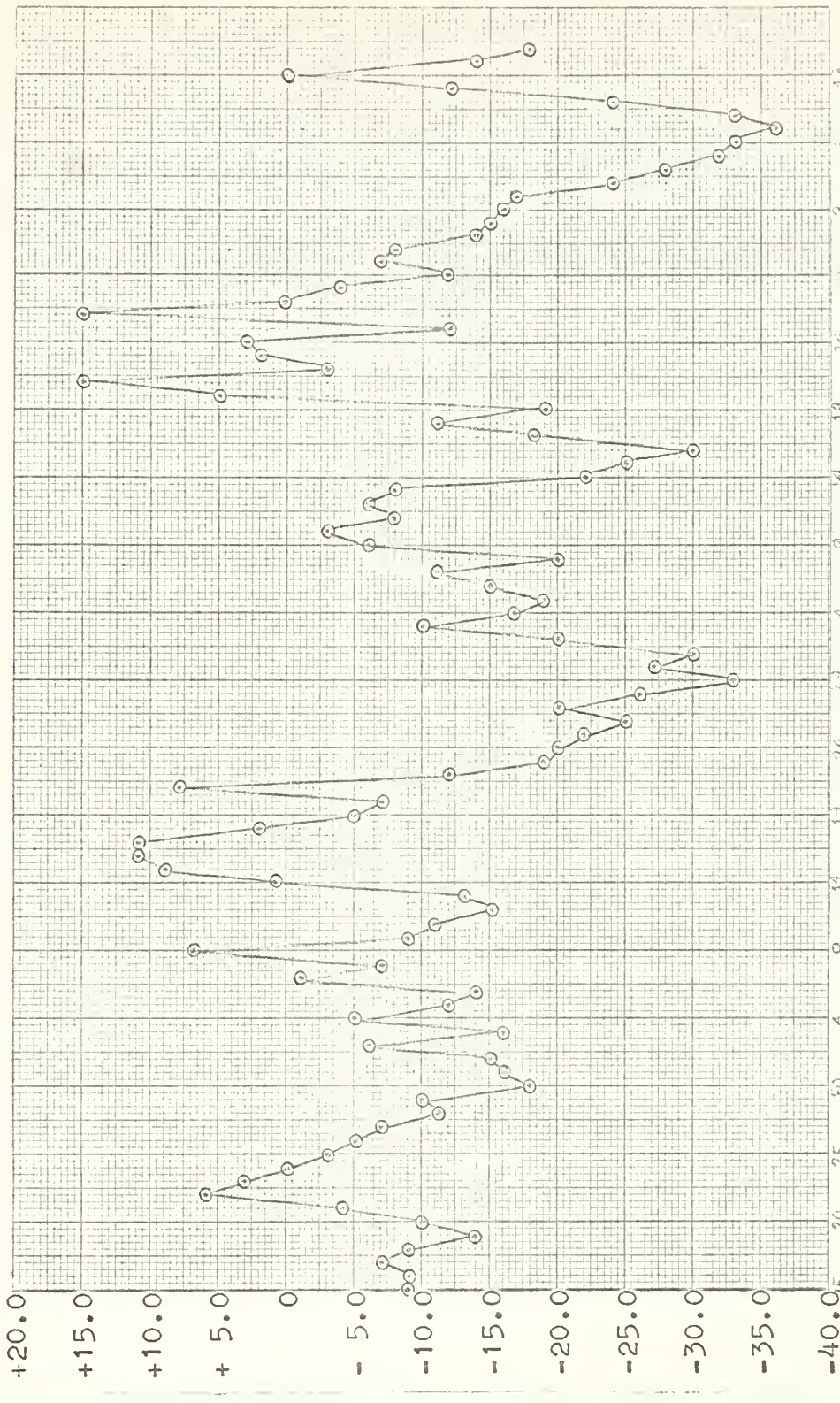

Figure 45: Seasonal trend of the temperature during the polar night at McMurdo Sound, Antarctica. (15 May - 15 August, 1957)

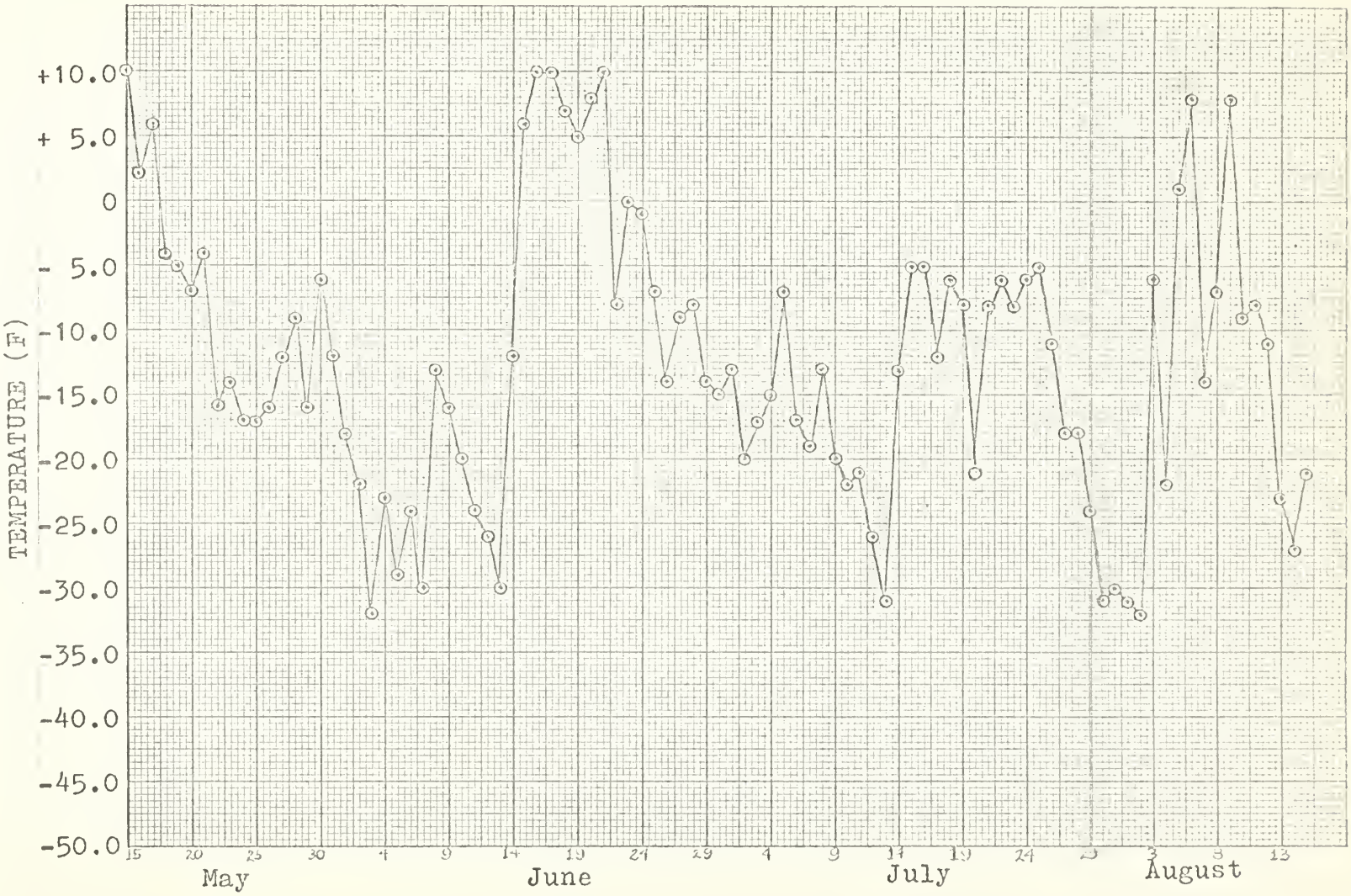

Figure 46: Seasonal trend of the temperature during the polar night at McMurdo Sound, Antarctica. (15 May - 15 August, 1958)

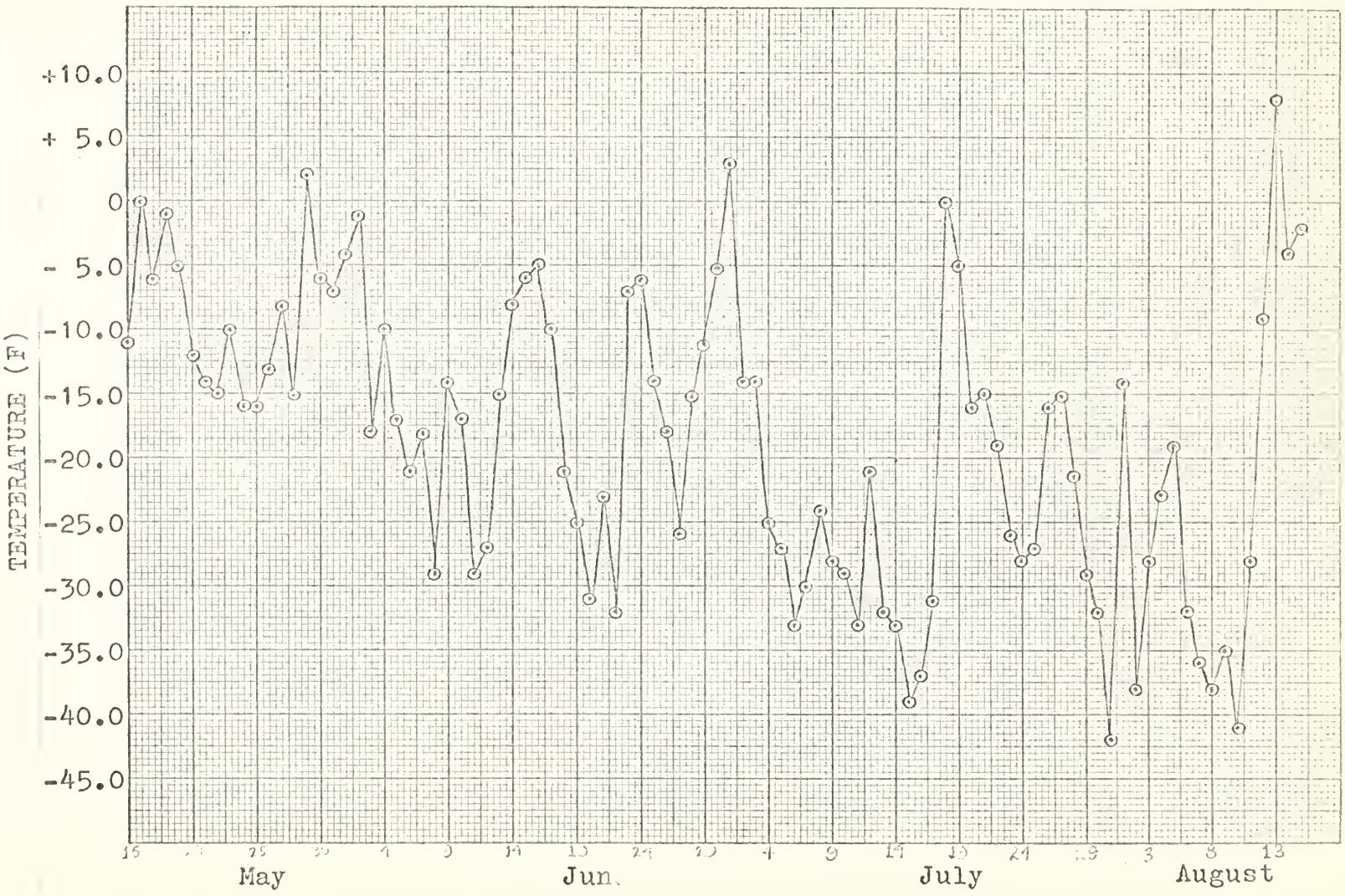

Figure47: Seasonal trend of the temperature during the polar night at McMurdo Sound, Antarctica. (15 May - 15 August, 1959)

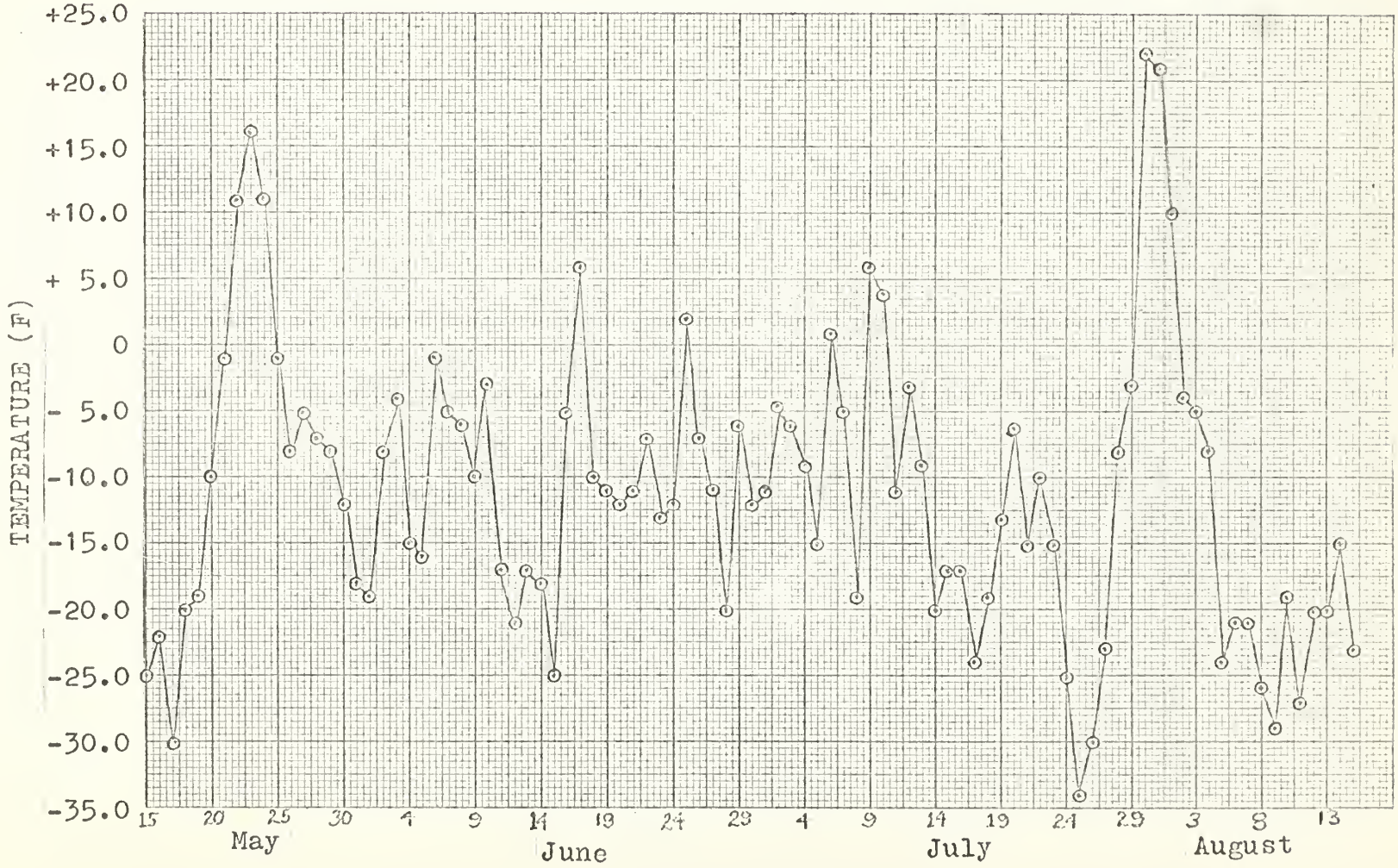

Figure 48: Seasonal trend of the temperature during the polar night at McMurdo Sound, Antarctica. (15 May - 15 August, 1960)

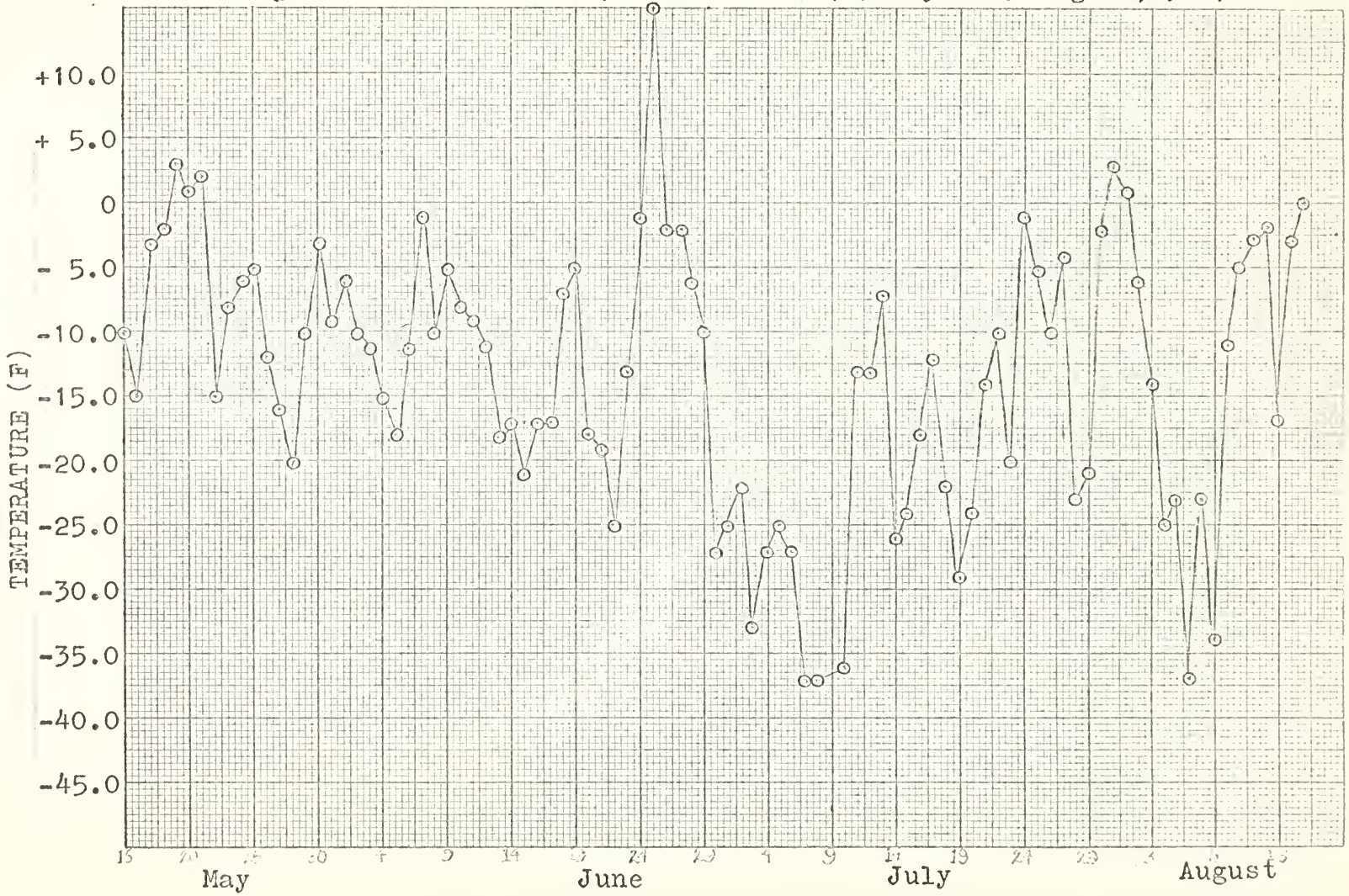

Figure 40: Seasonal trend of the temperature during the polar night at McMurdo Sound, Antarctica. (15 May - 15 August, 1961)

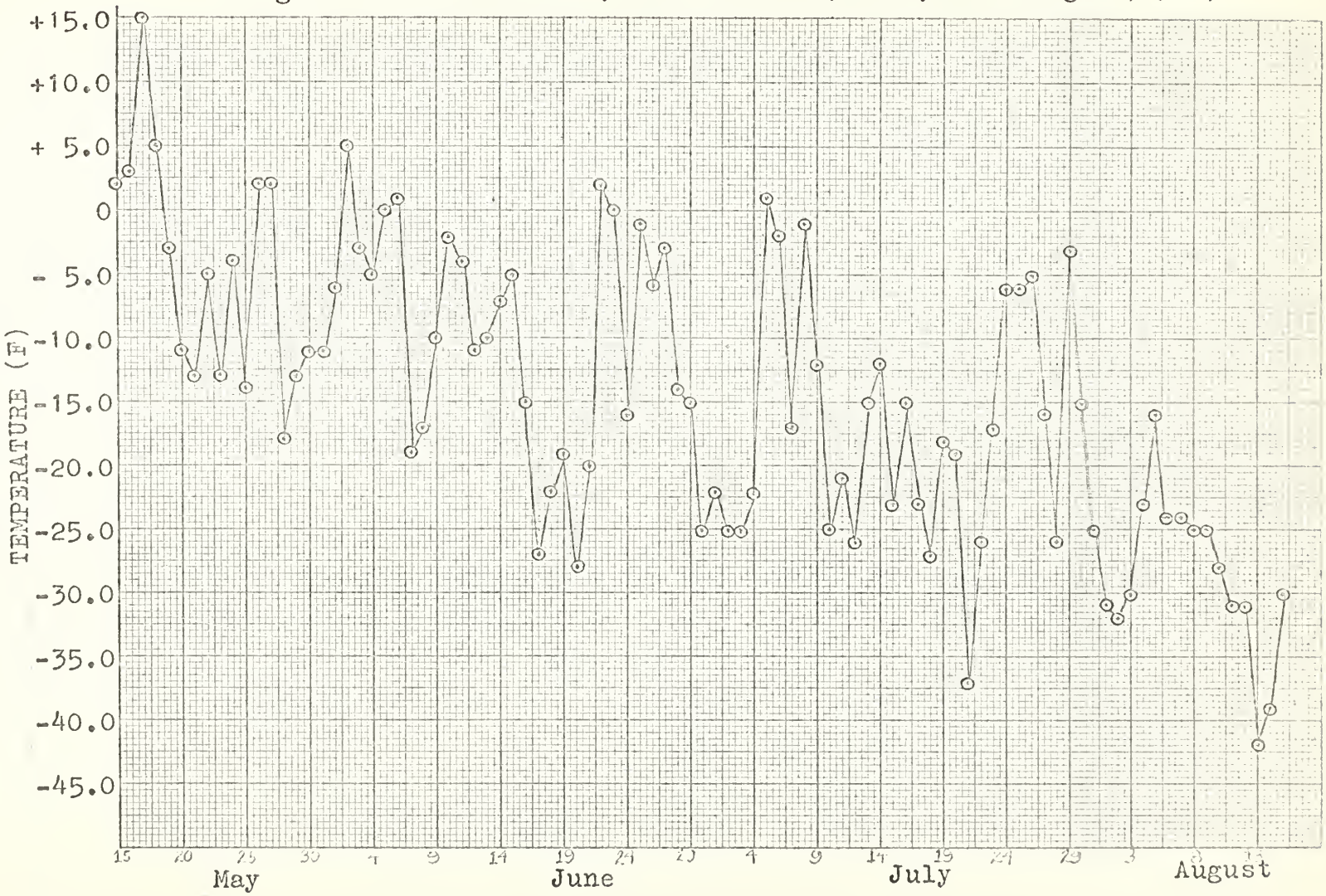

Figure 50: Mean seasonal trend of the temperature during the polar night at McMurdo Sound, Antarctica. (1956 - 1961)

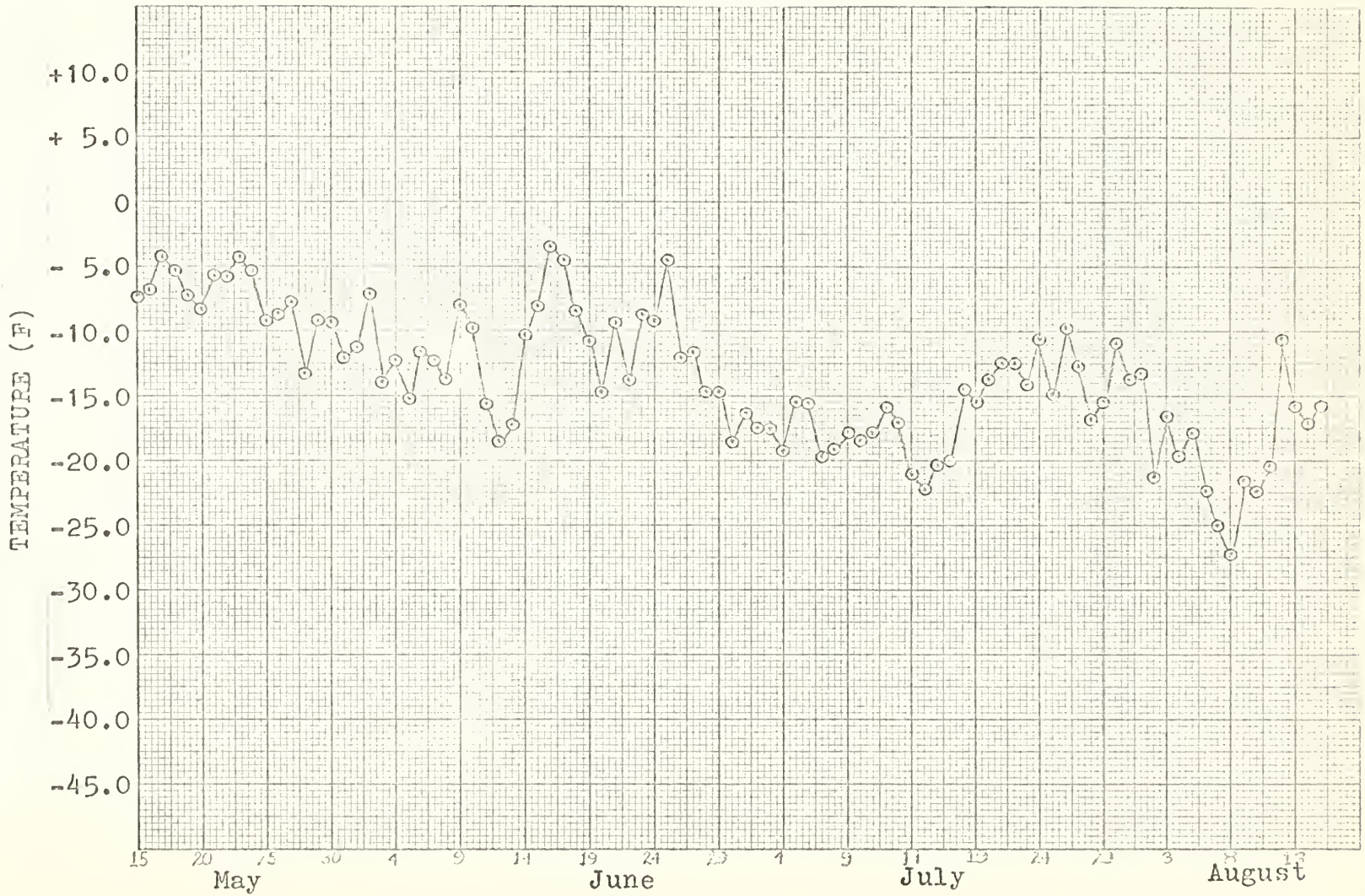

Figure 51

Schematic model of a proposed seasonal temperature trend for the polar regions

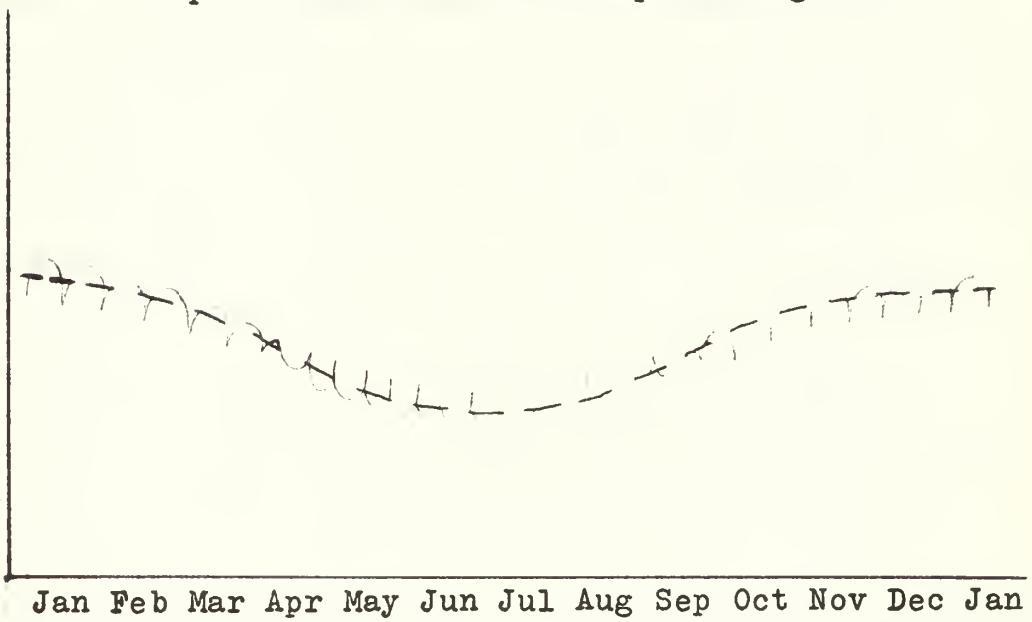

11. Discussion of random errors

Throughout this study, random errors have been mentioned as an important factor in the erratic behavior of various curves. For instance, the 2100 GCT maximum in the statistical bias curve of figure 7 was considered to be caused by the randomness of some of the data used in computing the mean values. The following discussion will illustrate that the 2100 GCT was, in fact, caused by random errors. Also, a computational scheme will be suggested, which reduces the effect of these errors.

The notation used is as follows:

M_i = temperature due to the meteorological influence at observation time i = 0,.., n,..,4

S_j = temperature due to the statistical bias

t_{mn} = total temperature = $M_n + S_j + e_{mn}$

m = 0,....,4

n = 0,...,3

e_{mn} = temperature due to the random error

σ^2 = variance of the single-observation random error = e^2_{mn}.

Subscripts:

m = row in matrix,

n = column in matrix,

i,j = chronological order of the temperature observation.

Consider table 9 to be a matrix of total temperature similar to table 3. The meteorological effect is constant

for any particular column, and the statistical bias is constant for any particular diagonal row. The errors are assumed to be random and uncorrelated in both the vertical and the diagonal directions.

Table 9

Generalized Theoretical Table of Mean Total Temperatures

S_j	M_0	M_1	M_2	M_3	M_4
S_3	t_{00}	t_{01}	t_{02}	t_{03}	t_{04}
S_2	t_{10}	t_{11}	t_{12}	t_{13}	t_{14}
S_1	t_{20}	t_{21}	t_{22}	t_{23}	t_{24}
	t_{30}	t_{31}	t_{32}	t_{33}	t_{34}

Using the column-averaging method, as explained in section 4, the following totals result from using the temperatures in table 9:

Column 1: $4M_0 + \sum_{j=0}^{3} S_j + \sum_{m=0}^{3} e_{m0}$

Column 2: $4M_1 + \sum_{j=0}^{3} S_j + \sum_{m=0}^{3} e_{m1}$

Column 3: $4M_2 + \sum_{j=0}^{3} S_j + \sum_{m=0}^{3} e_{m2}$

Column 4: $4M_3 + \sum_{j=0}^{3} S_j + \sum_{m=0}^{3} e_{m3}$.

Next, divide by four to obtain the column mean temperatures:

Column 1: $M_0 + \frac{1}{4}\sum_{j=0}^{3} S_j + \frac{1}{4}\sum_{m=0}^{3} e_{m0}$

Column 2: $M_1 + \frac{1}{4}\sum_{j=0}^{3} S_j + \frac{1}{4}\sum_{m=0}^{3} e_{m1}$

Column 3: $M_2 + \frac{1}{4}\sum_{j=0}^{3} S_j + \frac{1}{4}\sum_{m=0}^{3} e_{m2}$

Column 4: $M_3 + \frac{1}{4}\sum_{j=0}^{3} S_j + \frac{1}{4}\sum_{m=0}^{3} e_{m3}$.

Subtracting the column averages from their corresponding first-row entry yields an estimated value of the statistical bias for the various columns:

Column 1:
$$\frac{(M_0 + S_0 + e_{00}) - (M_0 + \frac{1}{4}\sum_{j=0}^{3} S_j + \frac{1}{4}\sum_{m=0}^{3} e_{m0})}{\frac{3}{4}S_0 - \frac{1}{4}(S_1+S_2+S_3) + \frac{3}{4}e_{00} - \frac{1}{4}(e_{10}+e_{20}+e_{30})}$$

Column 2:
$$\frac{(M_1 + S_1 + e_{01}) - (M_1 + \frac{1}{4}\sum_{j=0}^{3} S_j + \frac{1}{4}\sum_{m=0}^{3} e_{m1})}{\frac{3}{4}S_1 - \frac{1}{4}(S_0+S_2+S_3) + \frac{3}{4}e_{01} - \frac{1}{4}(e_{11}+e_{21}+e_{31})}$$

Column 3:
$$\frac{(M_2 + S_2 + e_{02}) - (M_2 + \frac{1}{4}\sum_{j=0}^{3} S_j + \frac{1}{4}\sum_{m=0}^{3} e_{m2})}{\frac{3}{4}S_2 - \frac{1}{4}(S_0+S_1+S_3) + \frac{3}{4}e_{02} - \frac{1}{4}(e_{12}+e_{22}+e_{32})}$$

Column 4:
$$\frac{(M_3 + S_3 + e_{03}) - (M_3 + \frac{1}{4}\sum_{j=0}^{3} S_j + \frac{1}{4}\sum_{m=0}^{3} e_{m3})}{\frac{3}{4}S_3 - \frac{1}{4}(S_0+S_1+S_2) + \frac{3}{4}e_{03} - \frac{1}{4}(e_{13}+e_{23}+e_{33})}$$

The next step will be to determine the variance of the statistical bias, in order to be able to compare it with the variance of the statistical bias computed by diagonal-averaging.

If σ^2 is the variance of a single-observation random error, then the variance of the first column-average equals

$$\left[\frac{1}{4}\left(e_{00}+e_{10}+e_{20}+e_{30}\right)\right]^2$$

$$= \frac{1}{16}\sum_{m=0}^{3} e_{m0}^2 = \frac{1}{16}\left(4\sigma^2\right)$$

$$= \frac{1}{4}\sigma^2 .$$

The variance of the statistical bias is then computed as shown below. Note in this connection that M_0 and $\frac{1}{4}\sum_{j=0}^{3} S_j$ are considered to be fixed numbers and therefore have zero variance.

For column 1: $\mathrm{Var}\left\{\left(\frac{3}{4}e_{00}\right)-\frac{1}{4}\left(e_{30}+e_{20}+e_{10}\right)\right\}$

$$= \frac{9}{16}\mathrm{Var}\, e_{00} + \frac{1}{16}\left(\mathrm{Var}\, e_{30}+\mathrm{Var}\, e_{20}+\mathrm{Var}\, e_{10}\right)$$

$$= \frac{12}{16}\sigma^2$$

$$= \frac{3}{4}\sigma^2 .$$

The other columns treated similarly will yield the same result, which is the standard deviation of the S_i.

The second method considered in section 4 is that of averaging the total temperatures diagonally. As explained previously, a diagonal average will produce the statistical bias, without having to subtract the average from the total temperature. As will be proven below, this method results in a more accurate estimate of the statistical bias than that arrived at through a column average. Using general notation we have

Diagonal sum: $4 S_j + \sum_{i=1}^{4} M_i + \sum_{i=1}^{4} e_{ij}$.

Average: $S_j + \frac{1}{4}\sum_{i=1}^{4} M_i + \frac{1}{4}\sum_{i=1}^{4} e_{ij}$

Variance in average: $\frac{1}{16} \text{Var} \sum_{i=1}^{4} e_{ij}$

$$= \frac{1}{16} \sum \text{Var}\, e_{ij}$$

$$= \frac{1}{16} (4\sigma^2)$$

$$= \frac{1}{4} \sigma^2 .$$

Note that the diagonal method reduces the variance in the statistical bias by a factor of three, compared with the variance resulting from the column method.

An important point that must be emphasized is that the reduction factor of three is valid only when the temperature observations are six hours apart. In other cases, where the observations are other than six hours apart, different reduction factors are valid.

A generalized derivation, similar to the one for the six-hour spacing, can be used to arrive at the values in table 10, which are the factors by which the variance in the statistical bias will be reduced if a diagonal average is used in computing the bias, rather than a column average.

Table 10

Reduction factor, R, for the error variance in the statistical bias

Δt	1	2	3	4	6	12	24/k
R	23	11	7	5	3	1	k-1

Δt = time between observations

= (24/k) hours

R = Reduction factor

k = 1,2,3,....,n

This discussion of random errors has shown that the best method for obtaining the statistical bias is by averaging the

temperatures in table 9 diagonally. A similar discussion would also prove that the best method for obtaining the meteorological influence is through a column average.

Figure 52 was plotted in order to provide a graphical comparison of the results of these two methods. The most striking feature of the figure is that using the diagonal average in computing the statistical bias has eliminated the 2100 GCT maximum.

Figure 52: Comparison of the total temperature variation with the meteorological and statistical variations.

(wind speed ≤ 15 kt; cloudiness ≤ 5/10)

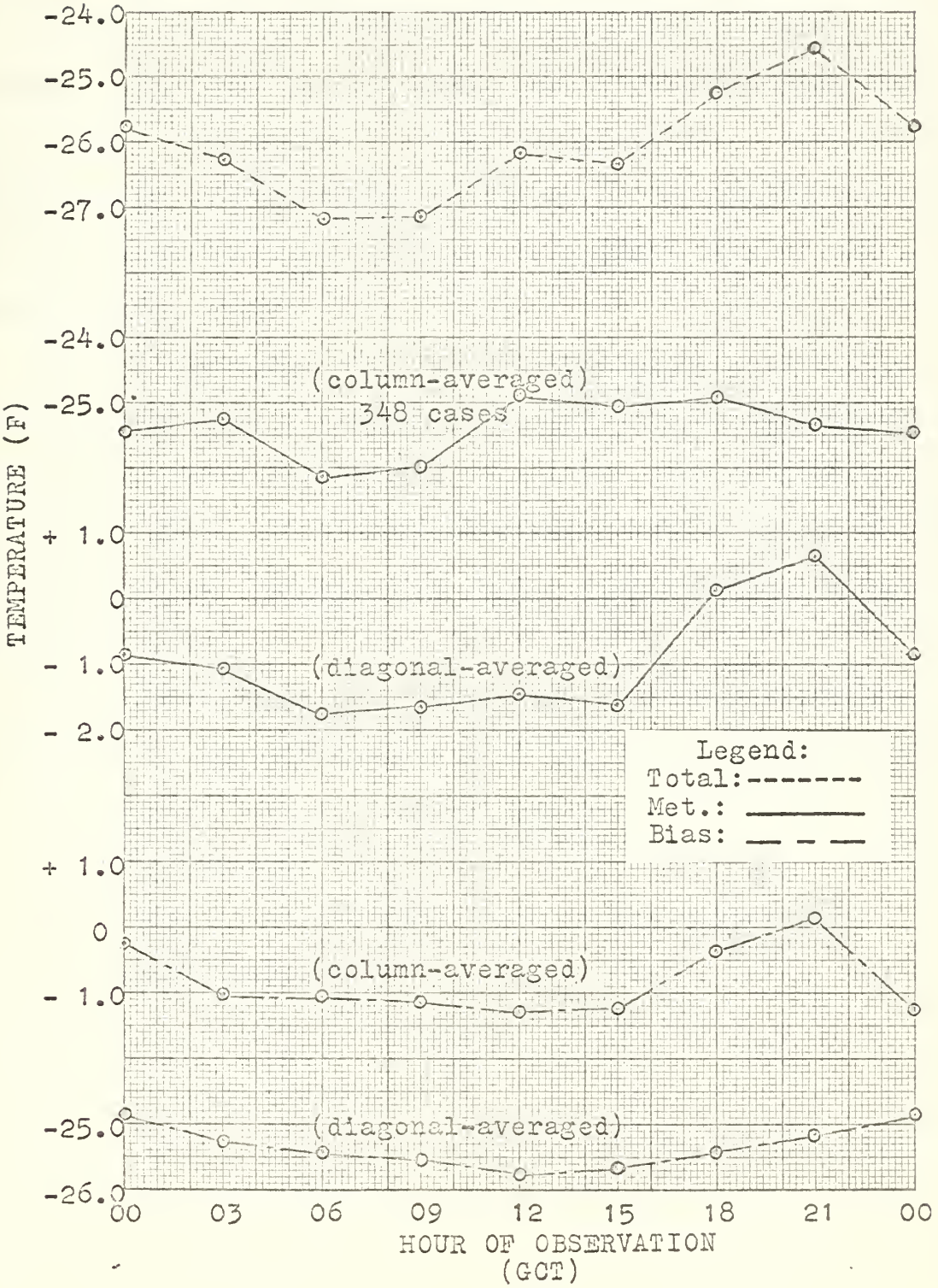

12. Conclusions and recommendations

The purpose of this investigation was to determine the nature of the diurnal temperature variation during the polar night at McMurdo Sound, Antarctica. The conclusion based upon data for the years 1956 through 1961 is that no diurnal temperature variation, in the normal sense, exists during the polar night. The maxima that appear in the daily temperature trend are due to synoptic fluctuations. The concave curvature between temperature peaks appears to reflect that of the seasonal cooling curve.

It is recommended that the column-averaging procedure should be used only for determining the meteorological component of the diurnal temperature variation. For computing the statistical bias, the diagonal-averaging method should be used. With this scheme, the variance in the statistical bias can be minimized.

For further study it is suggested that investigations, similar to the present one, be made for the following situations:

(1) summer season, when the sun never goes below the horizon;

(2) other polar stations, both in the winter and summer seasons.

BIBLIOGRAPHY

1. Hisdal,V., Norwegian-British-Swedish antarctic expedition, 1949-52 scientific results, vol.I, part 2, surface observations, Norsk Polarinstitutt, Oslo University Press, 1960.

2. Simpson, G.C., Meteorology, part I, discussion, British antarctic expedition 1910-1913, Calcutta, 1919.

3. Court, A., Antarctic atmospheric circulation, Compendium of Meteorology, Amer. Met. Society, Boston, Waverly Press, 1951.

4. Rouch, J., La variation diurne de la temperature dans l'antarctique, C. R. Acad. Sci., Paris, 1941.

5. Hisdal, V., The diurnal temperature variation during the polar night, Quarterly Journal of the Royal Meteorological Society, vol. 86, no. 367, 1960.

6. Bartels, J., Neue methoden zur berechnung und darstellung der taglichen luftdruckschwankung bei starken unperiodischen storungen diss. Gottingen, gedrukt in Bartels, 1923.

7. van der Bijl, W., Toepassing van statistische methoden in de klimatologie, Staatsdrukkerij en Uitgeverijbedrijf, 1952.

8. LeVasteau, T., Factors affecting the temperature of the surface layer of the sea, Commentations Physico-mathematicae, vol. XXV, no. 1, Societas Scientiarum Sennica, Helsinki, p. 27, 1960.

9. Conrad, V., and L. W. Pollak, Methods in climatology, Harvard University Press, pp. 133-139, 1950.

10. Carpenter, T. H., The distribution of the semidiurnal pressure oscillation on the antarctic continent, Journal of Geophysical Research, vol. 68, no. 8, p. 2211, 1963.